UNIVERSITY OF TEXAS AT AUSTIN
RESEARCH REACTOR LICENSE NO. R-129
DOCKET NO. 50-602

Response to Request for Additional Information Regarding License Renewal Request.

JULY 15, 2015

REDACTED VERSION*

Department of Mechanical Engineering
THE UNIVERSITY OF TEXAS AT AUSTIN
Nuclear Engineering Teaching Laboratory • Austin, Texas 78758
512-232-5370 • FAX 512-471-4589 • http://www.me.utexas.edu/~netl/

July 15, 2015

ATTN: Document Control Desk,
U.S. Nuclear Regulatory Commission,
Washington, DC 20555-0001

M. Balazik
Project Manager
Research and Test Reactors Licensing Branch

SUBJECT: Docket No. 50-602, Request for Renewal of Facility Operating License R-129

REF: UNIVERSITY OF TEXAS AT AUSTIN - REQUEST FOR ADDITIONAL INFORMATION REGARDING THE LICENSE RENEWAL REQUEST FOR THE NUCLEAR ENGINEERING TEACHING LABORATORY TRIGA MARK II NUCLEAR RESEARCH REACTOR (TAC NO. ME7694)

Sir:

Attached are *Analysis of Neutronic and Thermal Hydraulic performance of the University of Texas TRIGA Mark II Nuclear Research Reactor*, and response to referenced Request for Additional Information (RAI) related to items 7, 8.3, 10, 11, 13, 14, 15, and 35. We respectfully request an additional 90 days to support completion of the remaining RAIs.

Please contact me by phone at 512-232-5373 or email whaley@mail.utexas.edu if you require additional information or there is a problem with this submittal.

Thank you,

P. M. Whaley
Associate Director
Nuclear Engineering Teaching Laboratory
The University of Texas at Austin

I declare under penalty of perjury that the foregoing is true and correct.
Executed on July 15, 2015

Steven R. Biegalski
NETL Director

A020
NRR

ATT: 1. Request for Additional Information Items 7, 8.3, 10, 11, 13, 14, 15, and 35 with Responses
2. *Analysis of the Neutronic and Thermal Hydraulic Performance of the University of Texas TRIGA Mark II Nuclear Research Reactor*, July 2015

Attachment I: Request for Additional Information Items 7, 8.3, 9, 10, 11, 13, 14, 15 and 35 with Responses

RAI 7

The guidance in NUREG-1537 Section 4.5, "Nuclear Design," requests that the licensee provide a detailed description of analytical methods used in the nuclear design, including computer codes used to characterize technical parameters pertaining to the reactor. UT SAR Section 4.5 states that the "characteristics and operating parameters of this reactor have been calculated and extrapolated using experience and data obtained from existing TRIGA reactors as bench marks in evaluating the calculated data." Please provide comprehensive analysis of UT TRIGA behavior. Please describe the methods used for steady state neutronic (steady-state and kinetics) and thermal-hydraulic analysis and include comparisons with UT TRIGA measurements that demonstrate that those methods are appropriate to analyze the limits imposed by the UT TRIGA TS.

Response

The methods used for steady state neutronic (steady-state and kinetics) and thermal-hydraulic analysis of the UT TRIGA reactor are documented in *Analysis of the Neutronic and Thermal Hydraulic Performance of the University of Texas TRIGA Mark II Nuclear Research Reactor*, July 2015. The models used in analysis are validated by (1) comparison with experimental data, (2) comparison to comparable analyses, and/or (3) comparison to results using alternate codes.

RAI 8.3

[The guidance in NUREG-1537 Section 4.5.1, "Normal Operating Conditions," requests that the licensee define the limiting core configuration (LCC) which defines the highest power densities and temperatures achievable.] Please provide the technical parameters including analysis of "reactor kinetic behavior, basis reactor criticality, control rod worth, definition of the limiting core configuration (LCC), [etc.]" (NUREG-1537, Section 4.5.1). State whether the comparison of calculated and measured values demonstrates acceptable model development.

Response

Reactor kinetic behavior, reactor criticality, control rod worth, and the limiting core configuration are addressed in *Analysis of the Neutronic and Thermal Hydraulic Performance of the University of Texas TRIGA Mark II Nuclear Research Reactor*, July 2015. Validation by comparison of calculated and measured values assures acceptable model development.

RAI 9

UT SAR Section 4.5.3 refers to calculations made by General Atomics (GA) and the calculations are said to be applicable to UT TRIGA core parameters because of their similarity. The GA-4361 unit cell parameters are displayed and compared with UT TRIGA core parameters. Please provide the technical parameters that are applicable to UT TRIGA.

Response

Reference to the GA-4361 unit cell parameters is removed, superseded by the *Analysis of the Neutronic and Thermal Hydraulic Performance of the University of Texas TRIGA Mark II Nuclear Research Reactor*, July 2015.

RAI 10

UT SAR Table 4.21, "Limiting Core reactivity," displays Reference and Current control rod worths. In Table 4.14, please explain the origin of the values listed under the "Reference" column. Given the difference between the "Reference" and "Current" values of excess reactivity and shutdown margin, which values are being used in the UT TRIGA TS. The reference refers to the initial control rod worths as indicated in the 1992 SAR, as indicated in the description of Table 4.13.

Response

The paragraph preceding the table says "Based on the control rod worth values noted in Table 4.13 [4.14, Control Rod Worth (for the current core configuration)] and calibration data from June 29, 2011, the ability of the control rods to meet the specified limits is demonstrated in Table 4.21. When significant changes to the core configuration are made, verification that the core meets current requirements is accomplished including evaluation that the control rod calibration is valid or reestablishing the cone control rod worth calibration." Therefore the purpose of this table is document that control rod worth under the current core configuration meets requirements, noting the requirement to revalidate if the core configuration changes.

Nevertheless, this information is superseded by *Analysis of the Neutronic and Thermal Hydraulic Performance of the University of Texas TRIGA Mark II Nuclear Research Reactor*, July 2015.

RAI 11

The guidance in NUREG-1537 Section 4.5.3, "Operating Limits," requests that the licensee define the operating limits for its facility. However, the UT SAR does not provide sufficient information in this regard. Therefore:

(1) Please describe any limits or conditions on the evaluation of excess reactivity contributors, such as those due to temperature variations and poisons (e.g., xenon and samarium). Please provide calculations of full power reactivity defects for power, xenon, and samarium.

(2) Please provide calculations for excess reactivity and control rod worths, and evaluate whether they are in agreement with the analytical model and with UT TRIGA performance. Provide a discussion that describes the evaluation of these calculations to demonstrate acceptable reactor shutdown and shutdown margin. Include consideration of experiment reactivity.

(3) Please provide "a transient analysis assuming that an instrumentation malfunction drives the most reactive control rod out in a continuous ramp mode," (NUREG-1537, Section 4.5.3) of the reactor using a rate of withdrawal consistent with proposed UT TRIGA TS values of the maximum control rod withdrawal speed, reactivity rate, and the control rod scram time including uncertainties.

(4) Please provide all other applicable technical parameters, "excess reactivity, control rod worth, temperature coefficients, [etc.]" (NUREG-1537, Section 4.5.3).

Response

(1) There are no limits or conditions required related to excess reactivity contributors.

(2) Calculations and comparison of analytic models to observed parameters are provided in by *Analysis of the Neutronic and Thermal Hydraulic Performance of the University of Texas TRIGA Mark II Nuclear Research Reactor*, July 2015. Experiment limits are established to maintain potential transients within the limits of a pulse at the maximum reactivity addition. The addition of experiments with negative reactivity is not credited in shutdown margin calculations as contributing to shutdown margin. The removal of experiments with positive reactivity associated with experiments is not credited in shutdown margin calculations as contributing to shutdown margin.

(3) There is no reactivity transient possible with the control rod drives that would exceed the reactivity transient from a reactor pulse.

Nevertheless, methodology based on MATLAB SIMULINK in an RAI response by the DOW TRIGA reactor was implemented using NI LabVIEW Design and Simulation Suite (figure following) with minor modifications:

- Initial neutron generation time based on reactivity, (2)
- Specific heat capacity taken from *General Atomics E-117-833 The U-ZrHx Alloy: Its Properties and Use in TRIGA Fuel* – Simnad, 1980,
- LabVIEW implementation of Runge-Kutta as a variable time solver,
- Termination of rod withdrawal at scram, and
- Reactivity insertion as a ramp function.

Since the maximum historical control worth at the UTTRIGA was slightly more than $4, integral rod worth was used as $5. Scram time was set to occur at 60 seconds to avoid mitigating interaction. Control rod speeds were varied from 0.1% $Δk/k-s to 1.0% Δk/k-s in 0.1% increments.

The results are documented in *Analysis of the Neutronic and Thermal Hydraulic Performance of the University of Texas TRIGA Mark II Nuclear Research Reactor*, July 2015. As expected, peak power and peak temperature were bounded by maximum reactivity addition in pulsing analysis. Maximum fuel temperature for the fastest addition rate was 435°C at the maximum reactivity addition rate, below the scram setpoint.

(4) The specified technical parameters are documented in *Analysis of the Neutronic and Thermal Hydraulic Performance of the University of Texas TRIGA Mark II Nuclear Research Reactor*, July 2015.

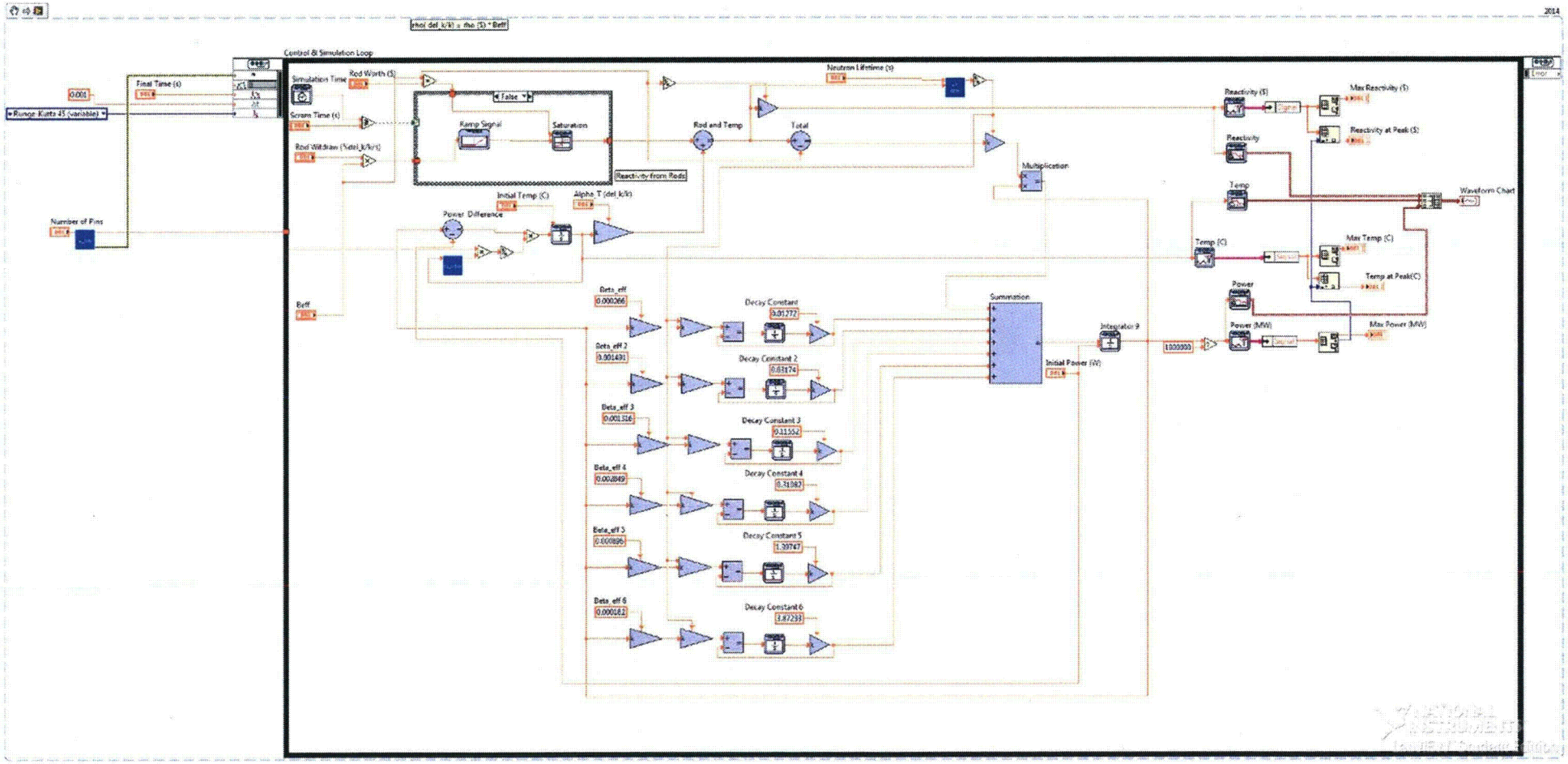
Control & Simulation Loop
Simulation Time
Rod Worth ($)
Scram Time (s)
Rod Withdraw (%del_k/k/s)
Ramp Signal
Saturation
Reactivity from Rods
Rod and Temp
Total
Neutron Lifetime (s)
Multiplication
Initial Temp (C)
Alpha_T (del_k/k)
Power Difference
Number of Fins
Final Time (s)
Runge Kutta 45 (variable)
Beff
Beta_eff
Beta_eff 2
Beta_eff 3
Beta_eff 4
Beta_eff 5
Beta_eff 6
Decay Constant
Decay Constant 2
Decay Constant 3
Decay Constant 4
Decay Constant 5
Decay Constant 6
Summation
Integration 9
Initial Power (W)
Reactivity ($)
Max Reactivity ($)
Reactivity at Peak ($)
Reactivity
Temp
Waveform Chart
Temp (C)
Max Temp (C)
Temp at Peak(C)
Power
Power (MW)
Max Power (MW)

RAI 13

UT SAR Section 4.5.4, Subsection C describes the use of the Bernath correlation which is typical for TRIGA analysis, but later UT SAR Section 4.6 states that the Biasi correlation is actually used for the evaluation of the DNBR. Please confirm that the Bernath correlation is used to characterize DNBR for UT TRIGA, or demonstrate the applicability of Biasi correlation to UT TRIGA analysis.

Response

Thermal hydraulic analysis was updated using the Bernath correlation and TRACE, see *Analysis of the Neutronic and Thermal Hydraulic Performance of the University of Texas TRIGA Mark II Nuclear Research Reactor*, July 2015.

RAI 14

The guidance in NUREG-1537 Section 4.5.2, "Reactor Core Physics Parameters," states that the supplied analysis should show that reactivity coefficients are sufficiently negative to prevent or mitigate any reactor transients. UT SAR Section 4.6 states, "Limits on reactivity are based not on the peak pulse power level, but on the final equilibrium power level associated with the reactivity." It also provides a series of statements on page 4-46 regarding pulse reactivity acceptability.

(1) The analysis provided in UT SAR, Section 4.6 is based upon Figure 4.21 which is said on page 4-34 (UT SAR) to display the fuel element reactivity coefficient. This figure does not display the fuel element reactivity coefficient. A version of this coefficient, believed to be from GA-7882, is displayed in Figure 4.2B. However, the applicability of this figure to UT TRIGA has not been established (e.g., there is no consideration of power level, burnup, etc.). Please provide clarification as to the relationship of the reactivity coefficient with the analysis provided in UT SAR Section 4.6.

(2) The basis for TS 3.2 "Pulsed Mode Operation," states that the reactivity limits are established so as to meet fuel temperature limits. However, this is inconsistent with the statements in UT SAR Section 4.6 as described above. Please revise the discussion in UT SAR Section 4.6 to support the UT TRIGA TS.

(3) UT SAR, Section 4.6 (p. 4-46) provides a series of statements regarding pulse reactivities and responses that are not supported by analyses. Please provide analysis supporting these statements in sufficient detail so that a confirmatory analysis can be performed.

Response

(1) The UTTRIGA fuel temperature coefficient was calculated in *Analysis of the Neutronic and Thermal Hydraulic Performance of the University of Texas TRIGA Mark II Nuclear Research Reactor*, July 2015, and used in analyses.

(2) The statement in Section 4.6 is incorrect, and will be revised to agree with the *Analysis of the Neutronic and Thermal Hydraulic Performance of the University of Texas TRIGA Mark II Nuclear Research Reactor*, July 2015.

(3) Section 4.6 will be revised to be consistent with See *Analysis of the Neutronic and Thermal Hydraulic Performance of the University of Texas TRIGA Mark II Nuclear Research Reactor*, July 2015.

RAI 15

The guidance in NUREG-1537 Section 4.6, "Thermal-Hydraulic Design," requests that the licensee provide information and analyses of thermal-hydraulic conditions in its reactor demonstrating that sufficient heat removal capacity exists for steady-state or pulsing operation at the maximum licensed power level. The fuel element and coolant conditions should be conservatively calculated, the DNBR correlation should be properly defined, and the resulting steady state DNBR at licensed power should be greater than 2.0.

(1) UT SAR Section 4.5.4 states that the TRACE analysis of the UT TRIGA DNBR used the Bernath correlation and determined that the DNBR is 5.9 for a 45 kW fuel element occurring at an elevation of 87 percent of the active fuel element height. However, typical analysis of TRIGA DNBR indicate that the power corresponding to DNBR of 1 is approximately 50 kW. Please review and revise these calculations, or provide the detailed results that confirm the calculated DNBR of UT TRIGA.

    Please describe the analytical methods used to determine the DNBR, including the core inlet and exit conditions assumed and other assumptions and correlations employed. This analysis should describe the parameters determined from the LCC such as peaking factors and limiting coolant inlet temperature and that the inlet temperature used for DNBR is a limiting value by showing how it corresponds to the primary pool water temperature measuring channel value.

(2) NUREG-1537, Section 4.6 describes that the licensee provide detailed "analyses for a pulsing reactor containing descriptions of the core configurations; the bases of the feedback coefficients; the calculational model and assumptions; the thermal-hydraulic evolution during a pulse; core, transient rod, and fuel characteristics that determine the shape and magnitude of a pulse; and the safety considerations that establish limits to pulse sizes." The UT SAR Appendix 4.1 provides a discussion of phenomenology; however, it does not demonstrate the acceptability of pulsing in UT TRIGA using parameters of importance that are demonstrated to be fully applicable to UT TRIGA.

    Please provide a comprehensive description of the calculational methods and the results that demonstrate the acceptability of design assumptions and TS for pulsing at UT TRIGA (e.g., the LCC, the approved power level, the pulse of reactivity inserted by the transient rod as allowed by TS, the value of the fuel temperature coefficient, the effective delayed neutron fraction, the prompt neutron lifetime, etc.). The analysis should demonstrate reactor overall behavior (e.g., power vs. time and fuel element temperature vs. time, etc.) and compliance of the leading fuel element in the LCC to safety limits (SL) as stated in the TS.

Response

(1) and (2) Sections 4.5 and 4.5 will be revised to be consistent with See *Analysis of the Neutronic and Thermal Hydraulic Performance of the University of Texas TRIGA Mark II Nuclear Research Reactor*, July 2015.

RAI 35

The guidance in ANSI/ANS-15.1-2007 Section 3, "Limiting conditions for operations," provides guidance and recommendations for the specifications pertaining to the limiting conditions for operation (LCO). This guidance is supplemented by NUREG-1537 Appendix 14.1. Some deficiencies and differences with the proposed UT TRIGA TS are described below. Please discuss these deficiencies and differences and revise accordingly.

(1) Section 3.1 of the guidance describes having specifications for fuel burnup, core configurations, and reactivity coefficients (if such coefficients establish required conditions). Such specifications are not present in the proposed UT TRIGA TS.

(2) Section 3.1 of the guidance describes that limits be placed on core excess reactivity and the corresponding regulatory interpretation includes provisions that account for experiment worth. Proposed UT TRIGA TS 3.1 "Core Reactivity," Specification A excludes consideration of experiments having positive reactivity.

(3) Section 3.1 of the guidance describes that limits be placed on the shutdown margin and states that this value "should be large enough to be readily determined experimentally, for example, ≥0.5% Δk/k or ≥0.50 dollar." Please provide an analysis and evaluation that demonstrates the ability to repeatedly measure core reactivity with sufficient accuracy to justify this small value of the shutdown margin.

(4) Section 3.2 of the guidance describes that a limit be established for the maximum control rod reactivity insertion rate for non-pulsed operation. The proposed UT TRIGA TS do not provide such a specification. This rate, and the control rod scram times, are typically justified through the analysis of an uncontrolled, control rod withdrawal transient.

(5) Section 3.2 of the guidance describes a specification for permitted bypassing of channels for checks, calibrations, maintenance, or measurements. Proposed UT TRIGA TS 3.3, "Measuring Channels," does not specify when it is permitted to bypass channels for checks, calibrations, maintenance or measurements.

(6) Proposed UT TRIGA TS 4.3 "Measuring Channels," contain Surveillance Requirements for the Fuel Temperature Channel and the Upper Level Radiation Monitor. However, there are no associated LCO specifications.

(7) Section 3.3 of the guidance describes specifications for leak or loss of coolant detection and a secondary coolant activity limit. No such specifications are found in the proposed UT TRIGA TS.

(8) Section 3.8.2 of the regulatory interpretations states that containers for experiments containing known explosive materials shall be designed such that the design pressure of the container is twice the pressure the experiment can potentially produce. Proposed UT TRIGA TS 3.6 "Limitations on Experiments," does not include such a specification.

Response

(1) No specified coefficients establish required conditions.

(2) In absolute terms, experiments with negative reactivity increase actual shutdown margin, but experiments with positive reactivity reduce actual shutdown margin. Experiments at UT are not credited in such a way as to reduce shutdown margin. This is conservative.

(3) Shutdown margin calculations are based on control rod reactivity worth. Control rod reactivity worth is based on a fit to a curve using data points from individual, independent measurements of time-dependent response to discrete control rod movements. Typical errors for individual data points in the curve fit are less than 1%, with a nominal maximum of 1-2% error.

Experience has shown reactivity balances to be repeatable a few cents of reactivity when considering comparable experiment configurations and burnup. Reactivity balance data for the first quarter of 2105 was collated and the data compared, including reactivity balance data (1) on sequential days of operation with shutdown periods long enough to allow significant xenon decay following power operations, and (2) sequential startups at low power where temperature was not a factor.

REACTIVITY BALANCE DATA, 1ST QUARTER 2015

DATE	$	Δ$
03/16/15	-0.50052	0.01297
03/13/15	-0.48755	
03/06/15	-0.19882	0.01454
03/04/15	-0.18428	
02/26/15	-0.53977	-0.01587
02/24/15	-0.55564	
02/19/15	-0.5396	0.02998
02/17/15	-0.50962	
02/12/15	-0.61461	0.02238
02/10/15	-0.59223	
02/03/15	-0.19229	0.00684
02/02/15	-0.18545	-0.02301
01/30/15	-0.20846	
01/26/15	-0.17187	0.01457
01/26/15	-0.1573	
01/16/15	-0.14302	0.03194
01/15/15	-0.11108	

Therefore the $0.29 limit, as currently approved for the UT TRIGA reactor, is appropriate.

(4) The "maximum control rod reactivity insertion rate for non-pulsed operation" and "control rod scram times" are not credited in analysis.

(5) Channels are not bypassed during operation for checks, calibration, maintenance or measurements. Automatic actions occur during pulse mode, including: (1) the gain of the NPP 1000 changes to capture the larger signal from the pulse, (2) the NP 1000 is bypassed, and (3) the NM 1000 is shifted a calibration mode (Mode 7). When exiting pulse mode these changes are automatically reversed.

(6) Fuel temperature has a limiting safety system setting which requires a measuring channel. The measuring channel has an operability requirement. Area radiation monitors are required to support personnel protection.

(7) The design of the secondary (chill water) coolant system is engineered to prevent pool to chill water leaks. Technical Specifications requires differential pressure that prevents such leakage. If the requirement is not met, Technical Specifications requires correction or shutdown and isolation of the chill water.

(8) The design and review occurs prior to operation. The design of experiments is incorporated in "Design Features," Section 5.4, "Experiments." Experiments that do not meet design requirements are not installed in the reactor, and are therefore not subject to limits on operations. The design features of experiments do not have surveillance requirements except as established though experiment approval (with the exception of reactivity limits) which is an administrative requirement. The Technical Specifications, Section 6.4 requires an experiment review, and the design criteria for encapsulation of known explosive material will be added to Section 5.4.

ATTACHMENT II

ANALYSIS OF NEUTRONIC (PART I) AND THERMAL HYDRAULIC (PART II) PERFORMANCE OF THE UNIVERSITY OF TEXAS TRIGA MARK II NUCLEAR RESEARCH REACTOR

LICENSE R-19

DOCKET 50-602

SUBMITTED TO THE NRC

IN SUPPORT OF THE UT TRIGA LICENSE RENEWAL

JULY 15, 2015

NEUTRONIC ANALYSIS OF THE UNIVERSITY OF TEXAS (UT) TRIGA REACTOR

TABLE OF CONTENTS

NEUTRONIC ANALYSIS OF THE UNIVERSITY OF TEXAS (UT) TRIGA REACTOR

LIST OF TABLES

NEUTRONIC ANALYSIS OF THE UNIVERSITY OF TEXAS (UT) TRIGA REACTOR

LIST OF FIGURES

THERMAL HYDRAULIC ANALYSIS OF THE UTTRIGA REACTOR

TABLE OF CONTENTS

THERMAL HYDRAULIC ANALYSIS OF THE UTTRIGA REACTOR

LIST OF TABLES

THERMAL HYDRAULIC ANALYSIS OF THE UTTRIGA REACTOR

LIST OF FIGURES

PART I

ANALYSIS OF NEUTRONIC PERFORMANCE OF THE UNIVERSITY OF TEXAS TRIGA MARK II NUCLEAR RESEARCH REACTOR

NEUTRONIC ANALYSIS OF THE UNIVERSITY OF TEXAS (UT) TRIGA REACTOR

1.0 Purpose and Discussion

Neutronic analysis evaluates operational characteristics of the reactor over the license term. Analysis is validated by benchmarking the model against historical performance from the initial core load to current values.

Analysis of the UT TRIGA reactor nuclear characteristics was performed using the SCALE code package[1], originally developed for the U.S. Nuclear Regulatory Commission, with some SCALE calculations supported by MCNP calculations. SCALE is an integration of codes in a plug and play framework that provides problem-specific calculations. SCALE includes deterministic and Monte Carlo radiation transport solvers, nuclear data libraries, and various computational and data-processing modules that process and integrate data shared between code routines and options.

Depletion and criticality calculations are performed for the UT TRIGA reactor. These calculations use the KENO Monte Carlo code for neutron transport, with the results of the KENO calculations used in ORIGEN for depletion/buildup calculations.

Fission and neutron absorption during reactor operation results in fissionable isotope depletion and buildup of transuranic isotopes and fission products. Depletion calculations (SCALE TRITON sequence) characterize material composition of the fuel from initial values to the composition at end of fuel life. Benchmarking is based on composition at specific core burnup values. The SCALE TRITON sequence requires multigroup cross-section libraries, which requires additional processing to correct for self-shielding.

Criticality calculations (CSAS6 sequence) are used to determine k_{eff} values for specific material compositions (with modifications by depletion calculations). The UTTRIGA SCALE model is configured to allow different control rod configurations; calculated k_{eff} values are used to determine excess reactivity and the integral (full-in to full-out) reactivity worth of individual control rods. The SCALE criticality sequence calculation can use either multigroup or continuous energy libraries, with continuous energy library calculations preferred.

Calculations of integrated neutroinc and thermal hydraulic performance required the use of data from TRACE, addressed separately.

2.0 SCALE MODEL

SCALE model development requires standardized input specifications for materials and physical geometry. The SCALE Standard Composition Library (SCL) defines material constants and isotopic composition for elements, specific mixtures, and compounds. The SCALE Generalized Geometry Package (SGGP) provides a standard method for developing a geometric model used in the sequences.

---

[1] *Scale: A Comprehensive Modeling and Simulation Suite for Nuclear Safety Analysis and Design*, ORNL/TM-2005/39, Version 6.1, June 2011 (ORNL Radiation Safety Information Computational Center, code CCC-785)

2.1 Materials

2.1.1 General

Material density in SCALE is based on standard material composition libraries, in units of either atomic density (atoms/cm^3 normalized to 1 barn), or mass density (g/cm^3). A user specified "density multiplier" adjusts from the standard library density to a non-standard specification. Standard composition library and density multiplier values for the UT TRIGA calculations are provided in Table 1.

SELF-SHIELDING CALCULATIONS

Neutron interaction is a function of material density and cross-section. The SCALE TRITON module is restricted to multigroup (energy-average) cross-sections, while the CSAS6 module is capable of using either multigroup or continuous energy cross-sections. Resonance self-shielding is not well characterized in multigroup calculations, and processing routines account for self-shielding. Flux varies spatially, and it is necessary that each material in each physical structure be uniquely identified for self-shielding correction routines. For example, although the cladding is essentially identical for all fuel elements, individual material specifications are required for each element to support self-shielding corrections. A single material specification is adequate for a continuous energy calculation.

Table 1: Material Specifications, Standard Composition Library Values

Material	ID	Density Multiplier	SCL Density	SCL Density Reference
Zirconium	1011-1127 alt. 1[2]	1	6.49	M8.2.2, Isotopes and Their natural Abundances
h2o[3]	2011-2127 alt. 2[1]	1	0.9982	M8.2.4, Compounds
ss304s[4]	311-427 alt. 3[1]	1	7.94	M8.2.5, Alloys and Mixtures
graphite	4	1	2.3	M8.2.4, Compounds
Aluminum	5	1	2.702	M8.2.2, Op. Cit.
dry-air[5]	6 alt. 6[1]	1	1.2E-3	M8.2.5, Alloys and Mixtures
h (h_2)	611-727	2.02E-3	1	M8.2.2, Op. Cit.
b4c	8	1	2.52	M8.2.4, Compounds
mo	9	1	10.2	M8.2.2, Op. Cit.
h-zrh2[6]	11-127	0.104-0.078	1	M8.2.3 Elements and Special nuclide Symbols
zr-zrh2	11-127	5.904-4.431	1	M8.2.3, Op. Cit.

[2] Continuous energy calculations; group energy libraries requires material specifications for resonance treatment
[3] Includes S(α,β) scattering kernels
[4] C (0.08%), Si (1.0%), P31 (0.045%), Cr (19.0%), Mn55 (2.0%), Fe (68.375%), Ni (9.5%)
[5] C (0.1026%), N14 (76.5081%), O16 (23.4793%)
[6] Hydrogen in zirconium hydride with S(α,β) thermal kernel

CORE MATERIAL LABELING

Unit cells are defined in all core positions where fuel might be used, consisting of the fuel element and contiguous spaces or structures. As noted above, self-shielding calculations require unique identification for every material in a geometric unit where self-shielding is important. Although zirconium, air, stainless steel, and water in and surrounding a fuel element can be represented by single material specifications in continuous energy calculations (material indices 1, 2, 3, and 6 respectively), multigroup calculations require unique specification for each material in each fuel element. For convenience, labels for materials in multigroup calculations are correlated with the fuel material identification in the element. For example, the element with fuel labeled as material 11 has zirconium fill rod material number 1011, water material number 2011, stainless steel material number 311, and hydrogen material number 611. Labeling is summarized in Table 1.

2.1.2 UZrH Densities

The initial of mass ^{235}U and ^{235}U-enrichment for each TRIGA fuel element received at the UT facility is documented in special nuclear material records to have a range of [redacted] grams of ^{235}U with enrichments ranging from 19.58% to slightly over 20%. Nominal value for TRIGA fuel uranium loading is 8.5%, but the mass in each fuel element but there is no specific assay value for (1) zirconium hydride mass, (2) actual fuel loading, or (3) total ZrH-U. There is no record of dimensional values for individual fuel elements, machined to fit cladding. Cladding is a commercially manufactured product with standardized engineering tolerances. Fuel expands slightly during reactor operation until it is well bonded to cladding, distributing mass across the available volume. Therefore nominal cladding dimensions are used to determine fuel volume, and nominal uranium loading to determine fuel mass.

The cladding of the fuel in fuel follower control rods is smaller than standard fuel elements, with correspondingly different volumes. The instrumented fuel element (IFE) configuration is machined to accommodate thermal couples in the fuel meat. IFE fuel volume is on the order of a few per-cent lower than standard fuel elements.

The UZrH fuel is manufactured as three [redacted] in ([redacted] cm) cylinders with a central [redacted] in ([redacted] cm) hole. After processing to increase hydride content, the central hole is filled with a zirconium rod. Outer diameter of a standard fuel element is [redacted] in ([redacted] cm), with the fuel follower diameter [redacted] in ([redacted] cm). The volume of the three fuel cylinders is given by equation 1:

$$V = L \cdot \pi \cdot \left(r_o^2 - r_i^2\right) \qquad 1$$

Where L is the total length ([redacted] cm), r_o is the outer radius, and r_i the inner radius. Standard fuel elements therefore have a volume of [redacted] cm^3, and FFCR fuel has a volume of [redacted] cm^3. However, the edges of the fuel are chamfered at a radius of [redacted] in ([redacted] cm), reducing the as-built volume slightly. Since (noted above) fuel expands during power operation the volume of the fuel is characterized as if the chamfers were not present.

Because of variation in composition (indicated above) and variation in fuel element power histories prior to use in the UT TRIGA located at the NETL (discussion to follow), fuel element materials were modeled for each element. Since assay values are available for the mass of ^{235}U and enrichment, ^{235}U and ^{238}U density is calculated directly as mass distributed over fuel volume. The SCALE standard library density for isotopes is 1 g/cm^3, the density multiplier therefore is the calculated density. The density of the

uranium 235 component in the fuel matrix is the mass (from assay value) distributed over the volume of the fuel, where the volume of the fuel is based on nominal dimensions (equation 2):

$$\rho_{235,Fuel} = \frac{m_{235}}{V_{Fuel}} \quad 2$$

The density of the uranium 238 component in the fuel matrix is determined by the ^{235}U mass and the enrichment (equation 3):

$$\rho_{238,Fuel} = \frac{\frac{m_{235}}{E_{235}} - m_{235}}{V_{Fuel}} \quad 3$$

Simnad[7] notes density of uranium of 19.07 g/cm^3, with the density of pure ZrH for H:Zr ratios 1.6 (ratio represented by X) or greater (equation 4):

$$\rho_{ZrH} = \frac{1}{0.1706 + 0.0042 \cdot X} \quad 4$$

For X=1.6, ρ_{ZrH}=5.640 g/cm^3; for X=1.7, ρ_{ZrH}=5.626 g/cm^3. Although the total mass of ZrH in each fuel element is not known explicitly, the ZrH density and volume in a fuel element can be used to determine the mass (equation 5).

$$m_{ZrH,Fuel} = \rho_{ZrH,Fuel} \cdot V_{Fuel} \quad 5$$

With the volume of the uranium distributed across the fuel element given by (equation 6):

$$V_U = \frac{m_U}{\rho_U} \quad 6$$

The mass of the ZrH in the fuel is calculated as (equation 7):

$$m_{ZrH,Fuel} = \rho_{ZrH} \cdot \left(V_{Fuel} - V_U\right) = \rho_{ZrH} \cdot \left(V_{Fuel} - \frac{m_U}{\rho_U}\right) \quad 7$$

Finally, the density of the ZrH distributed in the fuel element is given as (equation 8):

$$\frac{m_{ZrH,Fuel}}{V_{Fuel}} = \frac{\rho_{ZrH} \cdot \left(V_{Fuel} - V_U\right)}{V_{Fuel}} = \rho_{ZrH} \cdot \left(1 - \frac{m_U}{\rho_U \cdot V_{Fuel}}\right) \quad 8$$

The mass and enrichment of ^{235}U are known from assay, leading to density calculation (equation 9):

[7] *GA-117- 833 The U-ZrH Alloy: Its Properties and Use in TRIGA Fuel*, Simnad (1980)

$$\rho_{ZrH,Fuel} = \rho_{ZrH} \cdot \left(1 - \frac{m_{235}/E_{235}}{\rho_U \cdot V_{Fuel}}\right) \quad 9$$

Using ZrH ratio and assay values, the density of ZrH in the fuel matrix is calculated (equation 10a):

$$\rho_{ZrH,Fuel} = \frac{1}{0.1706 + 0.0042 \cdot X} \cdot \left(1 - \frac{m_{235}/E_{235}}{\rho_U \cdot V_{Fuel}}\right) \quad 10a$$

The mass ratios of Zr and H in ZrH are used to separate the density of the ZrH in the fuel matrix into components of Zr and H (equation 10b), where X represents the ratio of H to Zr:

$$\frac{91.224}{91.224 + X \cdot 1.00794} \text{ and } \frac{X \cdot 1.00794}{91.224 + X \cdot 1.00794} \quad 10b$$

Mass densities for 235U, 238U, ZrH, Zr, and H in fuel were calculated for individual fuel elements. However, groups of elements in the initial 1992 core were sufficiently similar in mass, enrichment, and burnup that the total number of material data sets was reduced from 87 to 40, discussion to follow.

2.1.3 Fission Product Density

The SCALE TRITON sequences automatically include specified fission product nuclides (in the ADDNUX subroutine) that will be tracked in coupled depletion (ORIGEN) and transport (KENO) calculations[8]. A large fraction of moderation in TRIGA reactors is attributed to hydrogen in the fuel. Scattering properties for hydrogen in zirconium hydride are substantially different than the elemental hydrogen and zirconium cross-sections. Therefore, hydrogen cross-sections in TRIGA fuel are specified as hydrogen in zirconium hydride (and zirconium specified as zirconium in zirconium hydride) with appropriate cross-section modification to simulate the UTTRIGA neutron physics. Some stable zirconium isotopes in TRIGA fuel are also high-yield fission products, which may not be well represented by the Zr in ZrH data. Isotope cross-sections can only be used once in ORIGEN so that using standard composition libraries for zirconium-hydride in conjunction with the zirconium implicitly included with ADDNUX will result in a fatal conflict in ORIGEN. It is therefore necessary to disable the automatic nuclide addition in SCALE depletion calculations with TRIGA fuel, and manually specify fission product nuclides that exclude stable zirconium fission products. Fission product contribution to total zirconium inventory is not large, and this approach is not expected to significantly affect calculations.

Table 2: Standard Added Nuclides

U-235	U-238	U-234	U-236	B-10	B-11	N-14	O-16	I-135
I-127	I-129	Np-237	Pu-238	Pu-239	Pu-240	Pu-241	Am-241	Cm-242
Pu-242	Am-243	Cm-243	Nb-93	Tc-99	Sn-126	Xe-131	Cs-133	Cs-134
Cs-135	Xe-135	Cs-137	Nd-143	Pr-143	Ce-144	Nd-145	Nd-146	Nd-147
Pm-147	Sm-147	Pm-148	Pm-149	Sm-149	Sm-150	Eu-151	Gd-152	Eu-153
Eu-154	Gd-154	Eu-155	Gd-155	Gd-156	Gd-157	Gd-158	Gd-160	Cm-244
Kr-83	Mo-95	Nd-148	Sm-151	Sm-152	Nb-95	Zr-95	Mo-97	Mo-98
Mo-99	Xe-133	La-139	Ba-140	Ce-141	Pr-141	Ce-142	Ce-143	Nd-144
Sm-153	Eu-156	Zr-93						

[8] SCALE Manual T1.3.7.5

The standard added nuclide sets in ADDNUX were developed for SCALE (Table 2) to represent the fission products with significant interaction probabilities. There are additional sets of fission product nuclides available to incrementally improve calculations, but calculations performed with the additional nuclides for both fresh core material composition and a heavily burned core showed insignificant absorption rates for the additional nuclides.

2.1.4 Control Rod Poison Density

The B_4C poison schematic (TOS2508226.C) specifies a minimum of 2.48 g/cm^3. Standard composition library density for B_4C is 2.52 g/cm^3. User specified density is therefore 98.4% of SCALE standard density.

2.2 GEOMETRY

2.2.1 General

SCALE geometry is based on nesting standard geometric shapes that contain standard materials, with complex geometries specified by excluding intersecting shapes. A collection of assembled geometric shapes is labeled as a "unit." SCALE standard geometries used in this model include cylinders (specified by radius, upper elevation, and lower elevation), hex-prisms (specified by the inner radius, upper elevation, and lower elevation), and truncated cones (specified by upper radius, upper elevation, lower radius, and lower elevation). Lattice structures are represented as specific geometric shapes positioned in an array format. The UTTRIGA model is displayed in Fig. 1a-1c, with graphite (reflector), water, and aluminum removed in Fig. 1c.

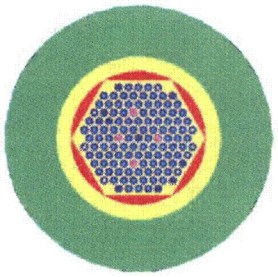

Figure 1a: Top View

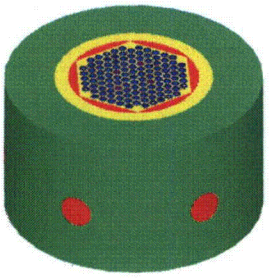

Fig 1b: Isometric

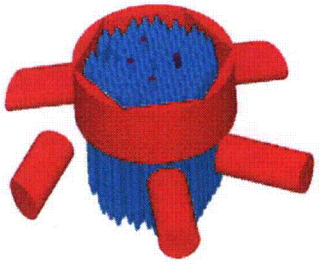

Fig 1c: Core and Air Spaces

2.2.2 Reflector and Core

The core volume is fabricated from an array of hexagonal-prism units (referred to as array or core positions), bounded by a hexagonal-prism extending from the top of the core to the bottom (representing the core shroud). Generally, each array unit includes a prism simulating the upper and lower aluminum grid plate, and a prism for the space between. Units that can be assigned to array positions include peripheral position units (simulating water and solid grid plates), fueled units, graphite rod units, water void units (simulating water and grid plates with penetrations), and the central thimble unit.

Sections of grid plate at the periphery of the core have no penetrations other than alignment holes and a set of small on-axis and radial holes that allow insertion of flux probes; these grid plate sections are

modeled as solid aluminum plates. Grid plate representations in peripheral positon are therefore solid structures, while other units have grid plate penetrations to accommodate fuel, graphite rods, water voids, or the central thimble. Grid plate unit geometry is provided in Table 3. Units with graphite dummy rods, control rods, or fuel elements are specified as the overall hexagonal structure in Table 3, modified to add graphite rods, control rods, or fuel to the central thimble.

Table 3: Unit Cell Structure, Geometry

Geometry	ID	Radius	Upper	Lower
Hexprism	30	2.177	32.309	-36.424
Hexprism	40	2.177	32.309	30.734
Cylinder	41	1.911	32.309	-36.424
Hexprism	50	2.177	-33.249	-36.424

2.2.3 Fuel Elements and Control Rods

Representation of fuel elements and control rods based principally on GA schematics T135210D210 (Fuel Element Assembly), T135210C212 (Reflector – Fuel Element), TOS210B229 (Disc), TOS210C232 (Cladding – Fueled Element), TOS210D213 (Fuel), TOS210B217 (Rod- Fuel Element), 21717-002 (Element Standard, [redacted], Standard Fuel Element assembly [redacted]), TOS250D225 (Control Rod – Fuel Follower), and TOS250B226 (Poison). A complete listing of fuel and control rod dimensions is provided in Table 4. Fuel elements are modeled as cylinders with conical shapes simulating top and bottom end fittings. Component dimensions from Table 3 were developed into unit specifications for fuel elements as indicated in Table 5.

Table 4: Component Dimensions

TYPE	COMPONENT	REFERENCE	Dia. (in.)	Dia. (cm)	Radius (cm)	Length (in.)	Length (cm)	Vol.[9] (cm^3)
FUEL	ZrH Fill Rod		[redacted]					
	FFCR ZrH-U	UT SAR 5/91 4-65						
	SFE ZrH-U	UT SAR 5/91 4-62						
GRAPH.	Lower graphite	T13210C212-1						
	Upper graphite	T13210C212-1						
Mo Disk	Mo Disk							
TR	AIR FLWR.	UT SAR 5/91 4-65						
CLAD	SFE (SS)	T135210D210						
	Inner	Outer less thickness						
	FFCR (SS)	UT SAR 5/91 4-65						
	Inner	Outer less thickness						
	TR (Al)	UT SAR 5/91 4-65						
	Inner	Outer less thickness						
POISON B_4C	FFCR B_4C	T0S2508226						
	TR B_4C	T0S2508226						

[9] Volume column values for fuel only
[10] Volume excludes zirconium "filler" rod
[11] [redacted]

FUEL ELEMENTS

GA schematic T135210C212 indicates the axial reflectors are [redacted] in ([redacted] cm) in diameter with length of [redacted] in ([redacted] cm) at the lower position and [redacted] in ([redacted] cm) in the upper position.

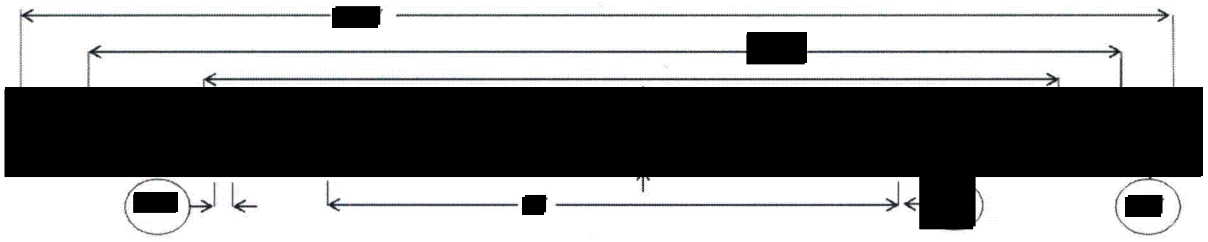

Figure
Figure 2: Standard Fuel Element

Table 5: Standard Fuel Element Unit Model

COMPONENT	Unit	Radius (cm)	Upper Z (cm)	Radius[12] (cm)	Lower Z (cm)	Excluded Units	Media
End fitting	60	[redacted]				na	3
Cladding	61					-62	3
Air Gap	62					-63 -64 -66 -67	6
Graphite	63					na	4
Fuel	64					-65	FUEL
Zr Fill Rod	65					na	1
Mo Disk	66					na	9
Graphite	67					na	6
End Fitting	68					na	3

FUEL FOLLOWER CONTROL RODS

The B_4C poison in TRIGA fuel follower control rods is manufactured to a diameter of [redacted] in. and length of [redacted] in. (drawing TOS2508226.C). Schematic values are used in analysis[13]. Fuel Follower Control rods are modeled as a set of cylinders (Table 6).

[redacted]

Figure 3: Fuel Follower Control Rod

[12] For truncated cones, with surfaces specifying an upper and a lower radius

[13] [redacted]

Table 6: Fuel Follower Control Rod Unit Model

COMPONENT	Unit	Radius (cm)	Upper Z (cm)	Lower Z (cm)	Length (in)	Length (cm)	media	
CLADDING (SS)	60	[redacted]					3 (SS)	60, 61-65, 67
(UPPER FIT)	--						--	
UPPER AIR	61						6 (Air)	61
(WELD)	--						--	
POS. AIR GAP	62						6 (Air)	62
POSION	63						7 (B4C)	63
WELD	--						--	
FUEL AIR GAP	64						6 (Air)	64
FUEL	65						FUEL	65 -66
ZIRC FILL ROD	66						1 (Zr)	66
(WELD)	--						--	
AIR FLLOWER (BOTTOM FIT)	67						6 (Air)	67

TRANSIENT (PULSE) ROD

The transient control rod is modeled as a set of cylinders (Table 7). The transient rod is protected by a guide tube. The guide tube surface has ½ in penetrations above the upper grid plate and below the lower grid plate to reduce the effects of fluid compression during operation (drawing T13S210D150). These penetrations were not modeled.

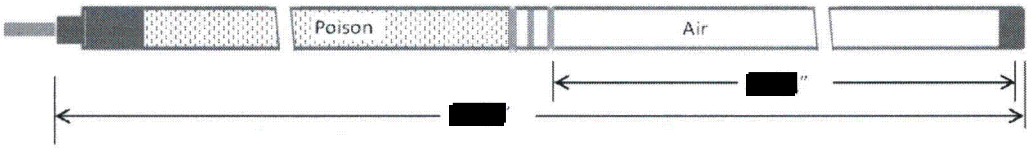

Figure 4: Transient Rod

Table 7: Transient Rod Unit Model

COMPONENT	Unit	Radius (cm)	Upper Z (cm)	Lower Z (cm)	Length (in.)	Length (cm)	media	
CLADDING (Al)	60	[redacted]					5 (Al)	60 -61 -63
(UPPER PLUG)	--						--	
Air at B4C	61						6 (Air)	61 -62
POSION	62						7 (B4C)	62
(weld)	--						--	
AIR FOLL.	63						6 (Air)	63
LOWER PLUG	--						--	

3.0 Calculations

Material composition of individual fuel elements vary in manufacturing (previously noted) and also from fission and transmutation during operation of the reactor. The neutron flux is not uniformly distributed across the core, so that co-irradiated individual fuel elements experience different burnups. Therefore

individual element composition was tracked according to the initial composition and specific core locations (Appendix 1) over core life to support model validation.

3.1 Initial Core

The UT TRIGA reactor became operational in 1992. Most of the initial core load was transferred from a previous UT TRIGA reactor located on the main campus.

3.1.1 Materials

For convenience, core positions (Fig. 5) are referred to as rings, labeled A (central thimble, CT) through G. The B ring is shaded green, C ring light blue-green, D ring rose, E ring light brown, F ring light blue, and the G ring yellow.

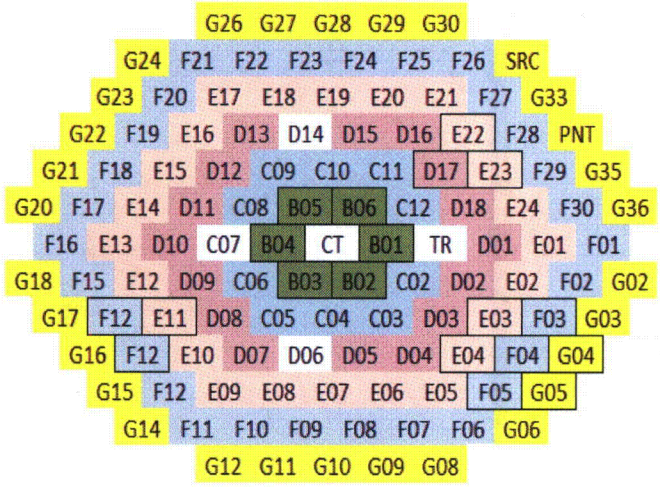

Figure 5: Core Positions

With the exception of elements in fuel followers (i.e., fuel follower control rods), the fuel elements in the initial core had prior burnup in other facilities. Most of the previously burned elements were used in the 250 kW TRIGA previously located on the main UT campus. A smaller set of fuel elements were manufactured more recently and irradiated in facilities that have higher rated power levels.

Burnup records for these previously irradiated elements include only total burnup (grams), with no information about the specific core configuration or location. Burnup records are based on a ratio of grams burned for each MWD, therefore the total burn (MWD) was determined as grams ^{235}U depleted divided by 1.05 g/MWD. Elements with operating history at the previous UTTRIGA were simulated as a burn at 250 kW for a time interval calculated as total burn (MWD) divided by 0.25 MW. A small quantity of lightly burned fuel was transferred from a GA TRIGA reactor and from a TRIGA reactor in Illinois. The Ill. TRIGA had a rated power of 1 MW. Some of the Ill. fuel had an initial H:Zr ratio of 1.7. All lightly-burned fuel elements decayed at least 1 year prior to use at the current UT TRIGA, and a 1-year decay intervals were included in burnup calculations.

In characterizing lightly burned fuel element composition for the initial core, similar elements were grouped (Table 8) based on ^{235}U loading, enrichment, and total burnup (MWD). Depletion calculations were performed on a single fuel element representative of each group to develop material data for subsequent calculations. Material data for these calculations for ^{235}U, ^{238}U, Zr, and H were formatted as

mass density while fission products (without stable zirconium isotopes) were introduced at an atom concentration of 1E-20 atom density (normalized to a barn), as recommended by the ORNL SCALE group (private communication). Mass densities (from the OPUS report module) for each representative element were used as materials for each fuel element in the "initial operational core".

Table 8: Summary, Initial Core Fuel Element Groups

GROUP	ELE.	POS.	g 235	W%	g 235 depl.	GROUP	ELE.	POS.	g 235	W%	g 235 depl.
A	6143	B-04	[redacted]	19.79	0.15		2983	F-26	[redacted]	20	0.69
B	5916	C-02	[redacted]	19.79	0.22		2979	F-25	[redacted]	20	0.69
C	5917	C-03	[redacted]	19.69	0.2	(M)	2983	F-26	[redacted]	20	0.69
D	5920	D-15	[redacted]	19.79	0.24		2906	E-06	[redacted]	20	0.69
	5921	B-01	[redacted]	19.79	0.24		2928	E-16	[redacted]	20	0.69
	5922	B-02	[redacted]	19.79	0.24		2932	E-19	[redacted]	20	0.69
	6886	B-05	[redacted]	19.69	0.24	N	2962	F-14	[redacted]	20	0.69
	6924	C-04	[redacted]	19.69	0.24		5283	B-06	[redacted]	20	0.69
	6926	C-05	[redacted]	19.69	0.24		2977	F-24	[redacted]	20	0.69
	6927	C-06	[redacted]	19.69	0.24		2974	F-21	[redacted]	20	0.69
	6928	C-08	[redacted]	19.69	0.24	O	2929	E-17	[redacted]	20	0.70
	6929	C-09	[redacted]	19.79	0.24		2950	F-05	[redacted]	20	0.70
	6930	C-10	[redacted]	19.69	0.24	P	2902	E-02	[redacted]	20	0.71
E	6889	C-11	[redacted]	19.69	0.24	Q	2905	E-05	[redacted]	20	0.72
	6932	C-12	[redacted]	19.69	0.24	R	2911	E-09	[redacted]	20	0.73
	5912	D-08	[redacted]	19.79	0.24		2912	E-10	[redacted]	20	0.71
	5913	D-09	[redacted]	19.79	0.24		2915	E-12	[redacted]	20	0.71
	5914	D-10	[redacted]	19.79	0.24	S	2918	E-13	[redacted]	20	0.71
	5915	D-11	[redacted]	19.79	0.24		2946	F-02	[redacted]	20	0.71
	5918	D-12	[redacted]	19.69	0.24		2969	F-18	[redacted]	20	0.71
	5919	D-13	[redacted]	19.79	0.24		2947	F-03	[redacted]	20	0.72
	6923	D-17	[redacted]	19.69	0.24	T	2975	F-22	[redacted]	20	0.72
	6925	D-18	[redacted]	19.79	0.24		2955	F-09	[redacted]	20	0.72
	5981	B-03	[redacted]	19.90	0.29	U	2940	E-23	[redacted]	20	0.72
F	6142	D-16	[redacted]	19.79	0.29		2971	F-20	[redacted]	20	0.72
	5904	D-07	[redacted]	19.79	0.3		2913	E-11	[redacted]	20	0.73
G	5902	D-04	[redacted]	19.79	0.31		2927	E-15	[redacted]	20	0.73
	5903	D-05	[redacted]	19.90	0.31		2930	E-18	[redacted]	20	0.73
	5844	D-01	[redacted]	19.79	0.32		2935	E-20	[redacted]	20	0.73
H	5845	D-02	[redacted]	19.79	0.32	V	2938	E-21	[redacted]	20	0.73
	5846	D-03	[redacted]	19.79	0.32		2954	F-08	[redacted]	20	0.73
I	2984	F-27	[redacted]	20	0.66		2957	F-10	[redacted]	20	0.73
J	2985	F-28	[redacted]	20	0.67		2968	F-17	[redacted]	20	0.73
K	2899	E-01	[redacted]	20	0.68		2970	F-19	[redacted]	20	0.73

Table 8: Summary, Initial Core Fuel Element Groups

GROUP	ELE.	POS.	g 235	W%	g 235 depl.	GROUP	ELE.	POS.	g 235	W%	g 235 depl.
L	2965	F-16	[redacted]	20	0.68	W	2908	E-07	[redacted]	20	0.74
	2910	E-08		20	0.68		2948	F-04		20	0.74
	2939	E-22		20	0.68		2960	F-13		20	0.74
	2959	F-12		20	0.68		2976	F-23		20	0.74
	2964	F-15		20	0.68	X	2903	E-03		20	0.75
M	2925	E-14		20	0.69	Y	2952	F-07		20	0.77
	2941	E-24		20	0.69	Z	2904	E-04		20	0.78
	2944	F-01		20	0.69	AA	3513	F-30		19.6	0.99
	2979	F-25		20	0.69	AB	5198	F-29		19.6	4.93

3.1.2 Initial Startup

Initial criticality for the UT TRIGA reactor at the Nuclear Engineering Teaching Laboratory (NETL) was accomplished on 02/13/1992. Criticality was attained with 3 fuel follower control rods (control element fully withdrawn, fuel fully inserted) and 56 standard fuel elements (including two instrumented fuel elements). Total mass of ^{235}U was [redacted] in the standard fuel elements and [redacted] in the three fuel followers. Critical fuel loading is displayed (Fig. 6) with labels:

- CT for the central thimble (water void)
- SFE for standard fuel rods
- TC for instrumented fuel elements
- GR for graphite rods
- S for the neutron source
- WV for water voids
- S2, S1 and RR for the fuel follower control rods (Shim 1 and 2, Regulating Rod)
- TR for the transient rod

A direct comparison between critical masses of the initial 1992 UT TRIGA core and the historical GA TRIGA cores is complicated by (1) differences in reflection, i.e. graphite rod and water void configurations, (2) prior power history for the UT TRIGA fuel elements, and (3) fundamental difference in core geometry. Nevertheless, the [redacted] ^{235}U in the UT TRIGA compares well with the [redacted] (approximately [redacted] water moderated) of fresh elements required in the prototypical GA TRIGA reactor.

3.1.3 Operational Loading

Fuel was loaded in the UT TRIGA reactor to support operation at 1.1 MW on 03/16/1992. The core contained 84 standard and 3 fuel follower elements (Fig. 7, labeling consistent with Fig. 6) with [redacted] kg ^{235}U. As previously noted, all the standard fuel elements in this configuration had prior power history, with 7.91 MWD generated at the UT Taylor Hall facility in 46 elements, and 41.07 MWD generated at General Atomics facilities in 56 elements; 15 fuel elements had operating history in the reactors at both The University of Texas at Austin TRIGA and General Atomics reactors.

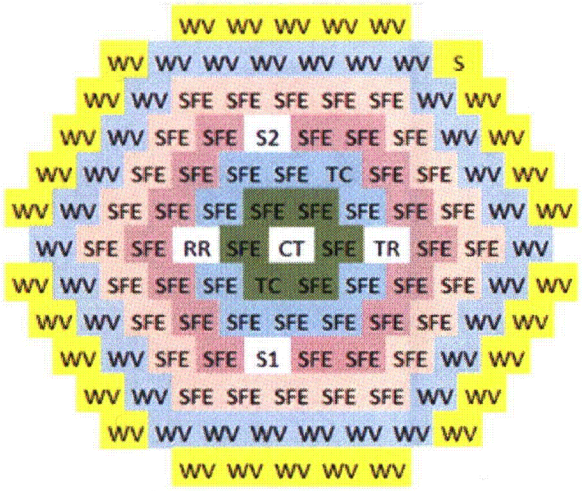

Figure 6: Initial Criticality

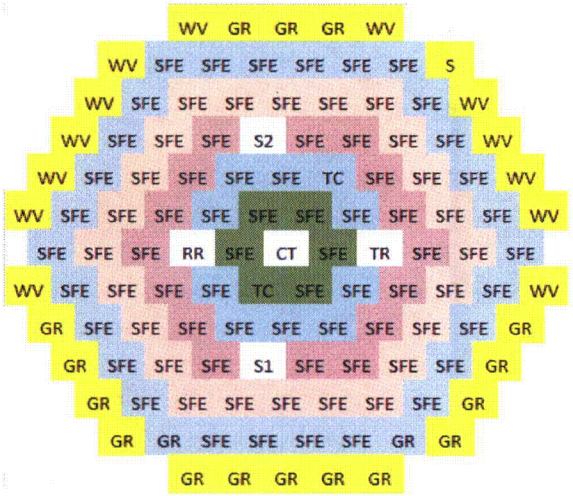

Figure 7: Operational 1992 Core

The initial operational core configuration existed from 01/28/92-03/16/92, with few configuration changes (principally changes in IFE configuration). Major changes to core configurations over the NETL TRIGA operating history (since 1992) include:

- Instrumented Fuel Element (IFE) relocation and replacement
- Insertion and removal of a three-element in-core experiment facility (D17, E22 and E23)
- Fuel insertions and movements to compensate for burnup
- Reflector changes (potential reactivity effects, although not a core change as defined)
    - Beam port and reflector flooding
    - Reflector replacement
- Comprehensive core reconstitution following reflector replacement
- Insertion and removal of a second 3-element in-core experiment (E11, F13, F14), and
- Insertion and removal of a seven- element in-core experiment facility (E03, E04, F03, F04, F05, G04, G05).

3.2 Configuration Changes Over Core Life

Instrumented fuel elements were moved or replaced 4 times between 1992 and 1998. The original three-element facility was installed for various operating periods between 1992 and 2001. Three-element facility installation required fuel movement from the core position to alternate locations with additional fuel added to compensate for the reactivity loss from displaced fuel. (Operating periods for experiment facilities range from days to several months, based on experiment needs.)

Table 9 provides a summary of information applicable to each configuration along with the date the configuration was established, the range of dates for which the configuration was active, the number of fuel elements in the configuration, experiment facilities in use, and the total burnup for the configuration. Note that prior to reflector replacement in 2004 there were only two configurations that did not use the intermittently installed three-element experiment facility, and dates for these configurations consequently overlap. After reflector replacement, the experiment facility positions were configured and left in place even when an experiment was not being performed, and experiment configurations after reflector replacement were not intermittent over short periods.

Reflector deformation was observed in 2002 from an apparent increase in internal pressure caused by water intrusion, which lead to beam port flooding. The reflector was intentionally flooded, then replaced in 2004. An attempt was made to model flooding as water in the reflector and beam port air filled spaces. The start date for simulating flooded spaces is a best estimate, not precise. As part of the reflector replacement, new core grid plates were designed incorporating two additional facilities, a three-element facility (in a lower reactivity-worth location) and a seven-element facility (at the core periphery). The new three-element facility has been used through several operating periods since 2004, and the seven element facility during one extended operational period.

Changes in core configuration were generally conducted in conjunction with fuel inspection or periodic maintenance outages. Fuel inspection and core reconfigurations occurred in 2002, 2004 (associated with the reflector replacement), 2005, 2006 (multiple times) and 2007.

This complex operating history was modeled as core configurations operated over discrete intervals. Fuel movement logs at the beginning of each configuration were used to identify which elements were located in core positions at the start of the configuration. Burnup for all operations was simplified as a single interval for which configuration was constant. When alternating configurations existed for periods during which an experiment facility was intermittently used, the burnup that occurred in each configuration was evaluated. Some configuration dates overlap as alternating positions were used to support experiment facility utilization.

During each burnup interval, operations occurred at a wide variety of power levels up to a maximum nominal power level of 950 kW. A T-6 SCALE depletion calculation was performed with a fuel temperature of 600°C for each configuration to develop a material data set (^{235}U, ^{238}U, and fission products) representative of fuel element composition at the end of each burnup interval. Lightly burned fuel elements were depleted in separate calculations (to develop a material data set based on initial assay and burnup data) prior to UT TRIGA burnup calculations.

Table 9: Core Configurations and Burnup

Configuration Date	Dates Active	No. of Elements	Installed Facilities	Core Burnup (MWD)	Acc. Burnup (MWD)
03/16/1992	1992-1999	87	Fully Fueled	31.07	31.07
03/04/1999	1999	90	3EL(A) CD	0.24	31.31
04/27/2000	2000-2001	89	Fully Fueled; Refl. flood	5.51	36.82
06/29/2000	2000-2001	92	3EL(A)	8.90	45.72
07/22/2002	2001-2002	95	3EL(A)	35.47	81.19
11/22/2002	2002-2004	103	3EL(A)	24.93	106.12
07/15/2004	2004-2005	102	3EL(B)); New Refl.	15.70	121.82
07/13/2005	2005-2007	104	3EL(B	64.71	186.53
07/24/2007	2007-2008	108	3EL(B)	18.35	204.88
06/11/2008	2008-2009	110	7EL(B)	21.29	226.17
06/23/2010	2010-2014	114	3EL(B)	52.88	279.05

Depletion sequence calculations assumed a constant power level over the time interval for the configuration (Table 10). Since the initial 3-element facility was used intermittently, time intervals prior to 2004 are a best estimate based on records of daily power history and core data. The last step in each depletion calculation is a 7-day decay time to assure minimal xenon poisoning in criticality calculations.

Table 10: T-6 Burn Parameters

CORE	START	END	MWD	DAYS	AVE PWR
87	03/16/92	10/26/99	31.07	2780	0.0112
90	03/04/99	10/26/99	0.24	236	0.2500
89	04/27/00	01/31/01	5.51	279	0.0197
92	06/29/00	07/18/01	8.90	384	0.0232
95	07/22/02	11/07/02	35.47	108	0.3284
103	11/22/02	03/17/04	24.93	481	0.0518
102	07/15/04	06/30/05	15.70	350	0.0449
104	07/13/05	07/02/07	64.71	719	0.0900
108	07/24/07	06/04/08	18.35	316	0.0581
110	06/11/08	06/14/10	21.29	733	0.0290
114	06/23/10	07/25/11	11.90	397	0.0300
114	06/23/10	08/02/12	24.54	771	0.0318
114	06/23/10	10/14/14	52.88	1574	0.0336

3.3 Reactivity Calculations

The UTTRIGA was modeled in SCALE as previously described. Calculations with SCALE were compared to integral control rod worth data.

3.3.1 SCALE Calculations

UT TRIGA criticality calculations using the CSAS6 sequence are based on the same model and material composition as the SCALE T6 depletion calculations, except for lattice cell data (not required for continuous energy libraries). Modifications of the SCALE input to adapt the depletion calculations to support criticality calculations include:

- Specifying continuous energy libraries
- Removing depletion-specific parameters (lattice data, burndata, OPUS
- Revising unit materials to single identification for non-fuel materials (since self-shielding calculations are not required for continuous energy library data)
- Simulating clean critical calculations with fuel temperatures of 300°C
- Developing fresh and burned fuel and fission product material files for each configuration
- For the current configuration, developing material data at intervals corresponding to control rod worth calibration data

The initial CASAS6 file (as modified) simulates all rods fully withdrawn. Four additional calculations are performed, with a single control rod inserted for each calculation (regulating rod, shim 1, shim 2, and the transient rod). Where β is the effective delayed neutron fraction, k_{ARO} is k_{eff} (transport calculation) with all control rods out, and k_{RiO} is k_{eff} with control rod *i* out:

- Excess reactivity with all control rods removed is calculated as:

$$\$ = \left(\frac{\Delta k}{k}\right) \div \beta = \frac{k_{ARO} - 1}{k_{ARO}} \div \beta \qquad 11$$

- Total integral control rod worth (with a single control rod inserted) is calculated as:

$$\$ = \left(\frac{\Delta k}{k}\right) \div \beta = \frac{k_{ARO} - k_{R_iO}}{k_{ARO} \cdot k_{R_iO}} \div \beta \qquad 12$$

Table 11: Calculated Reactivity Values

CORE	DATE	MWD	RR	±	SH1	±	SH2	±	TR	±	EXCESS	±
87	03/16/92	0	$3.57	0.010	$2.52	0.010	$2.90	0.010	$3.06	0.010	$9.20	0.018
87	10/26/99	31.07	$3.79	0.012	$3.21	0.011	$3.10	0.012	$2.96	0.012	$7.88	0.017
90	03/04/99	31.07	$4.58	0.013	$4.09	0.013	$2.94	0.014	$2.56	0.014	$7.60	0.016
90	10/26/99	31.31	$4.09	0.013	$2.85	0.013	$2.03	0.013	$2.25	0.014	$7.00	0.017
89	04/27/00	31.31	$4.17	0.013	$3.18	0.012	$2.26	0.012	$2.63	0.012	$8.04	0.016
89	01/31/01	36.82	$3.82	0.012	$2.88	0.012	$2.31	0.011	$2.81	0.011	$6.31	0.014
92	06/29/00	36.82	$4.92	0.014	$3.31	0.015	$2.40	0.015	$1.87	0.015	$7.46	0.015
92	07/18/01	36.82	$4.16	0.013	$2.95	0.012	$2.86	0.012	$2.16	0.013	$7.18	0.015
95	07/22/02	45.72	$4.55	0.015	$3.58	0.014	$2.67	0.014	$1.61	0.013	$7.02	0.015
95	11/07/02	81.19	$4.46	0.015	$3.48	0.014	$2.68	0.014	$1.31	0.014	$6.11	0.015
103	11/22/02	81.19	$3.90	0.011	$2.78	0.011	$3.37	0.012	$2.62	0.011	$7.36	0.014
103	03/17/04	106.12	$3.95	0.012	$2.48	0.012	$3.08	0.013	$1.63	0.012	$3.89	0.009

Table 11: Calculated Reactivity Values

CORE	DATE	MWD	RR	±	SH1	±	SH2	±	TR	±	EXCESS	±
102	07/15/04	106.12	$3.26	0.010	$3.45	0.010	$2.38	0.010	$3.02	0.010	$6.56	0.014
102	06/30/05	121.82	$3.12	0.009	$3.35	0.010	$3.24	0.009	$3.32	0.010	$8.42	0.018
104	07/13/05	121.82	$3.75	0.012	$3.22	0.011	$2.97	0.011	$2.81	0.012	$8.87	0.018
104	07/02/07	186.53	$3.27	0.003	$3.18	0.007	$2.62	0.007	$2.86	0.008	$7.64	0.005
108	07/24/07	186.53	$2.51	0.008	$1.46	0.008	$3.10	0.008	$2.30	0.008	$7.72	0.017
108	06/04/08	204.88	$3.25	0.010	$2.06	0.011	$2.66	0.010	$2.25	0.010	$7.70	0.017
110	06/11/08	204.88	$4.33	0.004	$2.49	0.004	$2.95	0.004	$1.85	0.004	$8.06	0.005
110	06/14/10	226.17	$4.09	0.004	$2.74	0.004	$2.74	0.004	$1.83	0.004	$7.54	0.005
114	06/23/10	226.17	$2.79	0.002	$2.39	0.003	$2.60	0.003	$2.52	0.003	$8.50	0.005
114	07/25/11	237.26	$3.11	0.002	$2.43	0.002	$2.67	0.002	$2.37	0.002	$8.33	0.002
114	08/02/12	250.7	$3.20	0.003	$2.43	0.003	$2.81	0.003	$2.60	0.003	$8.28	0.005
114	10/14/14	261.79	$2.41	0.004	$2.05	0.004	$2.74	0.004	$2.43	0.003	$5.38	0.006

3.3.2 Reactivity Measurements

Control rod calibrations are performed experimentally under surveillance procedure SURV-6, and excess reactivity determinations are documented with SURV 3 (Table 12). Control rod installation began 1/28/1992, and standard core fuel loading began 2/10/1992. The initial control rod reactivity worth calibration was completed on 03/31/1992, although excess reactivity was not determined until completion of initial testing in July when both SURV-3 and SURV-6 were performed.

Table 12: Reactivity Surveillance Data

DATE	MWD	Excess	RR	SH1	SH2	TR
07/01/92	0.00	$5.57	$4.08	$3.03	$3.17	$3.26
08/10/93	3.98	$5.61	$3.97	$3.00	$3.18	$3.24
10/25/94	6.44	$5.56	$3.99	$2.93	$3.19	$3.21
08/10/95	8.70	$5.46	$4.02	$2.98	$3.18	$3.21
03/05/96	9.65	$5.48	$4.02	$2.98	$3.18	$3.21
07/23/96	10.62	$5.50	$4.02	$2.98	$3.18	$3.27
01/29/97	11.73	$5.49	$4.02	$2.98	$3.18	$3.27
09/11/97	12.79	$5.44	$4.08	$3.00	$3.18	$3.22
01/23/98	14.48	$5.40	$4.08	$3.00	$3.18	$3.22
07/23/98	17.97	$5.40	$4.06	$3.06	$3.20	$3.23
07/02/99	26.00	$5.00	$4.05	$3.01	$3.22	$3.23
04/27/00	31.31	$5.53	$4.50	$3.48	$2.73	$2.36
06/30/00	34.76	$4.56	$4.50	$3.48	$2.73	$2.36
09/07/00	34.91	$5.50	$3.90	$3.02	$3.24	$3.17
07/30/01	45.81	$4.59	$4.19	$3.24	$2.94	$2.41
07/24/02	67.32	$4.09	$4.08	$3.16	$2.84	$2.47
11/14/02	81.29	$5.69	$4.30	$3.34	$2.75	$2.51
07/24/03	90.33	$5.20	$3.88	$3.31	$2.74	$2.46
07/29/04	106.23	$5.77	$3.33	$2.78	$3.25	$3.33

Table 12: Reactivity Surveillance Data

DATE	MWD	Excess	RR	SH1	SH2	TR
07/18/05	121.93	$5.55	$3.07	$2.94	$3.14	$3.28
07/19/06	145.21	$4.97	$3.09	$2.89	$3.02	$3.29
01/25/07	165.51	$4.47	$3.09	$2.89	$3.02	$3.29
07/25/07	186.65	$5.04	$2.84	$2.75	$3.30	$3.32
06/19/08	205.04	$4.45	$3.65	$2.35	$3.27	$2.04
06/25/09	214.05	$4.75	$3.99	$2.45	$3.36	$2.04
06/29/10	226.30	$5.79	$2.90	$2.54	$3.11	$3.14
06/29/11	236.82	$5.56	$2.83	$2.52	$3.07	$3.01
07/13/12	260.14	$4.83	$2.76	$2.47	$3.01	$3.04
07/16/13	281.57	$4.20	$2.75	$2.45	$2.91	$3.00
07/22/14	286.66	$4.70	$2.50	$2.74	$3.15	$3.17

3.3.3 Reactivity Calculations and Reactivity Surveillance Data

Excess reactivity was calculated using k_{eff} data with all rods fully withdrawn, and independently using the k_{eff} data from all rods fully inserted and the integral rod worth for each control rod.

$$SDM = \delta k_{ARI} + \sum_{i=1,4} \delta k_{RiO} \qquad 13$$

The limiting shutdown margin does not credit the most reactive control rod, and is therefore calculated as:

$$SDM = \delta k_{ARI} + \sum_{i=1,4} \delta k_{RiO} - \delta k_{R,max} \qquad 14$$

INTEGRAL CONTROL ROD WORTH COMPARISONS

Reactivity measurements and core configuration changes do not have a one-to-one correspondence. Calculated values and measured reactivity values were therefore compared based on burnup values (CORE, MWD and MEAS, MWD respectively) assumed in calculations and the burnup values corresponding to measured data between the start and end of the core configuration, indicated in Table 13, "CORE" column.

Table 13, Comparison of Reactivity Calculations to Surveillance Data

CORE (CALC)	MWD (CALC)	DATE	Burnup (MEAS)		Control Rod Worth					EXCESS
			MWD	ΔMWD	RR	SH1	SH2	TR	SUM	B
87	0	07/01/92	0.00	0.00	12.5%	16.7%	8.5%	6.2%	11.0%	-65.1%
		08/10/93	3.98	3.98	10.1%	15.9%	8.8%	5.6%	10.0%	-63.9%
		10/25/94	6.44	6.44	10.5%	13.9%	9.1%	4.8%	9.5%	-65.4%
		08/10/95	8.70	8.70	11.2%	15.3%	8.8%	4.8%	10.0%	-68.4%
		03/05/96	9.65	9.65	11.2%	15.3%	8.8%	4.8%	10.0%	-67.8%
		07/23/96	10.62	10.62	11.2%	15.3%	8.8%	6.5%	10.4%	-67.2%

Table 13, Comparison of Reactivity Calculations to Surveillance Data

CORE (CALC)	MWD (CALC)	DATE	Burnup (MEAS)		Control Rod Worth					EXCESS
			MWD	ΔMWD	RR	SH1	SH2	TR	SUM	B
		01/29/97	11.73	11.73	11.2%	15.3%	8.8%	6.5%	10.4%	-67.5%
		09/11/97	12.79	12.79	12.5%	15.9%	8.8%	5.1%	10.6%	-69.0%
		01/23/98	14.48	14.48	12.5%	15.9%	8.8%	5.1%	10.6%	-70.3%
		07/23/98	17.97	17.97	12.1%	17.6%	9.4%	5.3%	11.1%	-70.3%
		07/02/99	26.00	26.00	11.9%	16.2%	9.9%	5.3%	10.8%	-83.9%
89	31.31	04/27/00	31.31	0.00	7.3%	8.7%	17.1%	-11.6%	6.3%	-45.3%
		06/30/00	34.76	3.45	7.3%	8.7%	17.1%	-11.6%	6.3%	-76.2%
		09/07/00	34.91	3.60	-7.0%	-5.2%	30.1%	16.9%	8.1%	-46.1%
92	36.82	07/30/01	45.81	8.99	0.8%	9.0%	2.9%	10.4%	5.2%	-56.4%
95	45.72	07/24/02	67.32	21.60	-11.6%	-13.3%	5.9%	34.9%	1.1%	-71.7%
95	81.19	11/07/02	81.29	35.57	-3.7%	-4.1%	2.5%	47.9%	7.5%	-7.4%
103	81.19	07/24/03	90.33	9.14	-0.5%	16.0%	-23.1%	-6.5%	-2.3%	-41.5%
102	106.12	07/29/04	106.23	0.11	2.0%	-24.2%	26.7%	9.4%	4.5%	-13.6%
104	121.82	07/18/05	121.93	0.11	-22.0%	-9.4%	5.5%	14.3%	-2.5%	-59.8%
		07/19/06	145.21	23.39	-21.2%	-11.3%	1.7%	14.6%	-3.7%	-78.5%
		01/25/07	165.51	43.69	-21.2%	-11.3%	1.7%	14.6%	-3.7%	-98.4%
108	186.53	07/25/07	186.65	0.12	11.5%	46.9%	6.1%	30.7%	23.2%	-53.1%
110	204.88	06/19/08	205.04	0.16	-18.7%	-6.1%	9.8%	9.4%	-2.8%	-81.2%
	204.88	06/25/09	214.05	9.17	-8.6%	-1.8%	12.2%	9.4%	1.8%	-69.8%
114	226.30	06/29/11	236.82	10.52	-9.9%	3.5%	13.1%	21.1%	7.4%	-49.9%
114	237.26	07/13/12	260.14	22.88	-10.1%	3.6%	13.4%	20.9%	7.5%	-57.4%
114	261.79	07/13/12	260.14	-1.65	12.7%	16.8%	9.0%	20.0%	14.6%	-11.3%
		07/16/13	281.57	19.78	12.4%	16.1%	5.9%	18.9%	13.3%	-28.0%
		07/22/14	286.66	24.87	3.6%	25.0%	13.0%	23.3%	16.6%	-14.4%

The difference between the burnup assumed in calculation and the burnup associated with the measurement is also noted (ΔMWD). For deviation in excess reactivity, calculations were made based on all rods fully withdrawn (column label Excess - A) and independently balancing the reactivity for all rods fully inserted against the sum of the integral worth of all control rods (column label Excess - B). The deviation (ε) of the calculated reactivity values (ρ_{rod}^{calc}) from the surveillance data (ρ_{rod}^{meas})was calculated in Table 13 as:

$$\varepsilon = \frac{\rho_{rod}^{meas} - \rho_{rod}^{calc}}{\rho_{rod}^{meas}} \qquad 15$$

As previously noted, configurations with 3 element facilities usage prior to the 102 core involved intermittent configuration changes, but were approximated as a single burnup interval for calculations. The reflector and beam ports partially flooded prior to the 102 configuration then intentionally flooded to stabilize internal reflector pressure. A new reflector and grid plate were installed prior to establishing the 102 element configuration. The calculation for the current core configuration was conducted at three burnup values, corresponding to surveillance data. Although the regulating rod error is higher than desired, the total integrated rod worth matches surveillance data well and the calculated values for

the regulating rod exceed the values in surveillance data. Therefore calculation of the limiting shutdown margin (with the most reactive rod fully withdrawn) is conservative.

3.4 Fuel Temperature

Observations of current core operation in 2015 (Table 14) provides fuel temperature associated with the instrumented fuel elements (in core positions B03 and B06) and reactivity data, correlated to operation at specific core power levels.

Table 14: Observed Data

CORE PWR	Fuel Temp 1 B03		Fuel Temp 2 B06		REACTIVITY INSERTED
kW	°C	°K	°C	°K	
1	21	294	21	294	$7.72
100	84	357	91	364	$8.07
250	159	432	173	446	$8.62
500	243	516	263	536	$9.46
750	300	573	320	593	$10.04
950	340	613	363	636	$10.41

Core peaking factors are developed from SCALE physics calculations. Fuel temperatures as a function of element power is developed from TRACE thermal hydraulic calculation data. An average fuel element temperature is developed from core peaking factors (that characterize the fraction of core power in the element) and the average fuel element temperature associated with the element power.

3.4.2 SCALE and TRACE Calculations for Power Distribution

SCALE calculations were performed to determine the fission distribution across all elements in the core (Fig. 8). The distribution across elements is used to calculate the power produced in individual elements. The distribution within a fuel element is used as input to thermal hydraulic calculations to determine the radial and axial power profile. The distribution within a fuel element is 2-dimensional. The fuel element geometry is segmented into equal volume partitions, but variation along single axis at selected locations are provided in Fig. 9 and 10.

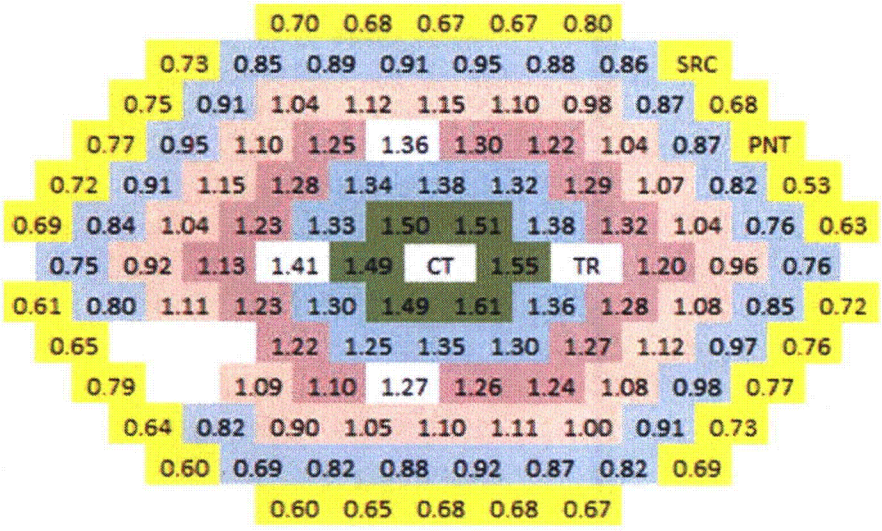

Figure 8: 114 Core Peaking Factors

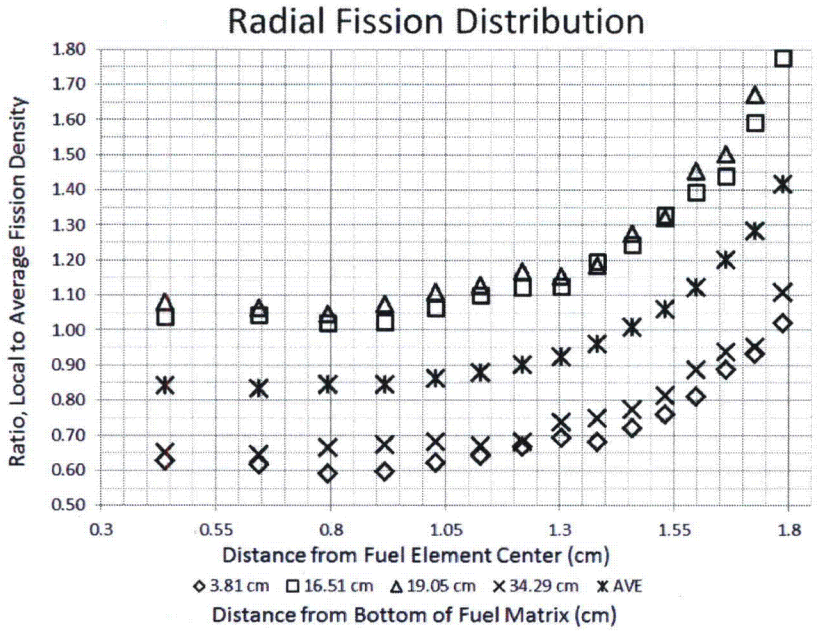

Figure 9: Radial Peaking Factor

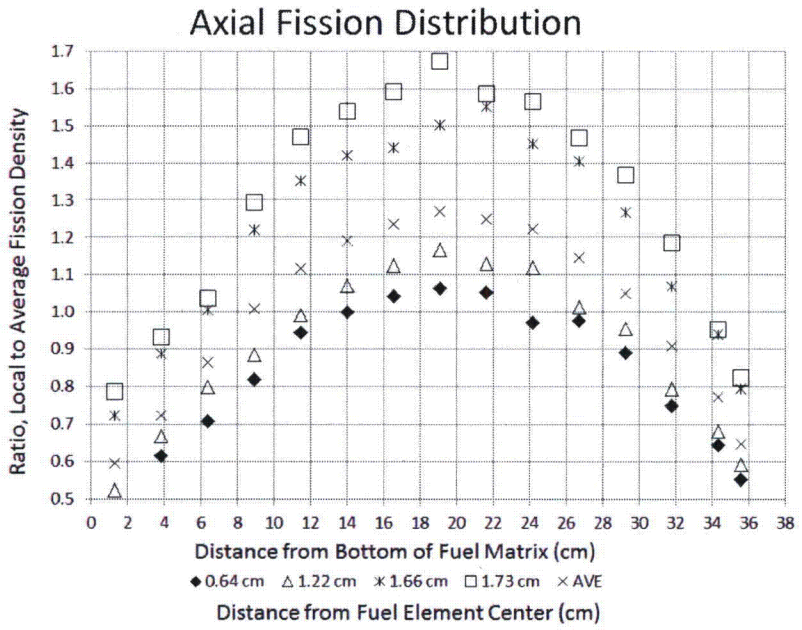

Figure 10: Axial Peaking Factor

Data from thermal hydraulic analysis provides a relationship between element power, monitored, maximum and average element fuel temperature (Fig. 11) for a single fuel element. The monitored temperature is the temperature at the location of the center thermocouple. The maximum fuel element temperature is taken as the maximum temperature in the zirconium fill rod. The average fuel temperature includes the zirconium fill rod and the fuel matrix.

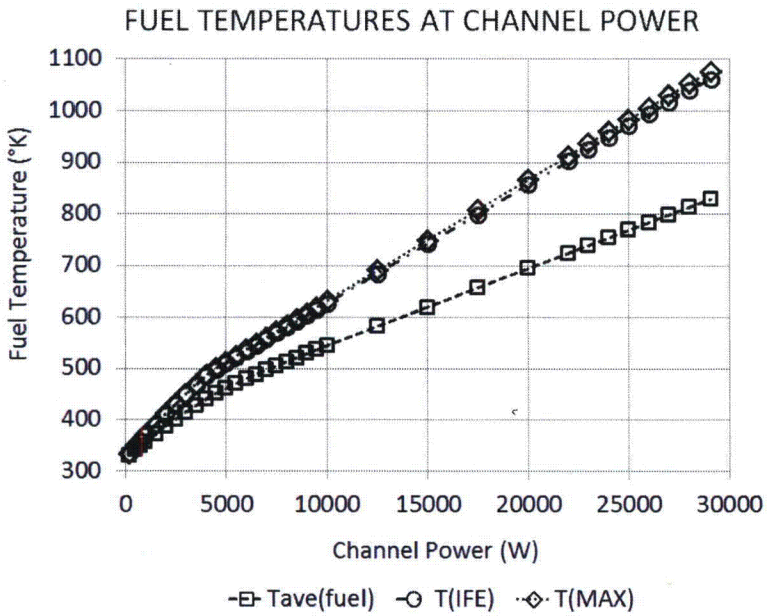

Figure 11: Monitored and Average Fuel Temperatures for Channel Power

3.4.3 Core Fuel Temperature Based on Measurement

The power level of each fuel element in the 114 element core was calculated from the peaking factor and the core power level (Fig. 8). The average core fuel element temperature for a specified core power is taken as a linear average of the temperature (including the zirconium fill rod and fuel matrix segments) for all equal volume segments in the fuel elements. The temperatures in the positions corresponding to FT1 and FT2 were calculated based on the power level in the installed instrumented fuel element positions (B03 and B06) at each power level. Core average temperature at power is therefore directly correlated to measuring channel indication (Fig. 12).

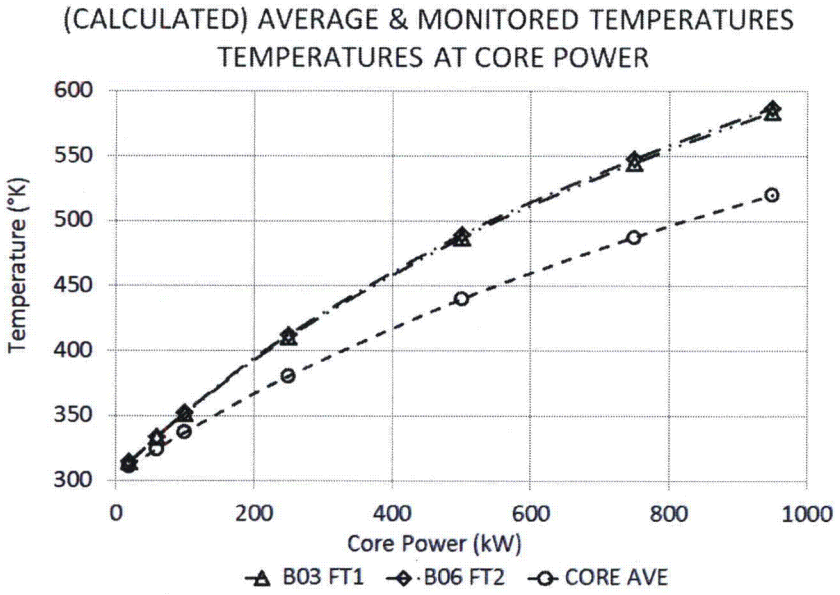

Figure 12: Calculated Core Average and FT1/FT2 Temperatures, 114 Element Core

3.4.4 Comparison

Based on the correlation from Fig. 11, the FT1 and FT2 measurements are used to calculate the average fuel temperatures at each power level used in measurements (Table 15). Using the measuring channel data as the basis for comparison (observed values and average fuel temperature based on the observation), the calculated values were compared to the values from observation. The FT2 measuring channel data has good agreement with the calculated values (Table 16). The FT1 channel agreement is qualitatively similar, but agreement is less than for FT1; this issue will be discussed in greater detail as part of the thermal hydraulic analysis. The results indicate modeling provides a reliable means of predicting reactor behavior.

Table 15: Average and Monitored Fuel Temperatures (°K)

Power	AVERAGE FUEL TEMPERATURE			BO3 FT1		BO6 FT2		Excess
kW	SCALE	FT1	FT2	SCALE	Meas.	SCALE	Meas.	Reactivity
1	305	300	298	306	298	306	294	$4.29
100	337	320	331	368	335	368	357	$3.93
250	380	344	372	446	380	446	432	$3.39
500	440	373	420	546	432	546	516	$2.55
750	487	392	453	621	465	621	573	$1.97
950	520	407	477	673	491	673	613	$1.60

Table 16: Comparison
Measuring Channel to Calculated Temperatures

Average Fuel Temperature		Measuring Channel	
FT1(SCALE)	FT2(SCALE)	FT1(SCALE)	FT2(SCALE)
-1.6%	-2.3%	-2.7%	-4.1%
-5.4%	-1.8%	-9.7%	-3.0%
-10.5%	-2.2%	-17.3%	-3.2%
-18.0%	-4.7%	-26.5%	-5.7%
-24.4%	-7.5%	-33.6%	-8.4%
-27.9%	-8.9%	-37.0%	-9.8%

3.6 Fuel Temperature Reactivity

Fuel temperature coefficient is the change in change in reactivity with respect to the change in fuel temperature. The fuel temperature measuring channels are related to average fuel temperature, as previously indicated. Excess reactivity as a function of core average fuel temperature (Fig. 14) exhibits a linear relationship, with the slope representative of the fuel temperature coefficient for the observed data in Table 15. The slope of the line representing excess reactivity as a function of core average fuel temperature based on the FT1 measuring channel shows a reactivity coefficient of -0.0169 $/°K, with FT2 at -0.0162 $/°K.

Independent calculations using SCALE were developed to determine excess reactivity response to fuel temperature changes. Calculations were performed with SCALE using ENDF/VII the continuous energy cross-section libraries corresponding to 300 °K and 600 °K. Temperature correction is not available to continuous energy libraries, so a second set of calculations was performed using the 238 energy group library. The fuel temperature coefficient based on SCALE calculations is -0.0157 $/°K for both the continuous energy and the group energy data.

The maximum difference between all of the fuel temperature coefficients is 7%. The agreement between the fuel temperature coefficients using measuring channels and SCALE calculations provides confidence that the SCALE model is capable of simulating the UTTRIGA reactor behavior as a function of fuel temperature changes.

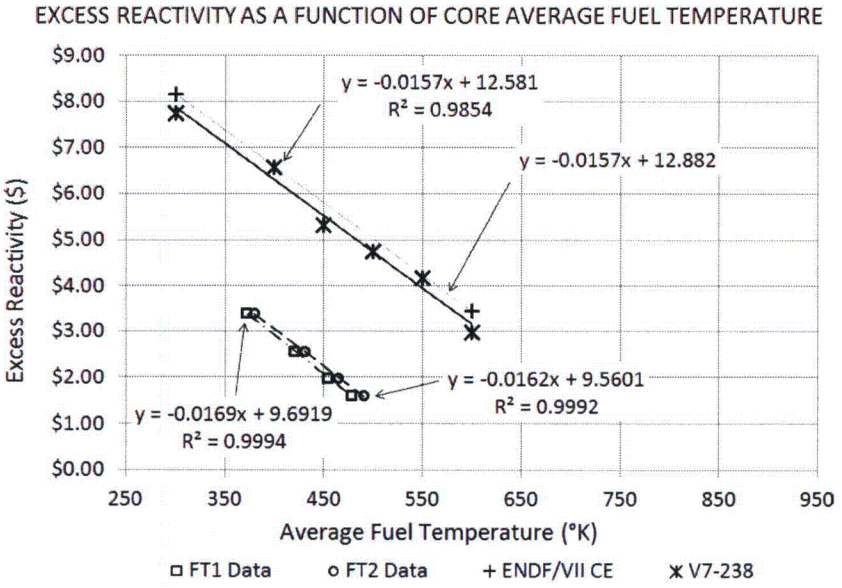

Figure 13: Reactivity and Average Fuel Temperature

3.7 Pulsing

Power and temperature data for the most recent pulses performed using the current core (32 total measurements, Table 17) was compared to calculations utilizing SCALE and TRACE data (Figs. 16 and 17). A correlation was developed for the core fuel element average temperature and the monitored fuel temperature for the current 114 core.

Table 17: Pulse Data

PULSE	DATE	CALC	MAX OBS			SCALE/TRACE CALC		
			POWER	FT2	FT_{ave}	POWER	FTB	FT_{ave}
368	05/10/12	2.269	916	338	204	937	346	208
369	05/21/12	2.324	992	343	207	1020	358	215
371	05/21/12	1.840	411	263	161	425	252	155
370	05/21/12	2.316	999	343	207	1006	356	214
359	05/21/12	2.324	1002	344	207	1020	358	215
372	07/20/12	1.840	411	263	161	425	252	155
373	07/20/12	1.884	441	275	168	468	261	160
374	08/22/12	2.332	1014	348	210	1032	360	216
375	08/28/12	2.392	1096	357	215	1123	373	224
376	08/31/12	2.340	1033	353	212	1042	362	217
378	11/01/12	2.660	1616	404	242	1595	431	258
380	11/02/12	2.699	1672	408	244	1670	441	262
381	11/12/12	2.219	834	330	199	867	335	202
382	11/13/12	2.660	1591	403	241	1595	431	258
383	11/13/12	2.660	1607	405	242	1595	431	258
384	11/20/12	1.899	470	276	168	483	264	162

Table 17: Pulse Data

PULSE	DATE	CALC	MAX OBS			SCALE/TRACE CALC		
			POWER	FT2	FT_{ave}	POWER	FTB	FT_{ave}
385	28 n0v 12	2.324	992	343	207	1020	358	215
386	12/18/12	2.357	1052	351	211	1070	365	220
387	02/20/13	1.910	476	275	168	495	267	163
388	02/20/13	1.918	486	286	174	503	269	164
389	04/08/13	1.918	486	279	170	503	269	164
390	04/09/13	2.047	628	297	180	647	297	180
391	04/29/13	1.438	118	192	121	132	164	105
392	04/29/13	1.918	489	274	167	503	269	164
393	06/12/13	1.895	470	274	167	480	264	161
394	06/12/13	1.918	493	278	170	503	269	164
395	06/28/13	1.938	502	278	170	523	273	167
396	07/19/13	1.955	513	281	171	542	277	169
397	10/22/13	2.726	1722	421	251	1727	446	266
398	11/22/13	1.161	21	125	82	29	110	73
399	11/22/13	1.914	472	270	165	499	268	164
400	11/22/13	2.634	1519	397	238	1538	426	254

The peaking factors for each element were used to determine the power in each element for a range of power levels from 100 kW to 1100 kW (in steps of 100 kW). The core average fuel temperature for each power level was taken as the average temperature of all the fuel elements. The temperature of the B03 element at the thermocouple location was then correlated to the average fuel temperature (Fig. 15).

The formulation of the in-hour equation by Johnson, Lucas, and Tsvetkov (INL/EXT-10-19953, *Modeling of Reactor Kinetics and Dynamics*, 2010) was implemented in Matlab. Precursor group constants were taken from *Reactor Dynamics and Controls*, Weaver (1968).

$$\frac{d\phi}{dt} = \frac{\rho(t) + \alpha_f \phi\left(T_F(t) - T_{F,0}\right) + \alpha_m \cdot \left(T_m(t) - T_{m,0}\right) - \beta_{mix}(t)}{\Lambda} \cdot \phi(t) + \sum_{i=1}^{6} \lambda_i \cdot C_i(t) + Q(t) \qquad 16$$

With the precursor rate of change as:

$$\frac{dC_i}{dt} = \frac{\beta_i^{mix}}{\Lambda} \cdot \phi(t) - \lambda_i \cdot C_i(t) \qquad 17$$

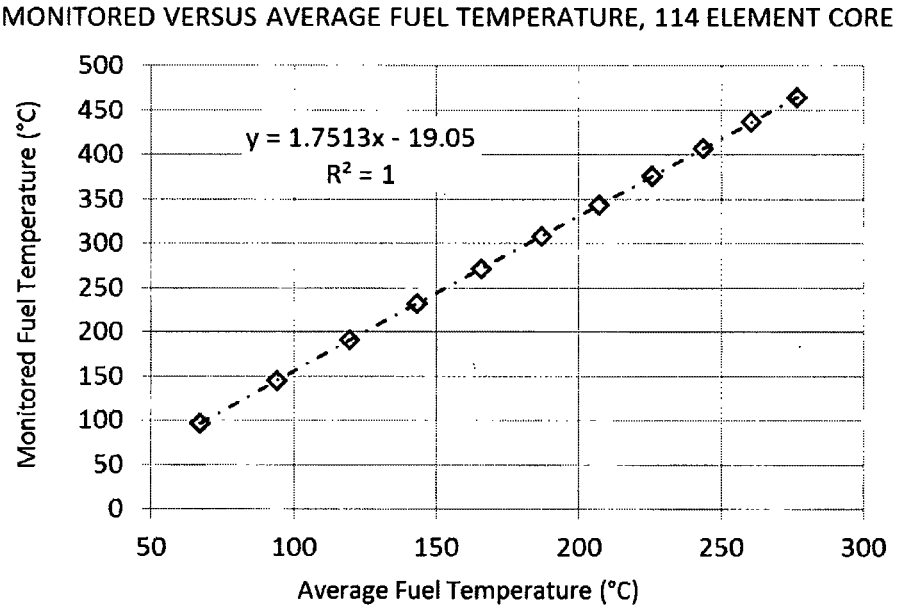

Figure 14: Correlation of Current 114 Element Core Average Fuel Temperature to Measuring Channel Temperature

And the fuel temperature rate of change as:

$$\frac{dT_F}{dt} = \frac{P_{eff}}{m \cdot c_p} - \gamma \cdot (T_F - T_m) \qquad 18$$

Where

Φ is the neutron flux, proportional to power
ρ is the pulsed reactivity
α is the temperature coefficient, subscripted F for fuel, m for moderator
T is the temperature, subscripted F for fuel, m for moderator
β_{mix} is the effective delayed neutron fraction for the 235/238 fuel
Λ is the prompt neutron lifetime, taken as the generation time
λ_i is the decay constant for the groups of delayed neutron precursors
C_i is the concentration of the groups of delayed neutron precursors
Q is the contribution from the neutron source

Simplified by assuming adiabatic conditions (i.e., water temperature does not change) and neglecting source neutrons:

$$\frac{d\phi}{dt} = \frac{\rho(t) + \alpha_f \phi \left(\int \frac{P_{eff(t)}}{m \cdot c_p} dt - T_{F,0} \right) - \beta_{mix}(t)}{\Lambda} \cdot \phi(t) + \sum_{i=1}^{6} \lambda_i \cdot C_i(t) \qquad 19$$

The temperature feedback coefficients are evaluated as:

$$\alpha_x = \frac{d\rho}{dT_x} \qquad 20$$

The rate of temperature change of the fuel is calculated as:

$$\frac{dT_F}{dt} = \frac{P_{eff}}{m \cdot c_p} - \gamma \cdot (T_F - T_m) \qquad 21$$

The prompt neutron lifetime (51.9 μs) was taken from the average of SCALE the value from SCALE calculations supporting fuel temperature reactivity calculations. Fuel density was calculated by the methodology of Simnad (op. cit.). The effective delayed neutron fraction was calculated using k_{eff} data generated by the MCNP model for the UT TRIGA, using the expression:

$$\beta eff = 1 - \frac{kp}{kp + d} \qquad 22$$

The effective delayed neutron fraction is 0.007036 ± 0.000729, compared to the nominal value of 0.007. Calculations of peak pulse power were compared (Fig. 16) to the measured values from surveillances (SURV7) recorded in Table 17.

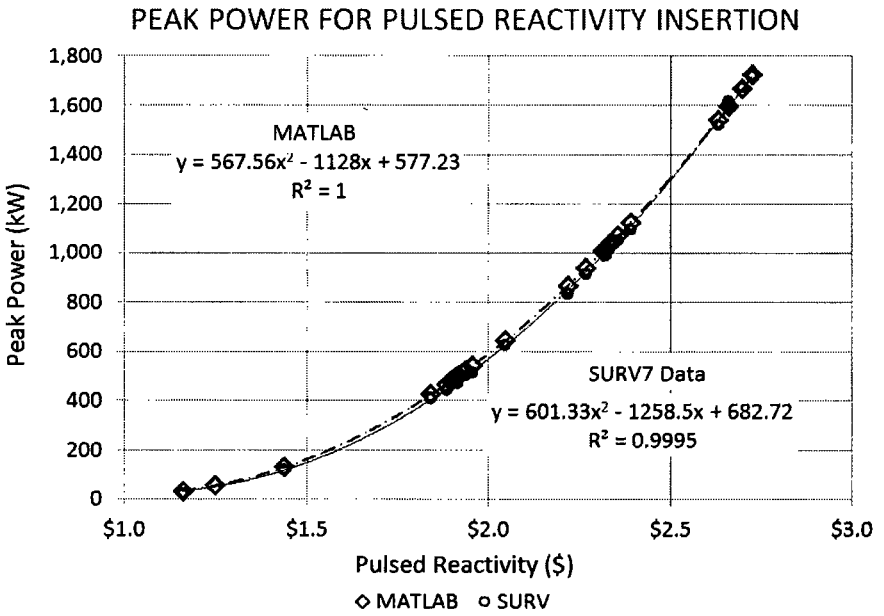

Figure 15: Pulsed Power Levels

The core average temperature calculated for each pulse using MATLAB was adjusted by the correlation (Fig. 17) to simulate the fuel temperature measuring channel response.

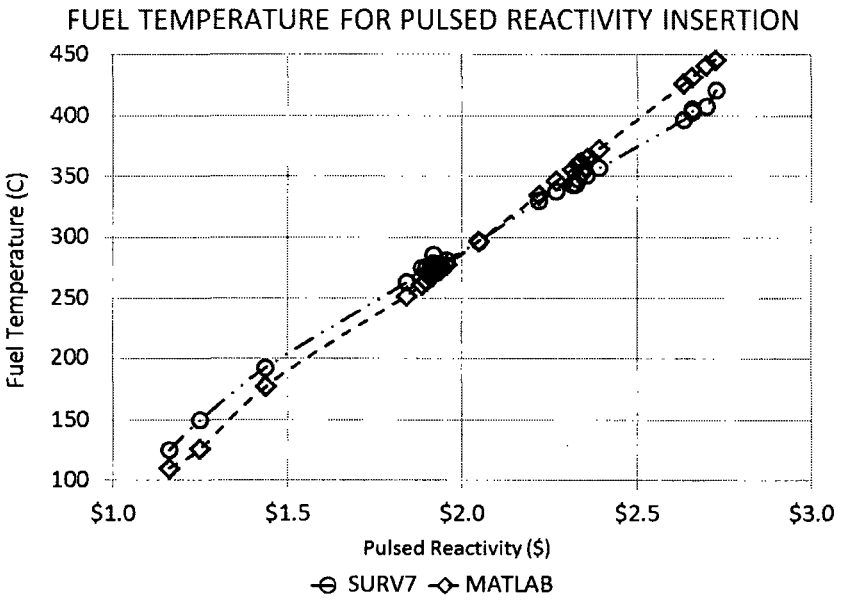

Figure 16: Pulsed Fuel Temperatures

The agreement between calculated and measured data provides confidence that the UTTRIGA reactor models are capable of simulating reactor behavior resulting from sudden reactivity insertions.

4.0 RESULTS

Nuclear data for a limiting core configuration are calculated. The total integral worth of each control rod, the total integral worth of all control rods, and excess reactivity for calculation were compared to surveillance measurements.

4.1 Nuclear Data

The prompt neutron lifetime for the 80 element core is taken as the generation time. The generation time is calculated by SCALE to be 4.71405E-05 ± 4.36711E-08 s at 300°K and 4.80039E-05 ± 4.56268E-08 s at 600°K.

Using methodology previously described, the fuel temperature coefficient of reactivity is evaluated to be -0.0153 $/°C (Fig. 18).

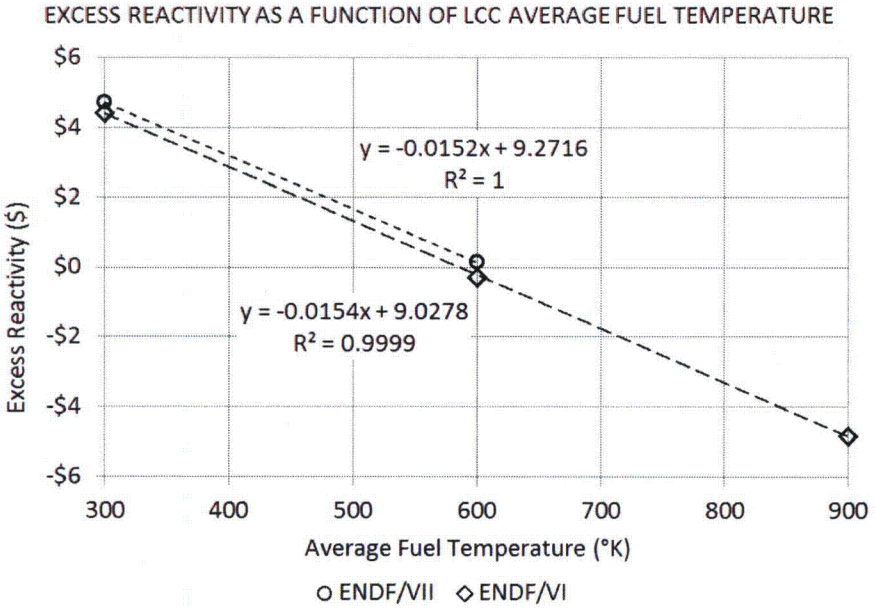

Figure 17: LCC Excess Reactivity and Fuel Temperature

4.1 Peaking Factors

The fission density calculated by SCALE was used to determine the ratio of power produced in each fuel element to the average power per element in the core (Fig. 19).

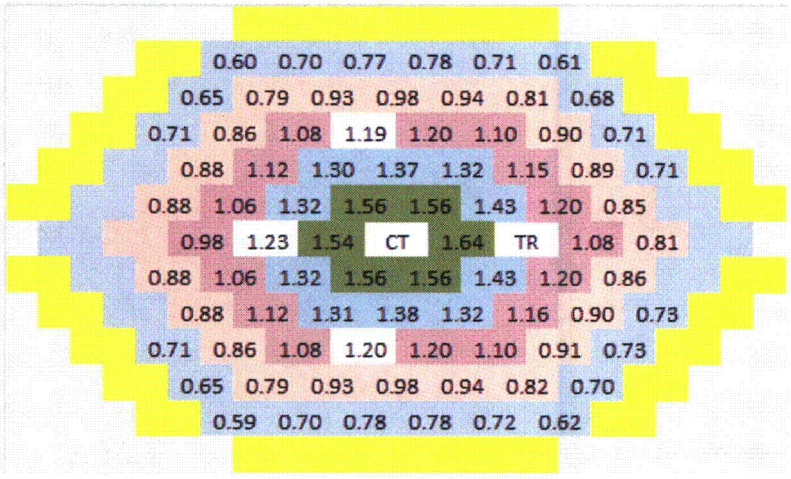

Figure 18: LCC Peaking Factors 80 Element Core

The distribution of power within a fuel element in the B ring was determined for a 15X15 cylindrically segmented fuel element, with radial and axial dimensions of each segment established to bound equal volume segments. The fission density for the sum of segment in each radial position was compared to the average of all radial positions (Fig. 20), and the fission density for the sum of all segments at specific axial positions similarly compared to the average of all axial positions (Fig. 21). Because of self-shielding effects, tallies at radial locations near the center of the fuel have large errors.

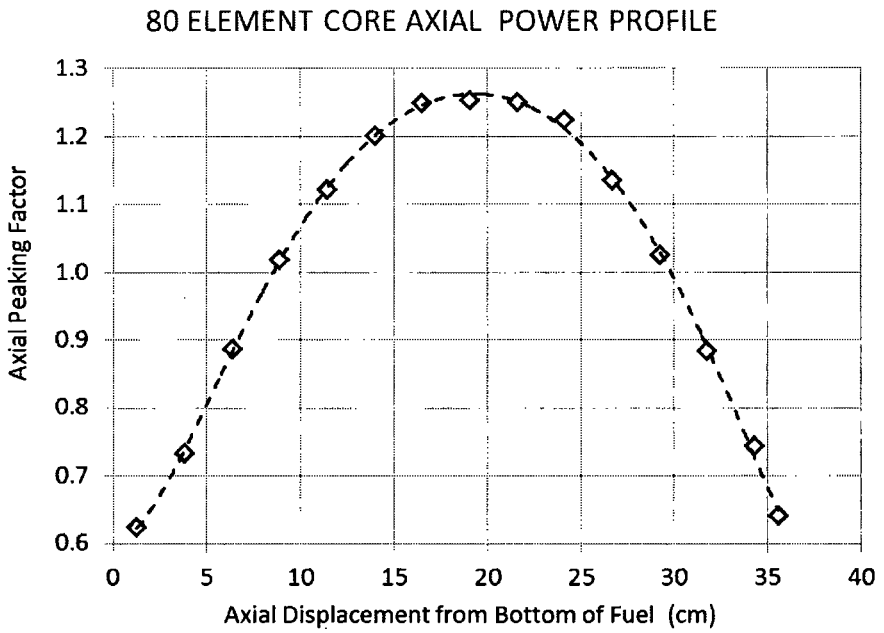

Figure 19: LCC Axial Peaking Factors

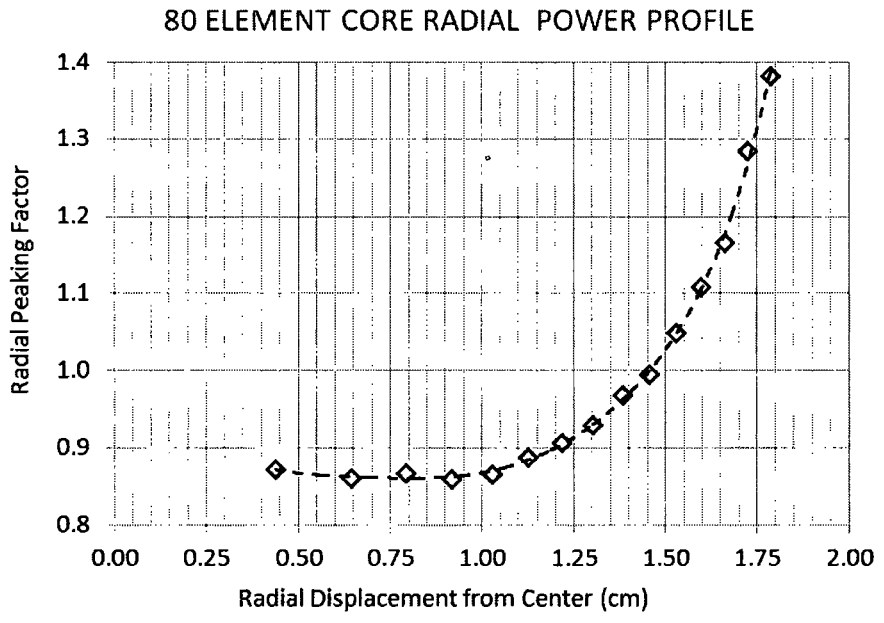

Figure 20: LCC Radial Peaking Factors

4.2 Fuel Temperature

Using thermal hydraulic data generated by TRACE, with input assumptions for the minimum permitted pool level and the maximum permitted pool temperatures, functional relationships were developed for power produced in an individual fuel element and (1) the average fuel temperature, (2) the temperature at the location of the center thermocouple, and (3) the maximum temperature in the fuel element (Fig. 22).

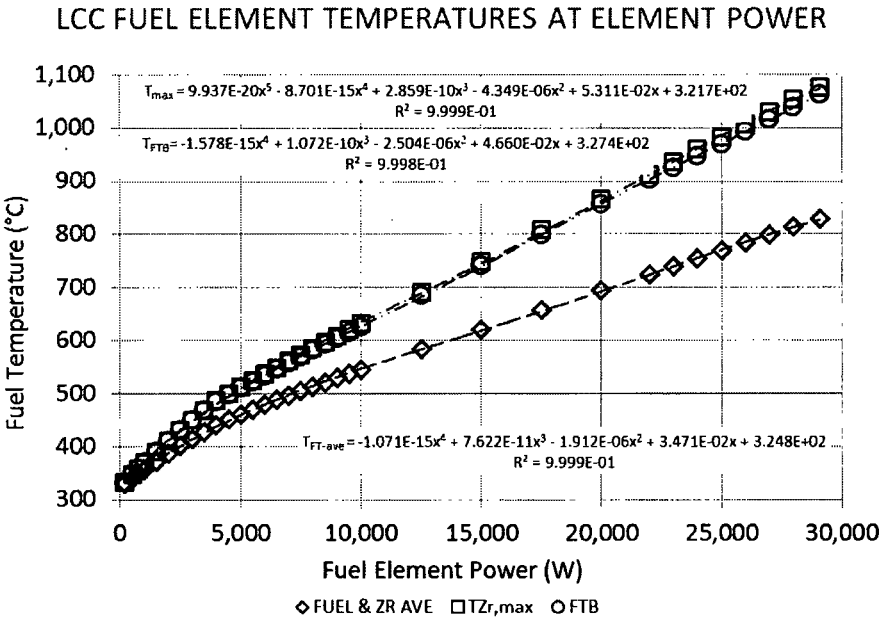

Figure 21: LCC Correlations of Fuel Temperatures and Element Power

The power produced in each fuel element was calculated by distributing the core power (for a range from 100 kW to 1210 kW) and then multiplying the average power by the peaking factor associated with element. The maximum temperature was calculated using the correlation in Fig. 22 with the fuel element producing the highest power. The fuel channel measuring temperature was simulated by applying the Fig. 22 correlation for the temperature at the thermocouple location to the B03 and B06 positions. The average fuel temperature was determined as the average of the temperature of each fuel element as determined by the correlation of Fig. 22. The results for fuel temperature at core power are provided in Fig. 23.

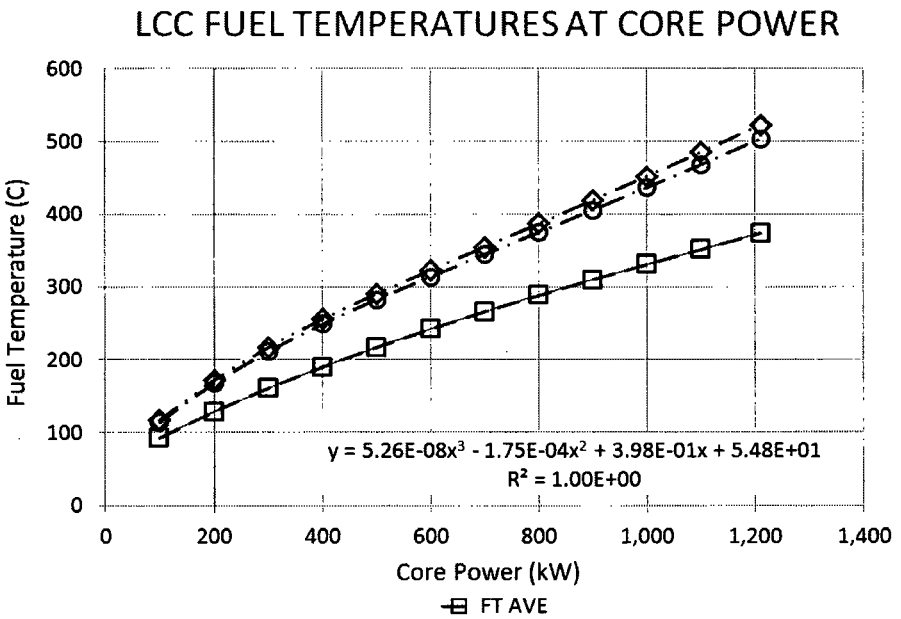

Figure 22: LCC Fuel Temperatures at Core Power for the 80 Element

Core at Limiting Pool Level and Temperature

4.3 Control Rod Worths

Criticality calculations were performed assuming all control rods fully inserted, all control rods fully withdrawn, and control rods individually inserted. Excess reactivity for each condition was calculated as:

$$\rho(\$) = \frac{1 - \rho_i}{\rho_i \cdot \beta_{eff}} \quad (23)$$

Table 18 values are noted ARI for all rods fully inserted, SH1 for shim 1 , SH2 for shim 2, RR for the regulating rod, and TR for the transient rod (with the remaining elements removed).

Table 18: LCC Reactivity Values

Config.	k_{eff}	±	$	Worth ($)
ARI	0.91680	0.00065	-12.964	17.697
ARO	1.03426	0.00061	4.732	NA
RR	1.00580	0.00065	0.824	3.908
SH1	1.00943	0.00064	1.335	3.398
SH2	1.01074	0.00063	1.518	3.214
TR	1.01132	0.0007	1.599	3.133

The worth of each condition ($\rho(\$)$) relative to the all rods out configuration (ρ_{ARO}) was calculated as:

$$\rho(\$) = \frac{\rho_{ARO} - \rho_i}{\rho_{ARO} \cdot \rho_i \cdot \beta_{eff}} \quad (24)$$

Shutdown margin with all control rods fully inserted is $8.9, calculated:

$$\rho_{SDM} = \rho_{ARO} - \rho_{RR} - \rho_{SH1} - \rho_{SH2} - \rho_{TR} \quad (25)$$

Shutdown margin with the most reactive rod fully withdrawn is $5.0, calculated:

$$\rho_{SDM} = \rho_{ARO} - \rho_{SH1} - \rho_{SH2} - \rho_{TR} \quad (26)$$

4.4 Pulsed Reactivity Response

Using the methodology previously described, the average fuel temperature in the core was correlated to the maximum temperature in the core and the fuel temperature measuring channel (Fig. 24).

Using a correlation (for 100 kW to 1,210 kW) between the core power and the average fuel temperature developed from Fig. 23, average fuel temperature is related to core power by:

$$T_{F,ave} = 5.26 \cdot 10^{-8} \cdot P^3 - 1.75 \cdot 10^{-4} \cdot P^2 + 0.398 \cdot P + 54.8 \quad (27)$$

The fuel temperature deficit from the temperature associated with operating at power was calculated from the fuel temperature coefficient for the 80 element LCC. The maximum pulse possible was determined by calculating excess reactivity at power as the reactivity deficit at power and the maximum allowed excess reactivity.

The MATLAB code for solving the in-hour equation was modified for the fuel mass and the prompt neutron lifetime (based on SCALE results for the 80 element core) associated with 80 fuel elements. The pulsed reactivity, initial fuel temperature, and initial power level for a range of values from 100 kW to the power where a $1 pulse is possible were used as input to determine reactor response to pulsing at power (Table 19, Fig. 25).

Table 19, LCC Response to Pulsing from Power

Core Power	FT_{ave}	Temp Deficit	Excess δk	Peak Fuel Tem	Peak Power
kW	°C	$	$	°C	MW
50E-3	25	0.00	3.00	408	1763
100	93	-1.42	2.58	430	1232
150	111	-1.70	2.30	405	864
200	128	-1.96	2.04	382	578
250	144	-2.21	1.79	359	354
300	160	-2.45	1.55	337	188
350	175	-2.68	1.32	316	78
400	190	-2.90	1.10	299	19
450	203	-3.11	0.89	304	2.2

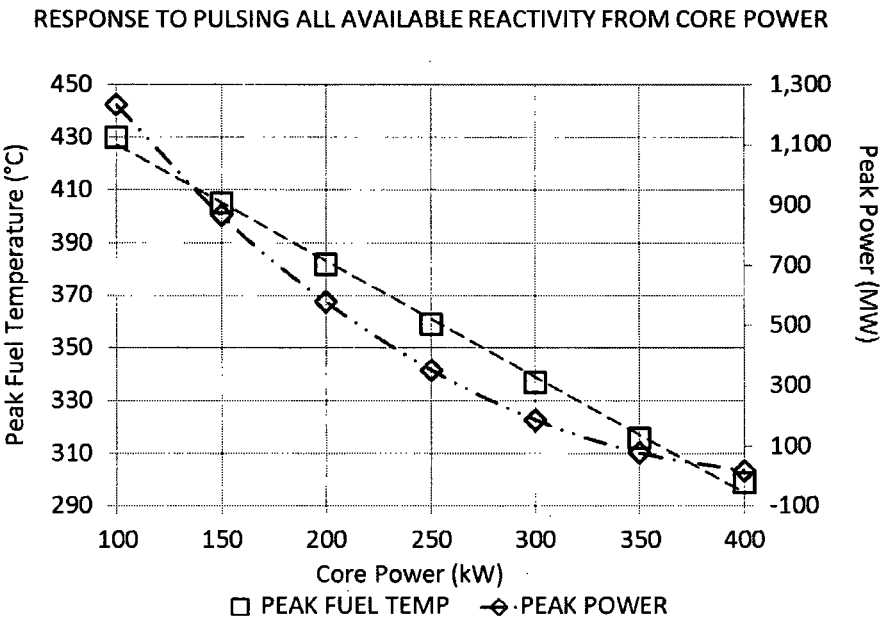

Figure 23: LCC 80 Element Core Response to Pulsed Reactivity Insertion

Although the initial fuel temperature is higher while operating at power, temperature associated with the operation limits the maximum pulse and therefore the maximum peak fuel temperature. At 100 kW core power, the maximum fuel temperature is approixmately 40°C greater than the temperature generate by a three-dollar pulse, and well within any limiting value. At slightly greater than 150 kW core power, the maximum power and temperature are lower than generated by a three-dollar pulse.

4.5 Control Rod Speed

The methodology for evaluating power and temperaure response to continuous control rod withrawal analysis by the DOW TRIGA reactor[14] using SIMULINK (a MATLAB product) was implemented for the UTTRIGA reactor using the LabVIEW Design and Simulation Suite. The UT TRIGA implementation was modifed to include (1) compensation for the initial neutron generation time based on reactivity, (2) speicific heat capacity from Simnad (op cit), (3) the use of the LabVIEW Runge-Kutta45 variable time solver, terminates rod withdrawal at scram (the DOW code continues rod withdrawl psot-scram), and adds reactivity with a ramp function based on rod speed (the DOW code uses a step function).

Table 20: Simulation of Continuous Control $5 Rod Withdrawal

Reactivity rate) %Δk/k-s	Peak Power MW	Temperature at Peak °C	Max Excess Reactivity $	Max Temp [60 s after] °C
0.1	5	35	1.050	128
0.2	12	40	1.133	258
0.3	20	44	1.189	364
0.4	29	47	1.235	394
0.5	37	50	1.274	408
0.6	45	56	1.309	417
0.7	56	56	1.341	423
0.8	62	62	1.369	428
0.9	74	61	1.399	432
1.0	81	66	1.423	435

In this analysis the scram time was set long enough after intiiation of the rod withdrawal to prevent the scram from terminating the transient. Therefore, no credit was taken for actuation of the power reactor trip in determining maximum power, total reactivity, and maximum fuel temperature during the rod withdrawal. The maximum control rod worth since the installtion of the UTTRIGA was slightly larger than $4; for reactivity additon rates from 0.002 to 0.1 %Δk/k-s of a $5 (integral worthl) control rod, the maximum power, temperature, and total reactivity are much less than the results of pulsing to $3 (Table 19), realted to the introduciton of temperature feedback on a time scale capable of regualting power.

[14] *Analysis of the Thermal Hydraulic and Reactivity Insertion behavior of the DOW TRIGA Research Reactor, Submitted to the NRC in Support of the DTRR License Renewal*, M. R. Hartman (03/12/2011)

5.0 Conclusion

Modeling the UTTRIGA reactor with SCALE and TRACE provides data consistent with experimentally determined values. Therefore, the models are expected to provide a reasonable estimate of reactor behavior.

When the models are applied to an 80 element core under limiting conditions of pool level and temperature, thermal hyraulic and temperature limts are preserved with a large margin. The current limit on pulsed reactivity insertion in TRGIA reactors restricts fuel temperature to less than 830°C, which does not occur for pulsing less than about $5.

Appendix 1: Fuel Element Core Locations

Element Utilization in Core

ELEMENT	87	90	89	92	95	103	102	104	108	110	114
2899	46	46	46	46	46	46	15	15	15	15	15
2902	47	47	47	47	47	47	86	86	84	84	84
2903	48	48	48	48	48	48	116	116	116	116	116
2904	49	49	49	49	29	29	114	114	114	114	114
2905	50	50	50	50	50	50	39	39	39	39	39
2906	51	51	51	51	51	51	35	35	30	30	30
2908	52	52	52	52	52	52	101	101	101	101	101
2910	53	53	53	53	80	80	28	28	28	28	28
2911	54	54	54	54	54	54	97	97	97	97	97
2912	55	55	55	55	55	55	84	84	86	86	86
2913	56	56	56	56	98	98	122	122	122	122	122
2915	57	57	57	57	57	57	76	76	76	76	76
2918	58	58	58	58	58	58	72	72	72	125	125
2925	59	59	59	59	59	59	24	24	24	24	24
2927	60	60	60	60	27	27	108	108	108	108	108
2928	61	61	61	61	61	61	34	34	34	34	34
2929	62	62	62	62	62	62	43	43	43	43	43
2930	63	63	63	63	63	63	118	118	118	118	118
2931		80				121	20	20	20	20	20
2932	64	64	64	64	64	64	36	36	48	56	48
2935	65	65	65	65	65	65	117	117	117	117	117
2938	66		66	66	17	17	111	111	107	107	107
2939	67	101	67	119	119	119	30	30	35	35	35
2940	68	102	68	100	100	100	89	89	89	89	89
2941	69	69	69	69	69	92	25	25	25	25	25
2943		112			123	123	40	40	40	40	40
2944	70	70	70	70	70	70	19	19	19	19	19
2946	71	71	71	71	71	71	77	77	77	77	77
2947	72	72	72	72	72	72	96	96	96	96	96
2948	73	73	73	73	28	28	121	121	121	121	121
2950	74	74	74	74	74	74	42	42	42	42	42
2951		66	75	75	43	43	103	103	103	119	119
2952	76	76	76	76	11	11				112	112
2954	77	77	77	77	26	26	123	123	123	123	123
2955	78	78	78	78	78	78	44	44	44	44	44
2957	79	79	79	79	97	97	106	106	106	106	106
2958		111	80	80	53	53	113	113	80	80	80
2959	81	81	81	81	81	81	29	29	29	29	29
2960	82	82	82	82	82	82	95	95	95	95	95
2962	83	83	83	83	83	83	32	32	32	32	32
2964	84	84	84	84	84	84	27	27	27	27	27
2965	85	85	85	85	85	85	17	17	17	17	17

Element Utilization in Core

ELEMENT	87	90	89	92	95	103	102	104	108	110	114
2968	86	86	86	86	96	96	102	102	102	115	115
2969	87	87	87	87	87	87	91	91	91	91	91
2970	88	88	88	88	45	45	110	110	110	110	110
2971	89	89	89	89	89	89	90	90	90	90	90
2974	90	90	90	90	90	90	38	38	38	38	38
2975	91	91	91	91	91	91	45	45	45	45	45
2976	92	92	92	92	92	69	107	107	111	111	111
2977	93	93	93	93	93	93	37	37	37	37	37
2979	94	94	94	94	94	94	26	26	26	26	26
2980				105	105	105	23	23	23	23	23
2983	95	95	95	95	95	95	21	21	21	21	21
2984	96	96	96	96	86	86	18	18	18	18	18
2985	97	97	97	97	79	79	11	11	11	11	11
2992				109	109	109	31	31	31	31	31
3013				114	114	114	14	14	14	14	14
3384										12	12
3496											72
3504											73
3513	99	99	99	99	99	99	93	93	93	93	93
3700											102
3703											74
5198	98	98	98	98	56	56	12	12	12		
5283	26										
5844	28	28	28	28	73	73	58	58	58	58	58
5845	29	29	29	29	49	49	46	46	46	46	46
5846	30	30	30	30	30	30	52	52	52	52	52
5902	31	31	31	31	31	31	63	63	63	63	63
5903	32	32	32	32	32	32	53	53	53	53	53
5904	34	34	34	34	34	34	64	64	64	64	64
5911					127	127	71	71	71	71	71
5912	35	35	35	35	35	35	55	55	51	51	51
5913	36	36	36	36	36	36	54	54	81	81	81
5914	37	37	37	37	37	37	67	67	67	67	67
5915	38	38	38	38	38	38	49	49	49	82	49
5916	17	17	17	17	66	66	88	88	88	88	88
5917	18	18	18	18	18	18	81	81	54	54	54
5918	39	39	39	39	39	39	48	48	36	36	36
5919	40	40	40	40	40	40	60	60	60	60	60
5920	42	42	42	42	42	42	73	73	73	104	104
5921	11	11	11	11	76	76	61	61	61	61	61
5922	12	12	12	12	12	12	98	98	98	98	98
5981	13										
5982		13	13	13							

Element Utilization in Core

ELEMENT	87	90	89	92	95	103	102	104	108	110	114
6142	43	43	43	43	75	75	68	68	68	68	68
6143	14	14	14	14	14	14	87	87	87	87	87
6886	15	15	15	15	15	15	50	50	50	50	50
6889	16	26	26	26	77	77	66	66	66	66	66
6923	44	75	44	115	115	115	57	57	59	59	59
6924	19	19	19	19	19	19	78	78	78	78	78
6925	45	45	45	45	88	88	59	59	57	57	57
6926	20	20	20	20	20	20	92	92	92	92	92
6927	21	21	21	21	21	21	62	62	62	62	62
6928	23	23	23	23	23	23	69	69	69	69	69
6929	24	24	24	24	24	24	51	51	55	55	55
6930	25	25	25	25	25	25	65	65	65	65	65
6931										83	103
6932	27	27	27	27	60	60	47	47	47	47	47
10146	33	33	33	33	33	33	33	33	33	33	33
10147	41	41	41	41	41	41	41	41	41	41	41
10148	22	22	22	22	22	22	22	22	22	22	22
10699									120	120	120
10700									124	124	124
10701								105	105	105	105
10702								109	109	109	109
10703									127	127	127
10704									100	100	100
10708		16	16	16	16	16	16	16	16	16	16
10810						101	74	74	74	126	126
10811						103	94	94	94	94	94
10812						104	79	79	79	79	79
10813						110	85	85	85	85	85
10814						111	99	99	99	99	99
10815						113	80	80	113	113	113
10816						120	75	75	75	75	75
10817						124	70	70	70	70	70
10878					13	13	13	13	13	13	13

PART II
ANALYSIS OF THERMAL HYDRAULIC PERFORMANCE OF THE UNIVERSITY OF TEXAS TRIGA MARK II NUCLEAR RESEARCH REACTOR

THERMAL HYDRAULIC ANALYSIS OF THE UTTRIGA REACTOR

1.0 Introduction

This report documents analysis of the thermal hydraulic characteristics of the UTTRIGA in support of renewal of the U.S. Nuclear Regulatory Commission facility operating license.

The UT Austin TRIGA Research Reactor (UTTRIGA) is a TRIGA Mark-II nuclear research reactor licensed to The University of Texas at Austin for operation up to 1.1 MW thermal power level. The geometry of the UTTRIGA core is based on seven concentric hexagons (designated as rings) that fix locations for fuel elements, graphite filled elements, and various experimental facilities. The core is surrounded by a modified cylindrical annulus in an aluminum container filled with graphite (neutron reflector), a rotary specimen rack (RSR), four beam port penetrations, and void spaces accommodating the RSR and beam port facilities. The core and reflector are located in an aluminum tank (pool) filled with high-purity water. The water acts as a neutron moderator, coolant, and radiation shield.

Thermal hydraulic modeling of the UTTRIGA was performed with TRAC/RELAP Advanced Computational Engine (TRACE) using the Symbolic Nuclear Analysis Program (SNAP) interface. Thermal hydraulic characteristics were developed from classical methods and corrections for UTTRIGA geometry using the computational fluid dynamics code FLUENT. Distribution of fission activity was developed from transport calculations in SCALE, a comprehensive modeling and simulation suite for nuclear safety analysis and design.

The thermal hydraulic codes TRACE are designed to perform best-estimate analyses of operational transients and accident scenarios by modeling physical geometry and thermodynamic conditions. TRACE was developed for commercial nuclear reactors applications, and RELAP has been widely used in characterizing research reactor thermal hydraulic performance. TRACE is the NRC's flagship thermal-hydraulics analysis tool consolidating and extending the capabilities of NRC's 3 legacy safety codes - TRAC-P, TRAC-B and RELAP. The Symbolic Nuclear Analysis Package (SNAP) is a graphic user interface that standardizes input and interaction for supported analysis codes.

NRC guidance[1] defines a "limiting core configuration" as the core that would yield the highest power density using the fuel specified for the reactor, with all other core configurations demonstrated to be encompassed by safety analysis for the limiting core configuration. The guidance references an "operational core." Analytical methods used to define the limiting core configuration are applied to the operational core, providing confidence that the model adequately supports limiting core configuration analysis.

2.0 General Description of Heat transfer at the UTTRIGA

Heat is generated in the fuel by the fission process. Cooling is required to maintain fuel temperature low enough to prevent challenges to cladding integrity. The UT TRIGA reactor operates in a natural convection-cooling mode. Heat transfer from fuel to the coolant in the core area is developed by generation of heat in the fission process, conduction of the heat to external surface of the fuel element, and heat transfer by convection from the fuel element surface to water in the core area.

Temperature increase of the water in the core area develops buoyancy forces that drive flow. The flow is diminished by momentum changes and friction (across the gird plates, fuel element end fittings, and fuel

[1] NURGE 1537, Guidelines for Preparing and Reviewing Applications for the Licensing of Non-Power Reactors, Format and Content

element cladding surfaces). Above a "critical" heat flux, coolant flow will not be adequate to prevent thermal hydraulic conditions from exceeding limits. This analysis demonstrates that operation at the maximum licensed power level has adequate margin to the critical heat flux.

3.0 Power Distribution

The distribution of heat generation across the fuel elements in the core is affected by the core configuration. The amount of heat generated in a specific fuel element can be characterized as a "peaking factor," the ratio of the power produced in that element to average (total heat distributed equally over all fuel elements). A larger number of fuel elements tend to exacerbate the peaking factor of higher power fuel elements. However, the average power per element is reduced by a larger number of fuel elements so that maximum power produced by a fuel element tends to decease. Determining the maximum power produced by a fuel element requires evaluation of peak to average power ratios for the core configuration. Distribution of heat production within a fuel element also varies spatially, affecting the distribution of fuel temperature in the element as well as localized heat transfer.

3.1 General

"Core power" refers to the total power produced by all fuel elements, and "average power" (per element) is the core power distributed uniformly across all fuel elements. The ratio of a specific fuel element power to the average power per element is referred to as core peaking factor. The hot channel is the fuel element producing the maximum power (the fuel element with the largest peaking factor) and the surrounding cooling flow. The fuel element and cooling channel geometry is reduced for thermal hydraulic calculations to a "unit cell" (repeatable geometry that can be used to replicate the geometry of the fuel in the core). Acceptable thermal hydraulic performance of the UTTRIGA is based on the heat generated in the unit cell corresponding to the hot channel.

Neutron flux has a spatial distribution across the core, causing variations in the rate of fission reactions in fuel elements. The variation is influenced by fuel element location, local geometry, and fuel element materials. SCALE transport codes calculate the fraction of total fissions generated in each element, allowing core peaking factors and the fuel element producing the most power to be identified directly.

Neutron flux also varies within fuel elements, creating spatial variations of heat production within the fuel matrix. More discretized fuel element modeling is used in SCALE to calculate the fraction of fissions occurring in segments of the fuel element. Segmentation allows development of a mesh of radial and axial fuel elements to define the heat-generation structure of the unit cell. SCALE reports the fraction of fission occurring in the segments, used to evaluate spatial variation in power production. These 2-dimensional distributions can be used explicitly in TRACE, while RELAP assumes the distribution can be decomposed into independent axial and radial factors. Analysis is core-specific to the extent that the power distribution specified for a specific fuel element varies with core configuration and burnup.

Fuel element material compositions were calculated for each element in neutronic analysis of the UTTRIGA SCALE model. The SCALE calculations used to develop fuel element material inventories are based on uniform fuel composition. However, burned-material and neutron-flux distribution are not independent; since neutron flux varies spatially, the products of neutron reactions are expected to vary. Limits on microprocessor capabilities prevent discretizing of the internal fuel element structure. The effects of this assumption are mitigated in thermal hydraulic analyses since maximum fuel burnup is correlated directly to maximum power production; higher burnup regions are likely to have lower power and lower local temperature compared to calculations with uniform material composition. Fuel in the center an element that has burnup will consequently generate less power in comparison to SCALE calculations that assume uniform material composition. Consequently the effect on fuel temperature

calculations is assumed to be conservative, and small.

Similarly, the initial SCALE calculations assumed a uniform fuel temperature for all fuel elements consistent with full power operation. However, fuel temperature and fission rate are not independent as elevated temperatures lower the fission cross section. Higher temperatures near the core midplane during reactor operation are likely to reduce the local fission rate. Consequently, the assumption of uniform temperature in SCALE calculations is expected to result in higher element peaking factor compared to actual reactor operations. Therefore, the effect on fuel temperature calculations is assumed to be conservative, and small.

Limiting pool water level (5 feet above the core) and pool water temperature (49 °C) bound the limiting core configuration, while nominal pool water level (6.25 feet above the core) and pool water temperature (~25 °C) apply to the remainder of the analyses.

3.2 Criticality Calculations

SCALE calculations were performed to determine first the minimum number of close packed fuel elements at ambient temperature (300°K) for criticality, and second the minimum number of close packed fuel elements required for operation at an assumed full power operating temperature (600°K). The minimum number of fuel elements required for criticality at power is the lowest number of fuel elements possible for the limiting core configuration. The actual limiting core configuration is selected by calculating margin to thermal limits for the single fuel element generating the highest power. Three assumptions are used to calculate the minimum number of fuel elements required.

(1) Calculations were performed with graphite dummy rods and then water voids in all positions which do not contain fuel.

(2) Calculations were performed using material specifications for fresh fuel. Since reactor operation reduces fissionable material and introduces fission product poisons into a fuel element, the number of fuel elements required to support full power operations with fresh fuel is the minimum. As the number of fuel elements increases, the distribution of heat generation over more fuel elements reduces the heat generated in the hot channel.

(3) Fuel material specifications are assumed to be the average initial (unirradiated) values of all TRIGA fuel elements possessed under the UTTRIGA reactor license.

Results of reactivity calculations from 40 to 89 fresh fuel elements at ambient (300°K) and an assumed uniform temperature consistent with full power steady stare operations (600°K) are provided in Fig. 1, with excess reactivity calculated as:

$$\$_{EX} = \frac{k_{eff} - 1}{k_{eff}} \cdot \frac{1}{\beta} \qquad 1$$

Minimum Number of Fuel Elements for Criticality and Operation

Criticality at ambient temperature requires a minimum of 55 fresh fuel elements. The minimum number required for criticality at full power operating temperature is 69 fuel elements. Although a maximum of 78 fuel elements can be loaded in a close packed core with graphite rods in the remaining core spaces and remain within the maximum excess reactivity limits, replacing graphite rods with water voids reduces excess reactivity and allows more fuel to be loaded. Actual loading that meets reactivity limits is

determined and validated experimentally.

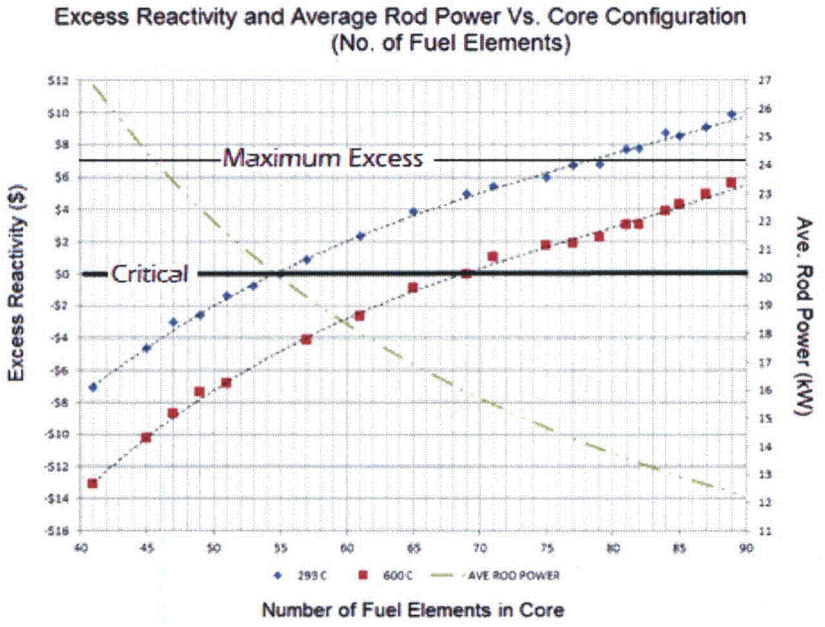

Figure 1, Excess Reactivity and Average Rod Power

Hot Channel Selection

Analysis (using SCALE) was performed for core configurations to evaluate peaking factors and the heat generated in each B ring element (Table 1 and Fig. 2) at the nominal core power of 1210 kW (1100 kW licensed power with a maximum potential instrument error of 10%).

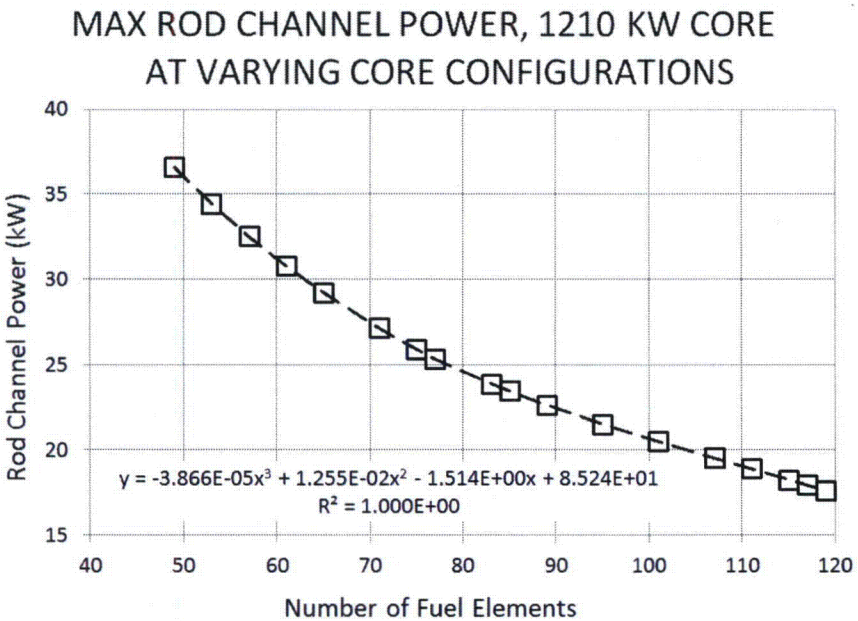

Figure 2, Maximum Channel Power at 1210 kW

The average fuel element power was calculated distributing the core power over the number of fuel elements in each configuration. The power generated in each element is the product of the applicable

peaking factor and the average power. The hot channel power values for the remaining cores demonstrate a definite and decreasing trend in the maximum hot channel power. The 80 element core is selected as the minimum number of elements in the limiting core configuration.

3.3 Power Distribution within Fuel Elements

Interactions in the outer radial reduce neutron flux in the inner radial segments of a fuel element, and statistics associated with fission rates near the center of the fuel element are challenging. The Monte Carlo calculations in areas of lower neutron flux in smaller dimensions require a significantly larger number of histories to reduce noise (piecewise variation). Consequently the SCALE model modification segmenting the fuel element axially and radially is based on equal volume segments (Table 1). Distribution fractions as used are the fraction of power in a specific segment to average fraction of power across 225 equal volume segments. Although fission distributions are calculated for each segment, distributions are provided in this report only for projections (1) near the radial and axial extremes, (2) at the respective centers, and (3) fuel element averages (to reduce complexity).

Table 1, Geometry for Fuel Segments

	Axial Segments			Radial Segments		
	z_1	z_2	z_{ave}	r_1	r_2	r_{ave}
1	19.05	16.51	17.78	0.3175	0.5603	0.4389
2	16.51	13.97	15.24	0.5603	0.7260	0.64315
3	13.97	11.43	12.7	0.7260	0.8604	0.7932
4	11.43	8.89	10.16	0.8604	0.9764	0.9184
5	8.89	6.35	7.62	0.9764	1.0801	1.02825
6	6.35	3.81	5.08	1.0801	1.1746	1.12735
7	3.81	1.27	2.54	1.1746	1.2621	1.21835
8	1.27	-1.27	4E-15	1.2621	1.3439	1.303
9	-1.27	-3.81	-2.54	1.3439	1.4210	1.38245
10	-3.81	-6.35	-5.08	1.4210	1.4941	1.45755
11	-6.35	-8.89	-7.62	1.4941	1.5638	1.52895
12	-8.89	-11.43	-10.16	1.5638	1.6306	1.5972
13	-11.43	-13.97	-12.7	1.6306	1.6947	1.66265
14	-13.97	-16.51	-15.24	1.6947	1.7564	1.72555
15	-16.51	-19.05	-17.78	1.7564	1.8161	1.78625

Fission generation data for each segment was used to calculate the fraction of fissions in the fuel element that occurred in each segment. Peaking factors in the axial or radial direction can be calculated by normalizing the sum of the fractions on the axis to the average of all summations on the axis.

The analysis for the core peaking factors of the current 114 element core is provided in in Fig. 3. In this analysis, the fuel element in position B02 produces the maximum power. Analyses for axial and radial variations in B04 for the 114 element core are provided in Fig. 4 and 5.

Axial Peaking Factors

Axial peaking factors were developed for cores representing slightly less than the minimum number of fuel elements required for full power operation, the initial UTTRIGA core, and the current core configuration. While there is some variation in the axial power distribution, the analyses reported in

Table 2 indicates suggest that axial power distribution for the specified locations is similar regardless of the core configuration. The results show that normalized axial power distribution is relatively stable over varying core configurations. Although specific power distributions were used to develop input for thermal hydraulic analysis the effect on axial distribution, and any associated errors, should be insignificant. The major effect on variations in power distribution is on core-wide, fuel-element peaking factors.

			0.63	0.65	0.77	0.56	0.65				
		0.61	0.76	0.88	0.97	1.12	0.84	0.89	H_2O		
	0.79	0.95	1.08	1.21	1.27	1.22	0.97	0.94	0.71		
	0.67	0.83	1.18	1.11	1.01	1.27	1.30	1.13	0.80	H_2O	
	0.61	0.84	0.94	1.32	1.21	1.25	1.35	1.28	1.21	0.91	0.54
0.66	0.77	1.03	1.16	1.25	1.53	1.52	1.41	1.44	0.94	0.60	0.00
	0.84	0.80	0.89	1.12	1.49	CT	1.46	TR	1.18	1.01	0.73
0.62	0.82	1.12	1.20	1.32	1.39	1.65	1.49	1.59	1.20	0.78	0.88
	0.63	H_2O	H_2O	1.05	1.27	1.40	1.27	1.33	1.34	1.07	0.85
	0.95	H_2O	0.97	1.05	1.12	1.36	1.43	1.23	0.97	0.93	
		0.72	0.74	0.92	1.01	1.14	1.12	1.04	1.05	0.77	
			0.53	0.76	0.64	0.92	0.87	0.81	0.77	0.78	
				0.59	0.72	0.70	0.74	0.66			

Figure 3, Peak to Average Power for 114 Element Core at 600 °K

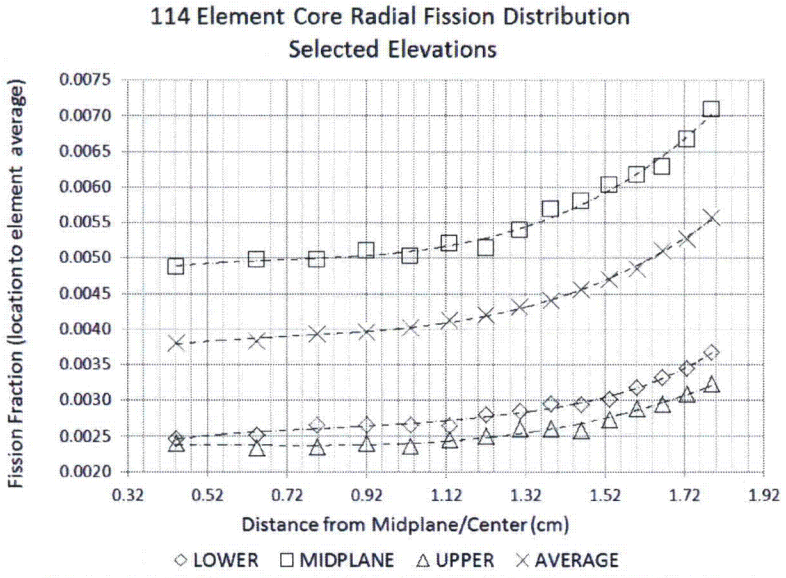

Figure 4, 114 Elements 600 °K, B04 Radial Power Distribution

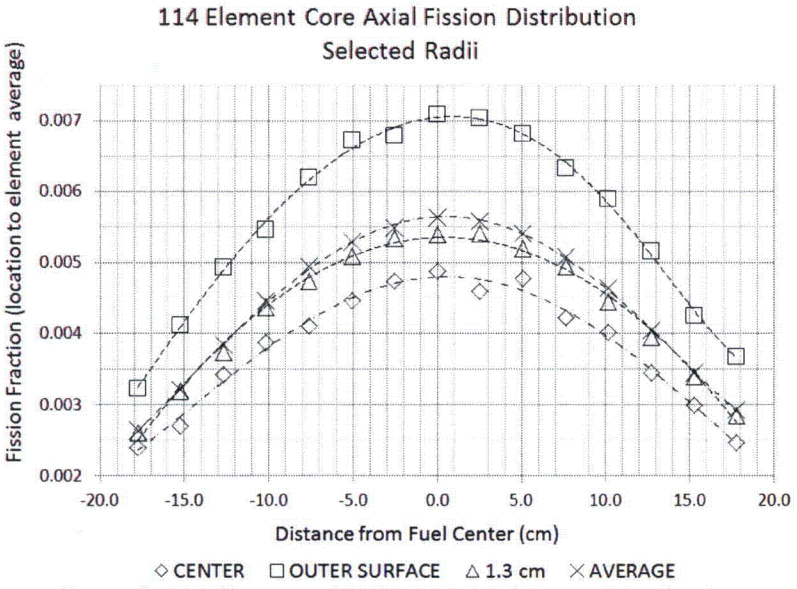

Figure 5, 114 Elements 600 °K, B04 Axial Power Distribution

Table 2, Fuel Element Axial Peaking Factors

Segment	No. of Fuel Elements in Core			AVE	DEV
	70	87	114		
1	0.65	0.63	0.66	0.64	1.83%
2	0.76	0.76	0.78	0.76	1.28%
3	0.91	0.90	0.91	0.91	0.52%
4	1.04	1.04	1.04	1.04	0.27%
5	1.14	1.14	1.14	1.14	0.26%
6	1.22	1.22	1.22	1.22	0.28%
7	1.26	1.27	1.26	1.26	0.40%
8	1.27	1.28	1.27	1.27	0.39%
9	1.25	1.25	1.24	1.25	0.65%
10	1.20	1.20	1.19	1.20	0.30%
11	1.12	1.12	1.11	1.12	0.47%
12	1.01	1.02	1.00	1.01	0.52%
13	0.87	0.87	0.87	0.87	0.36%
14	0.72	0.71	0.72	0.72	0.45%
15	0.60	0.59	0.59	0.59	0.76%

4.0 Thermal Hydraulic Modeling, Unit Cell Geometry and Thermal Hydraulic Characteristics

The flow channel unit cell cross section is based on the fuel element geometry, as illustrated in Fig. 6 (unit cell and the surrounding fuel elements). As illustrated, the unit cell is a fuel element and the surrounding flow area (end fittings have more complex geometry) circumscribed by a hexagon with an inner radius of ½ of the pitch. The cooling flow channel is modeled as a heated pipe with thermodynamic characteristics based on physical dimensions and properties of the coolant around the fuel elements. A large fraction of the unit cell is occupied by the fuel element, leaving a relatively small flow area. The complex geometry of the fuel element end fittings are approximated as hydrodynamic characteristics.

Since a regular hexagon can be decomposed into six equilateral triangles, a triangular unit cell is the smallest possible unit cell. However, RELAP and TRACE heat structures (described in a following section) have limited options for temperature analysis of sold structures; a cylinder can be used to develop a heat source, but a half-cylinder is not possible. This does not limit fluid analysis in thermal hydraulic calculations with a triangular unit cell, but limits the ability to calculate temperatures in the fuel element since the geometry of a triangular unit is ⅙ of the heat contribution from a single fuel element. Intrinsic properties used to calculate thermal hydraulic conditions are fully represented, but total heat for the cylindrical fuel element (used in material temperature calculations) in a triangular unit cell is not.

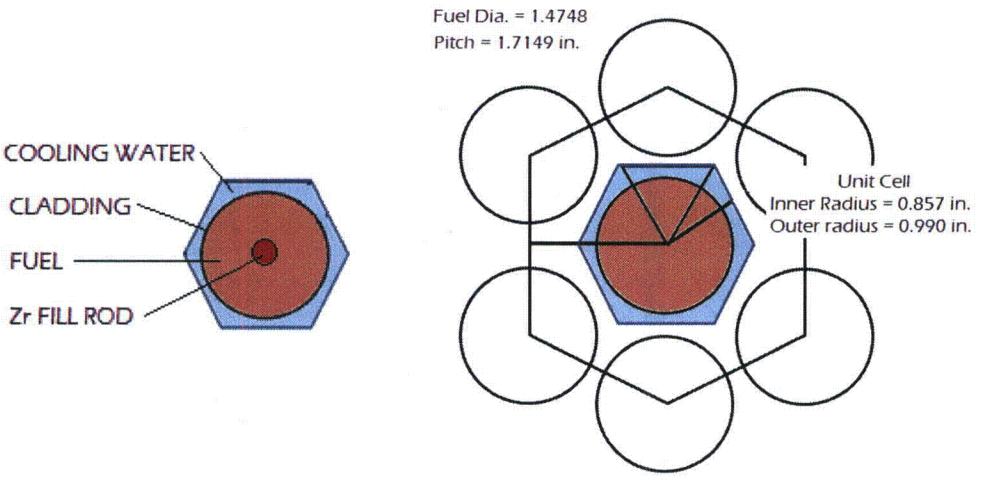

Figure 6, Flow Channel for UT TRIGA

The volume of the flow channel is calculated as the product of the flow area and length. The length of the TRIGA flow channel is defined for the heated (adjacent to fuel) and unheated surfaces of fuel element cladding. The heated length is divided into smaller sections for analysis, consistent with the axial segmenting indicated in Table 1. The geometries and thermal hydraulic parameters of the upper and lower gird plate/fuel element are calculated through equations 2-10, with results summarized in Table 3.

4.1.1 Unit Cell Geometric Parameters

The area of a regular polygon is calculated using the interior radius (r_i) and perimeter (P) as:

$$A = \frac{1}{2} \cdot r_i \cdot P \qquad 2$$

The unit cell is a hexagon (i.e., 6-sided perimeter) with each side one leg of an equilateral triangle; the height of the triangle is the hexagon's interior radius. The hexagon/triangle dimension (a) in terms of the internal radius is calculated:

$$a = \frac{2}{\sqrt{3}} \cdot r_i \qquad 3$$

Substituting 4.1 into 4.2, the cross sectional area of the hexagonal unit cell (A_{UC}) using the interior radius is therefore:

$$A_{UC} = \frac{1}{2} \cdot r_i \cdot \left(6 \cdot \frac{2}{\sqrt{3}} \cdot r_i \right) = 2 \cdot \sqrt{3} \cdot r_i^2 \qquad 4$$

The inner radius of the unit cell is ½ the distance between two fuel elements or ½ of the fuel element pitch (p_e) so that:

$$A_{UC} = \frac{\sqrt{3}}{2} \cdot p_e^2 \qquad 5$$

The cross sectional area of a fuel element (A_F) is calculated:

$$A_F = \pi \cdot \left(\frac{D_F}{2}\right)^2 \qquad 6$$

The area of the flow channel in the unit cell (A_{FC}) is the difference between the unit cell area (eq. 4.1) and the area occupied by fuel (eq. 4.2). Since the interior radius is ½ of the pitch, the area of the flow channel is calculated by:

$$A_{FC} = \frac{\sqrt{3}}{2} \cdot p_e^2 - \pi \cdot \left(\frac{D_F}{2}\right)^2 \qquad 7$$

Non-circular pipes are approximated as a pipe with an equivalent hydraulic diameter (D_h) with a wetted perimeter (P_W), where the hydraulic diameter is calculated as:

$$D_h = \frac{4 \cdot A_{FC}}{P_W} \qquad 8$$

The wetted perimeter is the length of the flow channel in contact with channel wall surfaces (i.e., the perimeter of the fuel element):

$$P_W = \pi \cdot D_F \qquad 9$$

Substituting equations 4.3 and 4.4 for flow area and perimeter into equation 4.5, hydraulic diameter is:

$$D_h = \frac{4}{\pi \cdot D_F} \cdot \left[\frac{\sqrt{3}}{2} \cdot p_e^2 - \pi \cdot \left(\frac{D_F}{2}\right)^2\right] = \frac{2 \cdot \sqrt{3}}{\pi} \cdot \frac{p_e^2}{D_F} - D_F = D_F \cdot \left[\frac{\sqrt{3}}{2} \cdot \frac{p_e^2}{D_F^2} - 1\right] \qquad 10$$

A summary of primary and calculated parameters is provided in Table 3.

9 3, Summary of Principle Thermal Hydraulic Values

Description	Var.	Value							
Fuel Element Pitch	P	1.714	in	0.142833	ft	4.35356	cm	0.043536	m
Fuel Element Diameter	*Dfuel*	1.4784	in	0.123200	ft	3.755136	cm	0.037551	m
Wetted Perimeter	P_W	4.64453058	in	0.387044	ft	11.79711	cm	0.117971	m
Fuel Cross Section/Area	A_{FC}	1.7166185	in^2	0.011921	ft^2	11.07494	cm^2	0.001107	m^2
Unit Cell Area	A_{Cell}	2.54420597	in^2	0.017668	ft^2	16.4142	cm^2	0.001641	m^2
Flow Channel Area	A_{FC}	0.82758747	in^2	0.005747	ft^2	5.339263	cm^2	0.000534	m^2
Hydraulic Diameter	D_h	0.71274154	in.	0.059395	ft.	1.810364	cm	0.018106	m

4.1.2 Unit Cell Thermodynamic Loss Factors

Pressure drops (head loss) across hydraulic components are the product of the fluid flow and factors such as the coefficient of friction between the fluid and the pipe wall, changes in flow area and diameter, flow channel surface roughness, and/or flow channel length. Within limits, the factors (K factors) are constant, the sum of the pressure drops in linear flow is additive. This analysis provides a traditional approach to evaluating the loss factors and loss factors reported by analysis and experiments conducted at the UT reactor, followed by the results of analysis and experiments conducted for the UTTRIGA facility.

Traditional Loss Factor Calculations

The impact of sudden expansion or contraction is principally in velocity changes. Bernoulli's equation applied to non-compressible fluids relates area and velocity. The K factors for sudden expansions or contractions are based on the ratio of the flow areas (Equation 7).

$$K_e = \left[1 - \frac{d_1^2}{d_2^2}\right] = \left[1 - \frac{A_1}{A_2}\right] \qquad 11$$

Other K factors are based on the magnitude of the direction change, the pipe surface roughness, and flow mode (turbulent, laminar, etc.). Calculations are simplified by using the Darcy-Weisback friction factor (f) as a multiplier on applicable aspects of system geometry. The friction factor is a function of the Reynolds number, wall surface roughness, and flow channel. The relationship is described in the Colebrook formula:

$$\frac{1}{\sqrt{f}} = -2.0 \cdot \log_{10} \cdot \left(\frac{\varepsilon}{3.7 \cdot D} + \frac{2.51}{\mathrm{Re} \cdot \sqrt{f}} \right) \qquad 12$$

In practice, the Moody chart (Fig. 7, a parametric representation of the friction factors) is frequently used to determine the friction factor. For reasonable and expected flow rates at the TRIGA reactor, the Reynolds number is between $1X10^4$ and $3X10^5$. Over this range, convergence exists for wall surface roughness values between $5X10^{-7}$ to $1X10^{-3}$. The broad range of surface roughness values indicates a very low sensitivity for roughness, and that any surface roughness within this range can be used without affecting the friction factor significantly. For comparison RELAP analysis conducted for DOW Chemical[2] reactor used surface roughness of 2.13E-6.

For losses in a straight pipe:

$$K = f \cdot \frac{L}{D} \qquad 13$$

For a 45° turn:

$$K_{45} = f \cdot 16 \qquad 14$$

For a 90° turn:

$$K_{90} = f \cdot 30 \qquad 15$$

[2] ANALYSIS OF THE THERMAL HYDRAULIC AND REACTIVITY INSERTION BEHAVIOR OF THE DOW TRIGA RESEARCH REACTOR, Submitted to the NRC in support of the DTRR License Renewal (M. H. Hartman, 03/12/2011).

Table 4: Channel End Geometry

Location	Component	Eff. Area
Bottom Entrance	Lower grid plate	1.2 cm^2
Bottom Exit	Lower End fitting/Channel	3.9 cm^2
Top Entrance	Upper End Fitting/ Channel	3.9 cm^2
Top Exit	Upper Grid Plate	1.2 cm^2

The K factor for elevations above the flow channel is based on a 45° turn out of the main channel (0.344) and sudden contraction at the upper grid plate (0.43). The K factor below the flow channel is based on a sudden expansion exiting the grid plate (0.9) and a 45° turn (0.344) into the main channel. Therefore the K factors are 1.244 at the inlet and 0.844 at the outlet. The results of calculations for K factors associated with the hydraulic parameters in Tables 3 and 4 and are provided in Table 5.

Table 5: Classical K factors

Location	Characteristic	K Factor
	45° Turn[3]	0.344
Inlet	Expansion	0.9
	TOTAL lower	1.244
	45° Turn	0.344
Outlet	Contraction	0.43
	TOTAL Upper	0.774

Correlation of K factors and flow are based on historical, experimental measurements with cylindrical pipes. Additional work validated this approach for rectangular ducts. In practice, non-circular cross sections are reduced to a flow area and hydraulic diameter with the length as measured for the pipe. However, the complexity of the TRIGA inlet and exit flow channel geometry is challenging. As fluid interacts with non-circular structures (or components), non-uniform surfaces can result in forces leading to secondary and/or internal flow paths that affect head loss/pressure drops. This suggests two potential issues using K factors calculated classically in analyzing thermal hydraulic response of the TRIGA reactor.

- The actual entrance and exit to the flow channel between the grid plates is directed by fins mounted on a conical shape that terminates in cylindrical alignment (bottom end fitting) and handling (upper end fitting) structures. The wetted perimeters and flow areas vary continuously from entrance and exit for each end fitting.

- The interface between adjacent fuel channels is not separated by a physical boundary. Differential pressure between adjacent flow channels at interfaces can support cross-channel flow.

Therefore thermal hydraulic analysis to support relicensing was developed[4] to:

(1) Model the UT TRIGA reactor using TRACE

(2) Develop an independent solution tool using MATLAB to calculate thermal hydraulic performance based on mass and energy balance and K factors,

[3] Friction factor times 16

[4] Development of Thermal Hydraulic Correlations for the University of Texas at Austin TRIGA Reactor Using Computational Fluid Dynamics and In-Core Measurements, A. D. Brand

(3) Develop a computational fluid dynamics model using FLUENT, and

(4) Conduct experiments to develop a UT TRIGA specific heat transfer correlation

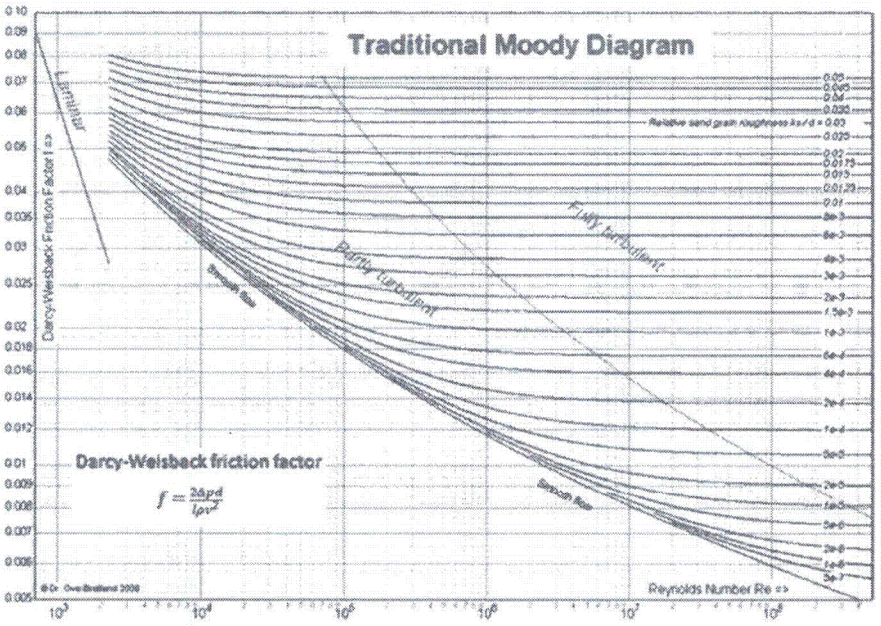

Figure 7, Moody Diagram

These methodologies were used to independently model thermal hydraulic performance from (1) first principles, (2) TRACE thermal hydraulics code, and (3) FLUENT computational fluid dynamics code. The results of experiments in the TRIGA core were used to evaluate UTTRIGA-specific K factors based on actual fuel element geometry. A summary of K values determined from both the traditional/classical method and the UT analysis is provided in Table 6, with a fractional deviation between factors provided. For comparison, RELAP work[5] performed for DOW Chemical facility used K factors of 2.26 and 0.63 for the lower and upper channels.

Table 6, K Factors

APPLICATION	CLASSICAL	FLUENT[6]	DEVIATION
Lower Channel	1.244	1.63	23.7%
Upper Channel	0.844	1.12	33.6%

The values determined from the UT research program were used in modeling for TRACE calculations.

4.2 Physical UTTRIGA Thermal Hydraulic Model

Standard TRACE components are structured to simulate physical characteristics of flow loop components. Descriptions of the TRACE components required to characterize the UTTRIGA hot channel are provided below, followed by the specific facility application.

[5] ANALYSIS OF THE THERMAL HYDRAULIC AND REACTIVITY INSERTION BEHAVIOR OF THE DOW TRIGA RESEARCH REACTOR, Submitted to the NRC in support of the DTRR License Renewal (M. H. Hartman, 03/12/2011).

4.2.1 Fluid System Component Modeling

TRACE analysis is based on modeling a set of representative, defined components where component characteristics are specified by the user to model the system. The UTTRIGA model uses Break , Pipe, Heat Structure, and Power Components. Heat structure material properties are used to calculate temperature distribution for fuel element components (zirconium fill rod, U-ZrH matrix, gas gap, and cladding).

a. Break: A break component is a boundary component normally used to provide a sink for liquid flows exiting the system. TRACE also uses a "Fill" as a similar component for inlet flows, but the fill flow rate is specified by the user while flow rate in a break is developed in calculations, and therefore not constrained. Since flow rates in the UTTRIGA model are developed by convection during reactor operation, the flow rate is not specified as an input. Therefore the use of a fill is precluded and breaks are used to specify both the entrance and exit conditions.

b. Pipe: The pipe component is a cylindrical volume containing water flow with various geometric and hydrodynamic properties. Analysis of the flow loop requires the flow across changes in elevation balance. Analysis requires limits on the magnitude of changes in adjacent flow areas.

b. Heat Structure: TRACE defines heat structures as rigid components that absorb, transfer, or radiate heat. A heat structure is specified by geometry, inner and outer radial boundary conditions, and material information. These attributes are specified in the "general" section. Power distribution is specified in the "Power Component" section of TRACE.

   Heat structure cells are axially uniform. Geometry is specified in the "Radial Geometry" section. Geometry includes both radial data which is constant along the axial length of the structure, and axial data that identifies surface areas for heat transfer. Initial conditions for the surfaces at each axial location are specified in "Initial Temperature." The gas gap heat transfer coefficient is explicitly specified the TRACE in the "Gas Gap HTC." Boundary conditions for heat transfer are specified for axial nodes/surfaces, linking the heat source to the heated lengths of the pipe to represent the active (fueled) part of the fuel element.

e. Power Component: The power component specifies how power is provided to the heat structure.

   The shape of power distribution in TRACE is managed by specifying the fraction of power supplied between the inner and outer radial boundaries at each axial node. The "power shape" section of the power component is used to specify a 2 dimensional distribution. The power distribution fractions are specified based on axial and radial locations that segment the fuel element.

   The Numerical solutions to the heat transfer equations are determined iteratively in TRACE. Iterative calculations with large step changes may lead to instability in solutions. A Power Table in the "general" section of the power component allows time based changes to simulate steps in calculation leading to a final power level.

f. Materials: TRACE has a limited set of material characteristics applicable to nuclear power plants. The default set of materials can be augmented by the user.

   User defined materials are defined either in a data table or a functional fit table. The functional fit is a 5^{th} order polynomial in temperature, although setting the coefficients to 0 can reduce the order of the polynomial. Properties are specified over a range of temperature, and include (1) density, (2) specific

heat , (3) thermal conductivity, and (4) emissivity.

4.2.2 UTTRIGA Application

TRACE components were assembled to model the thermal hydraulic performance of the unit cell flow channel as shown in Fig. 8. User supplied values for the source, downcomer, connecting pipe, fuel element, and sink simulate the thermal hydraulic characteristics of the components.

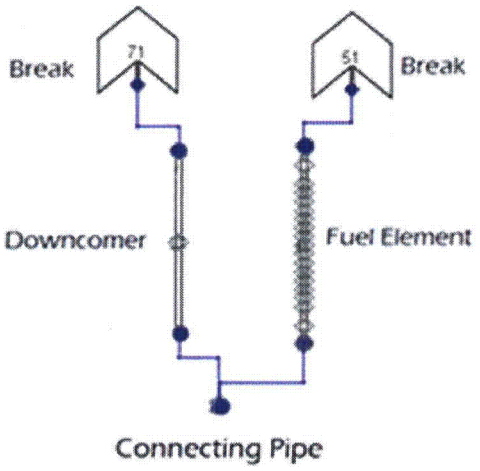

Figure 8, TRACE Model

a. Break Components applications:

The TRIGA hot channel pressure and temperature specifications are based on local environmental conditions (barometric pressure, confinement pressure regulation) and the pool (level and water temperature), specified as in the TRACE break component.

The NETL building is approximately 240 m above sea level, corresponding to 96 kPa at standard atmospheric conditions. The reactor bay confinement system is designed to control differential pressure to 0.06 in. (14.9 Pa) below atmospheric (minimal compared to atmospheric pressure). Total pressure at the top of the core is therefore:

$$p_T = 96\{KPa\} + p_{H_2O} \qquad 16$$

Pool water is a minimum of 5.25 m above the core, nominally 7.25 m. Constant pressure is established by setting the "rate of change" variable to zero in the break. Pool water temperature is limited to less than 49 °C, nominally 25-27 °C. Where g denotes the gravitational constant (9.8 $m \cdot s^{-2}$), the pressure (p_{H2O}) exerted by a column of water (at density ρ in $kg \cdot m^{-2}$and height h in m) is given by:

$$p_{H_2O} = \rho \cdot g \cdot h \qquad 17$$

A second break is connected to the exit of the core, simulating exit from the flow channel. Parameters associated with the exit are the same as the entrance. Pressure boundary conditions for

the limiting and nominal cases are provided in Table 7.

Table 7, Pressure Boundary Condition

Condition	Temp	Density	Height	Hydrostatic Pressure	Pressure	Pressure
	°C	$kg \cdot m^{-2}$	m	kPa	kPa	psia
Limiting	49	988.4881	5.25	50.9	146.9	21.3
Nominal	25	997.0479	7.25	70.8	166.8	24.2
	27	996.5162	7.25	70.8	166.8	24.2

b. Pipe applications:

Three pipes are used in modeling. One pipe represents movement of cooling flow from the top to the bottom of the flow channel. A second pipe moves flow to the entrance of the flow channel, connecting the down comer to the third pipe, the flow channel.

Down Comer/Cold Leg

Conservation requirements for calculations require balanced elevation changes, with a "downcomer" at the same length and area as the fuel element region. Instabilities can occur in TRACE calculations if adjacent volumes are sufficiently different, and the downcomer is segmented to meet the ratio criteria (for convenience, segmenting has equal lengths). Dimensions for the downcomer pipe are provided in Table 8.

Table 8, Down-comer Pipe

Length (segments)	0.09985 m
Length (total)	0.5991 m
Flow area	5.39E-4 m^2
Volume (segments)	5.38E-5 m^3
Volume (total)	3.23E-4 m^3
Hydraulic diameter	0.0183 m
Height Change (segments)	-0.09985 m
Height Change (total)	-0.5991 m

Connector

A pipe with two elbows (Fig. 9) connects flow from the downcomer to the unit cell flow channel. Dimensions of the connecting pipe are provided in Table 9.

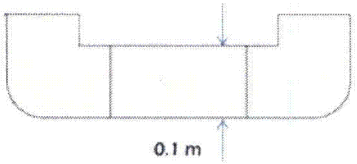

Figure 9, Cold Leg to Flow Channel Connector

Table 9, Connecting Pipe

SEGMENT	VOLUME	LENGTH	FLOW AREA	HEIGHT CHANGE
	m^3	m	m^2	m
1	5.38E-05	0.01	5.39E-04	-5.0E-3
2	5.38E-05	0.01	5.39E-04	0.0
3	5.38E-05	0.01	5.39E-04	5.0E-3

Unit Cell Flow Channel/Fuel Element Region

The flow channel for the fuel element region in the unit cell is modeled as a pipe. Specifications for the simulated fuel element cooling channel are provided in Table 10. Inlet and outlet geometry are reduced to loss factors (previously discussed K). The K factors as previously described are applied to the 2nd and the 19th segments.

Table 10, Specifications for Unit Cell Flow Channel

	VOL m^3	LENGTH m	FLOW AREA m^2	Δz m
1	5.14E-06	0.01905	2.70E-04	0.01905
2	2.43E-05	0.09	2.70E-04	0.09
3	6.86E-06	0.0254	2.70E-04	0.0254
4	6.86E-06	0.0254	2.70E-04	0.0254
5	6.86E-06	0.0254	2.70E-04	0.0254
6	6.86E-06	0.0254	2.70E-04	0.0254
7	6.86E-06	0.0254	2.70E-04	0.0254
8	6.86E-06	0.0254	2.70E-04	0.0254
9	6.86E-06	0.0254	2.70E-04	0.0254
10	6.86E-06	0.0254	2.70E-04	0.0254
11	6.86E-06	0.0254	2.70E-04	0.0254
12	6.86E-06	0.0254	2.70E-04	0.0254
13	6.86E-06	0.0254	2.70E-04	0.0254
14	6.86E-06	0.0254	2.70E-04	0.0254
15	6.86E-06	0.0254	2.70E-04	0.0254
16	6.86E-06	0.0254	2.70E-04	0.0254
17	6.86E-06	0.0254	2.70E-04	0.0254
18	2.43E-05	0.09	2.70E-04	0.09
19	5.14E-06	0.01905	2.70E-04	0.01905
Total	1.62E-04	0.5991	5.13E-03	0.5991

c. Heat Structure Application

The heat structure consists of 15 axial cells connected to the heated section of the flow channel (cells 3 through 17 of the unit cell flow channel pipe). "Outer surface boundary" conditions are connected to the unit cell pipe segments, with "Inner Surface Boundary Conditions" of 0.

Heat structure cells simulate the zirc fill rod at the center of the fuel element, ZrH-U fuel, the gap between the fuel and cladding, and the cladding. The UTTRIGA model includes:

- zirconium from a radius of 0 cm to 0.3175 cm (3.175E-3 m)
- zirconium-hydride from a radius of 0.3175 cm to 1.74117 cm (0.0174117 m), subdivided into 15 equal volume segments
- gap gases from a radius of 1.74117 cm to 1.8161 cm (0.018161 m)
- stainless steel 403 cladding from a radius of 1.8161 cm to 1.8263 cm (0.018263 m)

The gas gap heat transfer coefficient[7] of 2840 W m^{-2} K^{-1} is specified in TRACE as "Gas Gap HTC."

Power distribution is accomplished in the heat source geometry. The axial segments are divided

[7] Reference for the gas gap heat transfer coefficient

radially to provide equal volume segments. As previously discussed, heat generation is distributed in the heat structure based on SCALE transport calculations, based on the fission rate in each segment. The SCALE model provides data for each of the 225 segments of the radial and axial boundaries, and the complete distribution is used in TRACE (Power Component section).

d. Power component: Two sections of the power component module are used in the UTTRIGA model, "General," and "Power Shape."

General

Large changes in power can cause instability in calculation; the "Power Table" allows incremental steps at user specified times form a minimum to maximum power, allowing the calculation to stabilize. This function is accomplished in RELAP through a data table in the Control Systems section.

Power Shape

The 2-dimensional fission density profile as described previously is used in the TRACE power shape.

e. Materials: Material data is specified in the Thermal section of TRACE Materials section. A library of reactor material characteristics are provided, but only "gap gases" and "Stainless 304" apply to TRIGA fuel; characterization of ZrH-U fuel and zirconium is required.

The thermal conductivity of TRIGA fuel is noted to be 0.042 $cal \cdot s^{-1} cm^{-1} \cdot °C^{-1}$ (17.573 $W \cdot m^{-1} \cdot °K^{-1}$) [8], insensitive to temperature. The volumetric heat capacity calculated ($C_{,p}$, referenced to temperature T in °C) as:

$$C_{p(U-ZrH,1.6)} = 2.04 + 4.17x10^{-3} \cdot T \left\{ \frac{W \cdot s}{cm^3 \cdot ° C} \right\} \qquad 18$$

Specific heat capacity is calculated by normalizing the volumetric heat capacity by the density (ρ), with the density of the fuel in the matrix ($\rho_{U\text{-}ZrH1.6}$) calculated as:

$$\rho_{U-ZrH,1.6} \left\{ \frac{g}{cm^3} \right\} = \frac{1}{\frac{w_U}{\rho_U} + \frac{w_{ZrH}}{\rho_{ZrH}}} \qquad 19$$

With subscripts indicating Uranium and Zirconium-Hydride, the weight-percent of the components represented as w, the density of $ZrH_{1.6}$ ($\rho_{ZrH1.6}$) is reported as:

$$\rho_{ZrH,1.6} \left\{ \frac{g}{cm^3} \right\} = 0.1706 + 0.0042 \cdot 1.6 = 5.6395 \qquad 20$$

Calculations of U-ZrH density and heat capacity (specific C_p - as determined by $C_{p,v}$ normalized to the density) at a wide range of temperatures were performed (Table 4.10).

Thermal conductivity for the zirconium fill rod at the center of the fuel element was taken (even 100 temperature values) from the *Journal of Physical and Chemical reference Data (Volume 3, 1974,*

[8] Simnad, *The U-ZrHx Alloy: Its Properties and Use in TRIGA Fuel* (August 1980)

Supplement 1, Table 184), with intermittent values interpolated. Volumetric heat capacity data was taken from a compilation[9], with data interpolated by a curve fit. Mass-specific heat capacity used in TRACE is calculated as the ratio of the volumetric heat capacity to the density. Zirconium data is provided in Table 11.

Table 11, TRIGA Fuel and Zirconium Material Properties

TRIGA Fuel ($ZrH_{1.6}$-U)				Zirconium (Fill Rod)				
T	$C_{p,v}$	ρ	C_p	$C_{p,v}$	ρ	C_p	Conductivity	Emiss.
°K	$J \cdot m^{-3} \cdot K^{-1}$	$kg \cdot m^{-3}$	$W \cdot s \cdot kg^{-1} \cdot K^{-1}$	$J \cdot m^{-3} \cdot K^{-1}$	$kg \cdot m^{-3}$	$W \cdot s \cdot kg^{-1} \cdot K^{-1}$	$W \cdot m^{-1} \cdot K^{-1}$	
200	1.73E+06	6000.507	2.89E+02	1.71E+06	6520	261.7	25.2	0.8
300	2.15E+06	6000.507	3.59E+02	1.76E+06	6520	269.62	22.7	0.8
350	2.36E+06	6000.507	3.93E+02	1.81E+06	6520	276.91	22.1	0.8
400	2.57E+06	6000.507	4.28E+02	1.83E+06	6520	280.56	21.6	0.8
450	2.78E+06	6000.507	4.63E+02	1.85E+06	6520	284.21	21.3	0.8
500	2.99E+06	6000.507	4.98E+02	1.88E+06	6520	287.86	21	0.8
550	3.19E+06	6000.507	5.32E+02	1.90E+06	6520	291.51	20.85	0.8
600	3.40E+06	6000.507	5.67E+02	1.92E+06	6520	295.16	20.7	0.8
650	3.61E+06	6000.507	6.02E+02	1.95E+06	6520	298.81	20.8	0.8
700	3.82E+06	6000.507	6.37E+02	1.97E+06	6520	302.46	20.9	0.8
750	4.03E+06	6000.507	6.71E+02	2.00E+06	6520	306.11	21.25	0.8
800	4.24E+06	6000.507	7.06E+02	2.02E+06	6520	309.76	21.6	0.8
850	4.45E+06	6000.507	7.41E+02	2.04E+06	6520	313.41	22.1	0.8
900	4.65E+06	6000.507	7.76E+02	2.07E+06	6520	317.06	22.6	0.8
950	4.86E+06	6000.507	8.10E+02	2.09E+06	6520	320.7	23.15	0.8
1000	5.07E+06	6000.507	8.45E+02	2.10E+06	6520	322.53	23.43	0.8
1050	5.28E+06	6000.507	8.80E+02	2.11E+06	6520	324.35	23.7	0.8
1100	5.49E+06	6000.507	9.15E+02	2.14E+06	6520	328	24.3	0.8

[9] http://www.efunda.com

5.0 Model Validation

TRACE calculations were performed for flow channel/fuel element power levels from 200 watts to 29 kW. Fuel element and cooling temperatures are calculated as the TRACE heat structure. The temperature response to power generation was evaluated using the UTTRIGA model. Fuel temperature observations (operating data) at varying power level are provided (Table 12). The relationship between power level and (fuel element) component material temperature was evaluated from TRACE thermal hydraulic calculations. This methodology is based on flow channel analysis, while the temperature data is correlated to core power. Observations were compared with the two independent measuring channels. Temperatures calculated by TRACE consistent with the nominal thermocouple locations were compared to observations.

There is no measurement available for flow rates or heat fluxes that would allow comparisons with calculations of mass flow rate or critical heat flux ratio, CHFR (the ratio of fuel element local heat flux to the heat flux that could result in departure form nucleate boiling). Model validation is supported by comparing results to data associated with accepted reference work. Thermal hydraulic data from TRACE is used to calculate the mass flow rate and the ratio of heat flux at each power level to critical heat flux.

5.1 Temperature Calculations

Temperatures of materials in the TRACE heat structure for flow channels/fuel element operation at selected power levels are provided in Figs. 10 and 11 for selected power generation levels. Locations bounding the zirconium filler at the center of the fuel element, thermocouples, and cladding are marked for reference in Fig. 10.

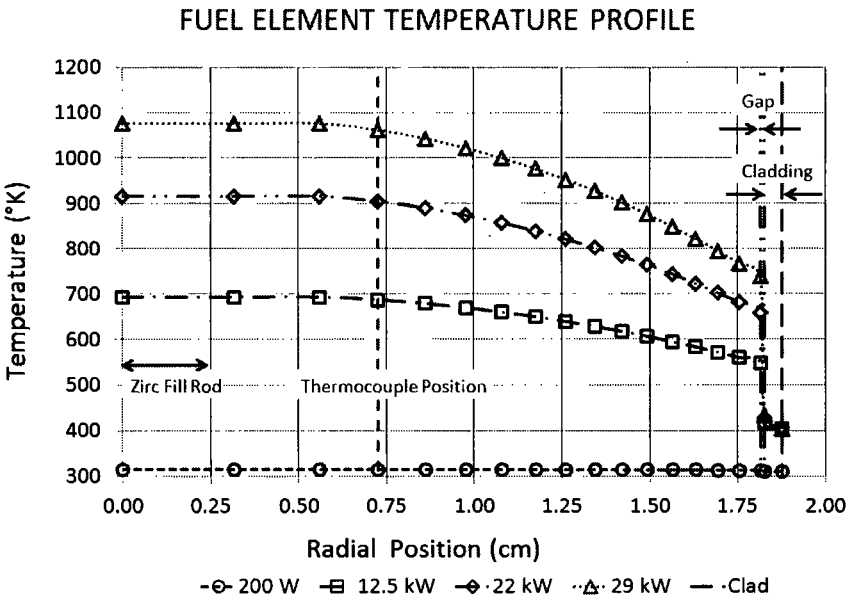

Figure 10, Fuel Element Temperature Radial Profile

5.1.2 Operating Data

Instrumented fuel elements (IFEs) are located in the B ring (currently B03 and B06). Power level, fuel temperature, and control rod position data are routinely recorded in nuclear engineering exercises at 20 kW, 60 kW, 100 kW, 500 kW, 750 kW and 950 kW. Data (taken in 2013) is provided in Table 12

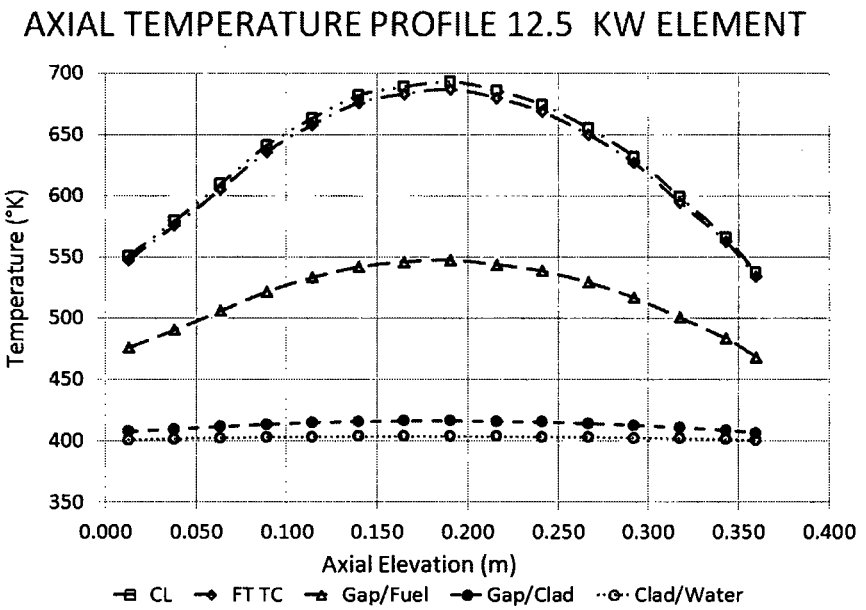

Figure 11, Fuel Element Temperature Axial Profile

Table 12, Operating Data

Core Pwr (kW)	FT1 °C	FT2 °C	Pool °C
20	27	32	19
60	47	60	19
100	68	86	19
250	136	171	19.4
500	221	264	20.7
750	278	331	23
950	319	370	23.4

Confirmatory measurements during the summer of 2014 showed minimal deviation from the 2013 measurements. Based on historical values and confirmatory measurements, temperature response to the heat generated during reactor operation is well characterized by the values in Table 12 and Fig. 12.

Core power is distributed non-uniformly across all fuel elements bas on the ratio of the power in an individual element to the average across all elements, or peaking factor. Fission data from SCALE burnup calculations modeling the fuel materials form the initial 1992 core to the current 14 element core was used to determine the peaking factors for B03 and B06. The B03 peaking factor was calculated to be 1.49, with the B06 peaking factor 1.52.

5.1.3 Comparing FT1 and FT2 Measurements to UTTRIGA Model Calculations

Pool temperatures varied during operation for measurement data points, while calculations are performed using a single value for pool temperature. Therefore, values from thermocouple readings were corrected to allow direct comparison between observed and calculated temperatures. Observed temperatures were modified by subtracting pool temperature and adding a 300°K correction to agree with pool temperature in calculations and perform unit conversion (Table 13, Fig. 11).

Table 13, Fuel Temperature Data

Core Power (kW)	B03 Power (W)	Corrected FT1 Temp °K	B06 Power (W)	Corrected FT2 Temp °K
20	261	308	267	313
60	784	328	800	341
100	1,307	349	1,333	367
250	3,268	417	3,333	452
500	6,535	500	6,667	543
750	9,803	555	10,000	608
950	12,417	596	12,667	647

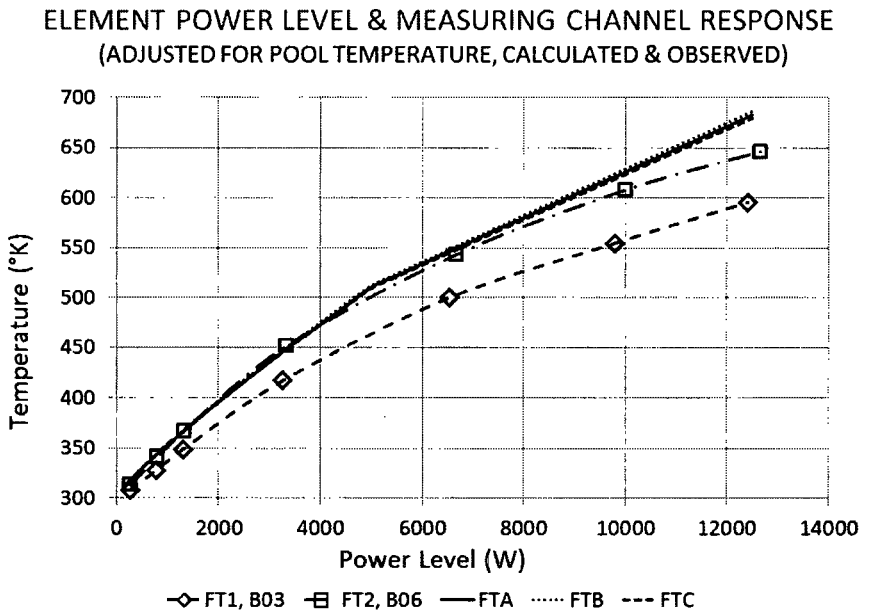

Figure 12, FT2 Temperature Response to Core Power Level

The FT1 data response is qualitatively similar to calculations (and FT2), but the FT1 indication diverges by about 12% from calculated temperatures.

The FT2 data is remarkably consistent with calculated temperatures, with some divergence at higher power (Fig. 12). The strong correlation between observed and calculated fuel temperatures for FT2 begins to deviate at core power levels greater than 750 kW, calculated B06 power greater than 1000 W. Calculations indicate conservative values (i.e., higher temperatures). There are several possible explanations.

As previously noted, flow channels are not well isolated from adjacent flow channels. Significantly different hydrostatic or hydrodynamic conditions at the boundary could affect flow rates. However, flow and local pressures calculated at power levels associated with adjacent fuel elements are not significantly different from values for the B03 position.

During full power operations, there is frequently a vigorous stream of bubbles entrained in coolant flow from the core to the pool surface. The onset of nucleate boiling occurs in circular TRIGA cores as low

as 210 kW[1]. However, subcooled nucleate boiling effects are extremely short range and cannot survive distance required to exit the flow channel. These bubbles have the potential to affect system dynamics. Nitrogen solubility decreases as depth and temperature increase[2]. The change in depth as water passes through the core causes a decrease of approximately 6% in nitrogen gas solubility. At 750 kW, the maximum water temperature result in an additional 41% decrease in solubility as cooling water passes through the channel. With a nearly 50% decrease in nitrogen gas solubility occurring over 38.1 cm of heated water, some nitrogen degassing is possible. Nucleate boiling from the fuel element surfaces may provide nucleation sites for evolution of nitrogen bubbles.

These effects are not modeled, but could contribute to a complex flow with additional mixing action. Potential for these mixing effects is minimized at the low water temperature changes associated with low power levels. Higher flow associated with better mixing would cause lower fuel temperatures in the B ring fuel elements as local water temperatures increase and affect nitrogen solubility. This mechanism is consistent with the observed deviation between fuel temperature measuring channels and thermal hydraulic calculations that occurs at power levels greater than about 750 kW.

5.1.4 FT1 and FT2 Comparisons

The close agreement between FT2 and calculated data in conjunction with the lower agreement between FT1 and calculated data prompted closer evaluation of FT1 and FT2. Both measuring channels qualitative response to power was similar (see Fig. 12), indicating the two thermocouples were responding in a similar manner, but the temperature indicated by the FT1 measuring channel was much lower than expected.

The FT1 and FT2 fuel elements (B03 and B06, respectively) are functioning at some fraction of the core power determined by the peaking factor. Fundamentally, heat transfer (Q) is based on temperature difference (T_{CL} as maximum fuel temperature, T_b as bulk cooling temperature, A as the heat transfer area) driving heat transfer though a system with an overall heat transfer coefficient (h):

$$Q = h \cdot A \cdot \left(T_{CL} - T_b\right) \qquad 21$$

The thermocouples in B03 and B06 are nominally located 0.762 cm from the center of the fuel element, with one installed an inch above the mid-plane, a second at the mid-plane, and a third an inch below the mid-plane. Consequently, the monitored temperature is slightly below the centerline temperature. However, the difference between the temperature at the nominal IFE position and the maximum centerline temperatures over a wide range of power levels is small, ranging from virtually no difference to a few per cent.

Factors implicit in the overall heat transfer coefficient depend on the magnitude of heat generated. Different power levels could have different heat transfer coefficients, but the small difference in power between B03 and B06 (indicated by the ratio of the peaking factors) would result in comparable heat transfer coefficients.

The difference in temperature between fuel measuring channel and coolant temperatures is therefore approximately proportional to power, where the heat transfer from B03 and B06 have approximately the

---

[1] *Thermohydraulics Analysis of the University of Utah TRIGA Reactor of Higher Power Designs,* P.M. Babitz, University of Utah, December 2012

[2] EIFAC. 1986. Report of the working group on terminology, format and units of measurement as related to flow-through and recirculation system. European Inland Fisheries Advisory commission. Tech. Pap., 49. 100 pp. & Multiphase Flow Dynamics. http://dx.doi.org/10.1007/978-3-642-20749-5_11 Springer Berlin Heidelberg 2012-01-01 A Kolev, Nikolaylvanov P 209-239

same constant of proportionality (a factor of $h \cdot A$). At a specific average core power, the ratio of the power produced in the two fuel elements with peaking factors PF_{B03} and PF_{B06} is:

$$\frac{PF_{B06}}{PF_{B03}} \sim \frac{(T_{FT1} - T_b)}{(T_{FT2} - T_b)} \qquad 22$$

The ratio of the peaking factors derived from SCALE calculations B03 and B06 in the 114 element core at nominal operating temperature is 0.98. However, the data in Table 13 shows ratios of values derived from FT2 and FT1 (in absolute temperature) to be approximately 0.91. The FT2 agreement with calculated data suggests that B06 the peaking facto is appropriate. Agreement can be forced by adjusting the FT1 peaking factor, but agreement is achieved only with values approaching 1.1, which is not considered likely.

Portable thermocouple instrumentation showed the two functional spare thermocouples in B06 to agree within a few degrees to the fuel temperature measuring channel at 950 kW operations. The unmonitored thermocouple in the instrumented fuel element of B03 was found to be significantly higher than the installed FT1 channel. The spare thermocouple in B03 was therefore installed in to the FT1 fuel temperature channel, and a test operation showed FT1 indication at a 950 kW test operation of 343°C (611°K).

Since application of the peaking factor for B06/FT2 resulted in agreement between calculated and measured data, and since an unrealistic peaking factor would be required to bring the B03 data into agreement, the transport calculations were not considered a likely source of the disagreement. Since the characteristic response to changes in power level indicated on FT1 and FT2 were qualitatively similar, neither the instrument nor the thermocouple was considered the likely source of the disagreement.

If the radial position of the thermocouple previously in the FT1 channel is different than the nominal value, the channel response would be qualitatively similar but biased to temperatures associated with the different positon. Inspection of calculated temperature data for 12500 W indicates fuel temperature is 605°K at the lower thermocouple axial position (1 in. below mid plane) at a radial position of 1.495 cm. This approaches the measured value of 596°K for the B03 power of 12417 W. Therefore as a test case, temperatures at a radial positon of 1.495 cm as a function of power were compared to measured data for with good agreement.

Although the non-nominal positioning of the thermocouple in B03 is a plausible explanation for the disagreement between FT1 and temperature calculated data, the thermocouple position cannot be directly measured or observed. Given the uncertainty in the FT1 data and the loss of confidence in historical temperature data (replacement of the thermocouple), FT1 data was disqualified for model validation.

5.1.5 Summary

Data from an installed fuel measuring channel (FT2) is used in comparing model calculations to observed data. The comparison of TRACE temperature calculations to the FT2 measuring channel gives confidence that the models predict reasonably accurate values for fuel temperature calculations. The calculations are less accurate, but conservative, at power levels exceeding about 750 kW.

5.2 Comparison to Reference Thermal Hydraulic Analysis

Benchmark data is not available to validate the use of TRACE for thermal hydraulic analysis, except to the extent that the model is capable of predicting fuel temperature where the fuel element is cooled by water

flow. Nevertheless, RELAP has a long history in analysis of TRIGA systems, and TRACE is the current platform endorsed by NRC (incorporating RELAP and TRAC codes). A comprehensive review of methods for predicting power at which critical heat flux occurs in TRIGA fuel is documented in ANL/RERTR/TM-07-01[3]; the report provides thermal hydraulic data for comparing the UTTRIGA calculations to a generic hexagonal TRIGA core:

- Mass flow rates calculated by the UTTRIGA model using TRACE are compared to the reference document (RELAP) values.

- Axial distribution of critical heat flux ratios from the UTRRIGA model using TRACE is compared to the reference document values.

5.2.1 Coolant Flow Rates

Data from ANL/RERTR/TM-07-01 (Fig. 4) for mass flow rate is used as reference for comparison of values calculated with the UTTRIGA TRACE model. The UTTRIGA cooling water inlet was assumed to be 30°C to be consistent with reference-data inlet cooling water temperature. Power levels considered in the reference extend considerably higher than the UTTRIGA data used in temperature comparisons.

The reference document was based on RELAP calculation, with a different algorithm for flow calculations. Calculated TRACE UTTRIGA model flow rates are within a factor of 2 of the reference calculation flow rates (Fig. 13). The difference in flow rates between the TRACE and the reference RELAP calculations is reasonable.

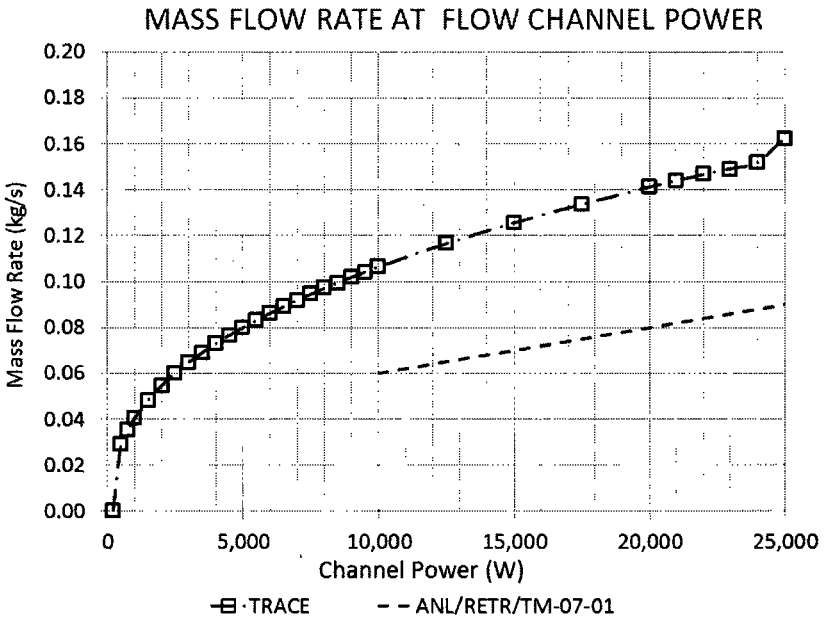

Figure 13, Comparison of Calculated Flow Rates for UTTRIGA and Reference Calculation

5.2.2 Critical Heat Flux Ratio Calculations

Critical heat flux ratio (CHFR) is the ratio of the critical heat flux (CHF) to the actual heat flux. The correlation for critical heat flux developed by Bernath is recommended for evaluating TRIGA fuel

[3] ANL/RERTR/TM-07-01, Fundamental Approach to TRIGA Steady-State Thermal-Hydraulic CHF Analysis (E.E. Feldman, Nuclear Engineering Division, Argonne National Laboratory) 2007

performance[4]. The Bernath correlation (where CHF_{BO} is the heat flux that results in burnout h_{BO} is the convection heat transfer correlation at burnout, $T_{W,BO}$ is the temperature of the cladding surface at burnout, and V is the fluid velocity, T_b is the cooling water bulk temperature, and dimensional variables as previously described determines the critical heat flux that results in burnout as:

$$CHF_{BO} = h_{BO} \cdot \left(T_{W,BO} - T_b\right) \quad 23$$

Where the heat transfer coefficient for burnout conditions is calculated:

$$h_{BO} = 10890 \cdot \frac{D_e}{D_e + D_i} + V \cdot \frac{48}{D_e^{0.6}} \quad 24$$

The formula predicting wall temperature at burnout is:

$$T_{W,BO} = 57 \cdot \ln P - 54 \cdot \frac{P}{P+15} - \frac{V}{4} \quad 25$$

Substituting equations 14 and 15 into equation 13 results in:

$$CHF_{BO} = \left[10890 \cdot \frac{D_e}{D_e + D_i} + V \cdot \frac{48}{D_e^{0.6}}\right] \cdot \left(\left[57 \cdot \ln P - 54 \cdot \frac{P}{P+15} - \frac{V}{4}\right] - T_b\right) \quad 26$$

The Bernath formulation is in "pound centigrade units," converted to BTU h^{-1} ft^{-2} by a factor of 1.8.

$$W_{CHF} = 1.8 \cdot \left[10890 \cdot \frac{D_e}{D_e + D_i} + V \cdot \frac{48}{D_e^{0.6}}\right] \cdot \left(\left[57 \cdot \ln P - 54 \cdot \frac{P}{P+15} - \frac{V}{4}\right] - T_b\right) \quad 27$$

The results of calculations of CHFR calculations at 29 kW based on TRACE shows reasonable agreement from the reference document (based on RELAP) at 30 kW. There is a slight shift in the location of the minimum CHFR that would be expected at higher flow rates as calculated for the UTTRIGA model).

5.2.3 Comparison to Reference Values

Critical heat flux calculations using the Bernath correlation and RELAP data were performed by Feldman (op. cit.) for typical TRIGA reactor configurations. The UTTRIGA TRACE ran stably up to 29,000 W, while the maximum RELAP calculation ran at 30,000 W. There is some difference in flow calculations are performed (previously noted). Nonetheless, the TRACE model shows results similar to the reference (Fig. 14), providing confidence that the model provides reasonable results in thermal hydraulic calculations.

[4] ANL/RERTR/TM-07-01,

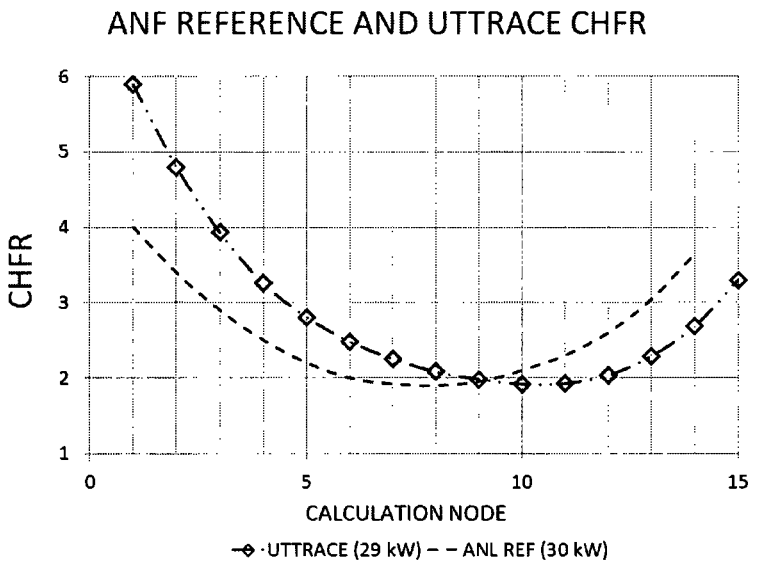

Figure 14, Comparison CHFR for Reference and UTTRIGA Model

6.0 Results

A limiting case and a nominal case were defined for analysis based on Technical Specifications and normal operating conditions in Table 7.

Calculations performed with TRACE are based on heat generation (or power) in an individual element. Power in an individual element is related to total core power by the number of fuel elements in the core and the individual element peaking factor.

Transport calculations were performed to evaluate the minimum number of fuel elements that could be loaded within reactivity limits and to determine peaking factors for each core configuration. The peaking factor data was used to determine the maximum power generated in a single fuel element assuming the maximum core power and maximum instrument error (1210 kW). Thermodynamic analysis with the UTTRIGA model was used to determine heat flux for the limiting channel.

6.1 Fuel Element Power at Maximum Core Power

A series of MCNP and SCALE (KENO) calculations were performed to determine k_{eff} and the maximum peaking factor for UTTRIGA cores loaded with varying numbers of fuel elements. Material specifications for the fuel were assumed to be the average of all fresh fuel present at the facility. Calculations were made assuming ambient temperature and 600°K (assumed to be consistent with full power operation). Calculations with water voids and graphite "dummy" rods in non-fuel spaces showed that the maximum peaking factors occurred with water voids.

6.1.1 Core Configurations and k_{eff}

Transport calculations with SCALE resulted in lower k_{eff} values than MCNP, therefore using the data from SCALE will reflect the minimum number of fuel elements to achieve conditions. Operating a power (nominal 600°K) requires a minimum of approximately 77 fresh fuel elements (Fig. 15).

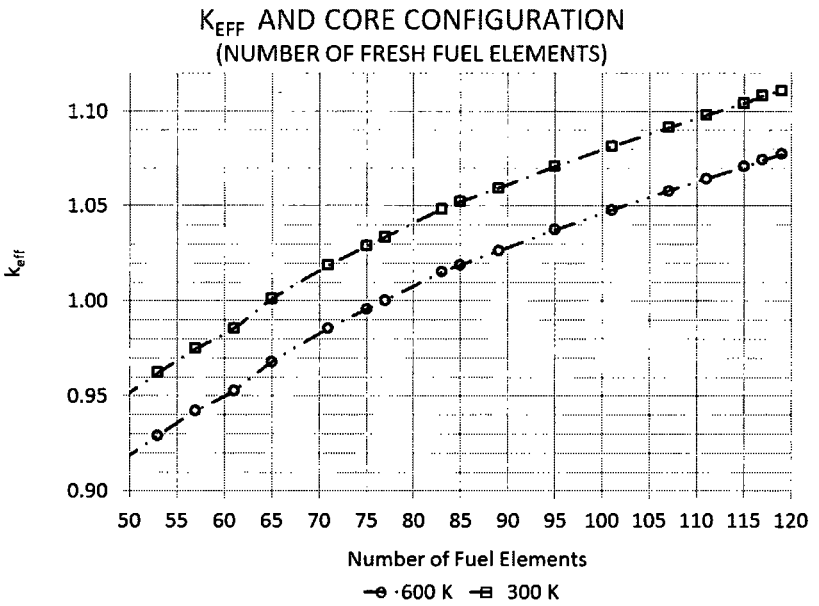

Figure 15, Criticality Considerations

At 80 elements, k_{eff} at cold clean critical conditions is the maximum permitted of 1.04. Therefore the limiting core configuration is expected to be in the range of 77 to 80 fresh fuel elements.

6.1.2 Maximum Fuel Element (Hot Channel) Power

The fission distribution data from the transport calculations was used to evaluate peaking factors for each fuel element. The maximum fuel element (hot channel) power was calculated assuming the maximum core power (license limit of 1100 kW with a 10% potential instrument error, or 1210 kW), the number of fuel elements in the core, and the maximum fuel element peaking factor. The k_{eff} values were not considered in calculations of fuel element power levels, i.e., not all configurations could achieve criticality at the specified temperatures. Values for maximum fuel element power for each configuration fell within a narrow range in MCNP and SCALE for both hot and cold calculations (Fig. 16).

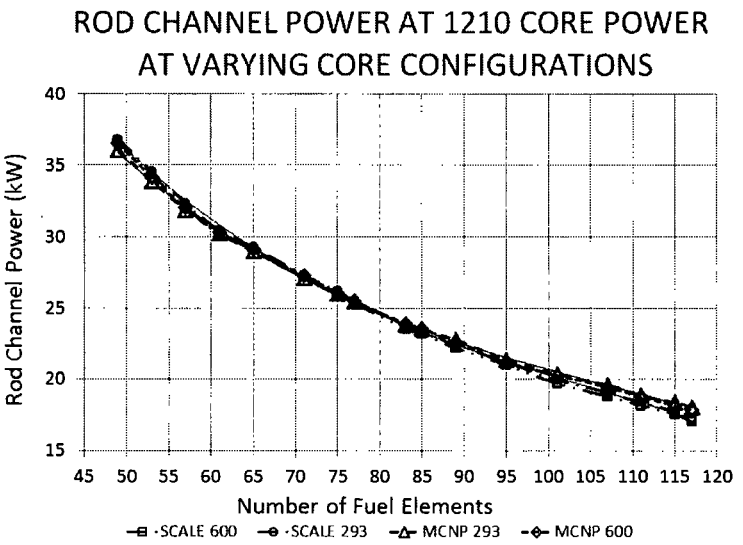

Figure 16, Maximum Element Power for 1210 kW Core (MCNP & SCALE at 300 & 600°K)

With a potential range of 77-80 fuel elements in the limiting core configuration, the power produced in the hot channel is expected to be approximately 23000-25000 W.

6.2 Fuel Temperature

The maximum fuel temperature is limited to prevent long term fuel degradation and short term cladding failure. Long term, stead- state operations with fuel temperatures greater than 750°C (1023°K) have resulted in morphological changes that expanded to the limit of the axial gas gap[5]. This is a long-term process, requiring extended intervals of operation at temperatures exceeding 750°C to develop the growth.

Historical temperature limits for TRIGA reactors prevent precipitous cladding failure from internal pressure. The limits are 950°C (1223°K) for cladding temperature greater than 500°C (773°K) , and 1150°C (1423°K) for cladding temperature below 500 °C. Following an operational event at a TRIGA conversion-fuel reactor, and additional limit of 830°C (1103°K) for pulsing operations has been imposed.
The maximum fuel temperature occurs in the fuel element that is generating the most heat, or the fuel element with maximum peaking factor. Reactor power is limited so that the fuel element with the maximum peaking factor does not exceed temperature limits.

The TRACE heat structure analysis calculates the fuel element temperature in axial and radial segments from the center of the fuel to the cooling water surrounding the fuel element. A series of calculations was performed to determine the maximum and average fuel temperature as a function of the power generated in a fuel element (Fig. 17). The maximum fuel temperature exceeds 1023°K (750°C) at approximately 26500 W.

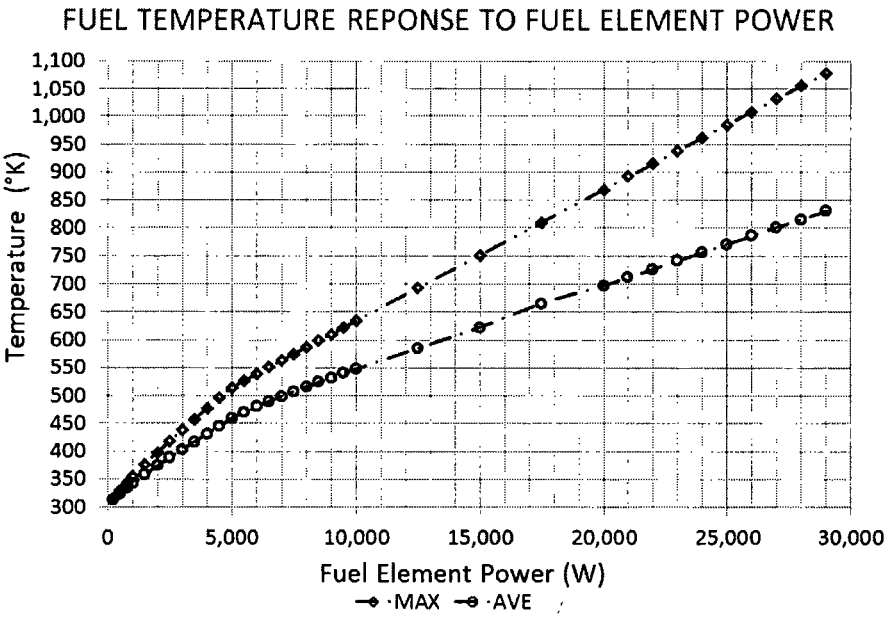

Figure 17, Fuel Temperatures as a Function of Element Power Level

Although there are two cases for consideration (nominal and limiting pool level and temperature), pool parameters are shown to have negligible effect on the maximum temperature and the temperature profile within the fuel element for a specified fuel element power level (Fig. 18).

[5] Need reference

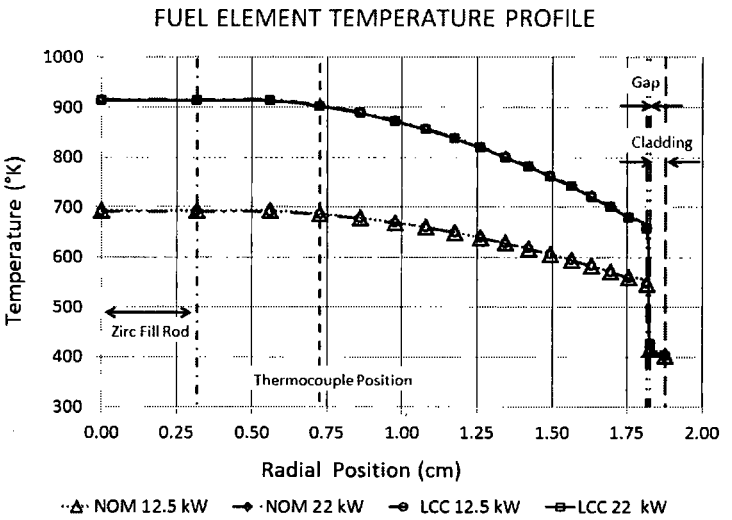

Figure 18, Fuel Element Temperature Profiles for Selected Element Power Levels

The temperature calculations demonstrate that the limiting core configuration will prevent exceeding fuel temperature limits for a fuel element power less than approximately 29000 W.

6.2.2 Fuel Temperature Measuring Channel Protective Action

As previously described, fuel elements with embedded thermocouples are installed to monitor fuel temperatures. Temperature monitoring by instrumented fuel elements provides assurance that reactor operation is terminated if limits are exceeded. However, the instrumented fuel element may not be in the position that produces the greatest power (i.e., the maximum temperature) in the core. Therefore the trip set point for the fuel temperature measuring channel is established at a level that initiates action to prevent the maximum fuel temperature in the B ring from reaching the limit regardless of the instrumented fuel element location. Since the peaking factor is calculated:

$$\frac{P_E}{P_C} = PF_E \qquad 28$$

The power generated in the instrument fuel element is a fraction of the power in the maximum heat element:

$$P_{IFE} = P_E \cdot \frac{PF_{IFE}}{PF_E} \qquad 29$$

Using SCALE and MCNP data at operating temperature as previously described, the minimum power that is being generated in a B ring fuel element is 93% (MCNP) or 94% (SCALE) of the maximum power being generated in any element in the core. The minimum power that is being generated in a C ring fuel element is 74% (MCNP) or 75% (SCALE) of the maximum power in the core. The minimum power in the core at full power is 31% (SCALE) or 33% (MCNP) of the maximum power being produced by the maximum element. Temperature response to power for representative factions were prepared and plotted against the power produced by the maximum heated fuel element. Fig. 19 demonstrates that if the instrumented fuel element power level is at least 70% of the maximum power level, a set point of 550°C is adequate to terminate operations if the maximum power element reaches 1023°K (750°C).

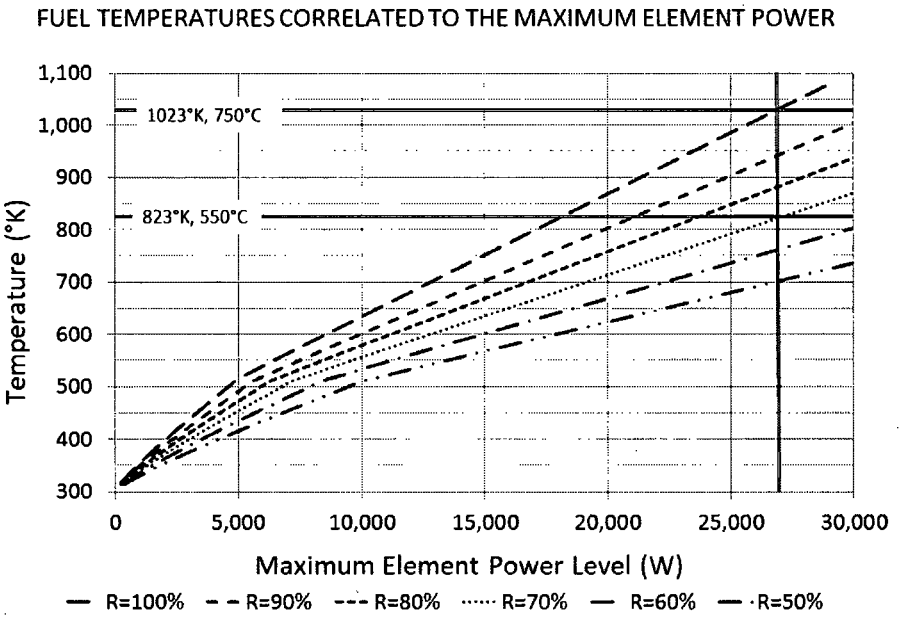

Figure 19, Maximum & Monitored Fuel Temperatures at Maximum Element Power

Table 14 , Limiting Temperatures

Application	°K	°C
Safety Limit for Cladding <500°C	1423	1150
Safety Limit for Cladding <500°C	1223	950
Limit for pulsing operations	1103	830
Limit for fuel growth	1023	750
Temperature Trip	823	550

The disagreement between FT1 and FT2 that lead to disqualification of the channel for model validation could be explained by a radial displacement from the nominal position. The effect of radial displacement of a thermocouple is similar to the effect of changes in peaking factor. Fig. 20 illustrates that data representing a thermocouple position at 1.6306 cm brings the calculation into close agreement with the measurement data, as does adjusting the temperature response data to reflect the IFE simulation operating at 70% of the power produced in the maximum power fuel element.

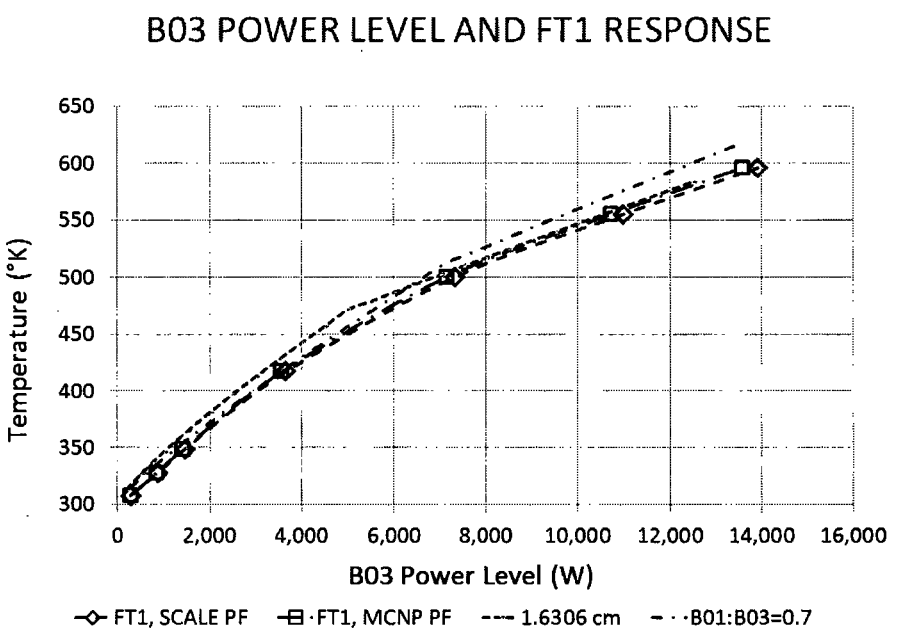

Figure 20, B03/FT1 Effects

6.3 Critical Heat Flux

Limiting the critical heat flux ratio (CHFR) in the hot channel assures that departure from nucleate boiling will not occur in the core. TRACE calculations were performed were performed using the limiting values for pressure and water temperature over a range of fuel element heat generation/power levels. Water temperature, pressure, and mass flow rate at each elevation were used to calculate critical heat flux using the Bernath correlation (Eqn. 5.8). The minimum ratio of heat flux to critical heat flux as a function of power level is provided in Fig. 21. For power levels less than about 30,000 W in a fuel element, critical heat flux ration remains above 2.0.

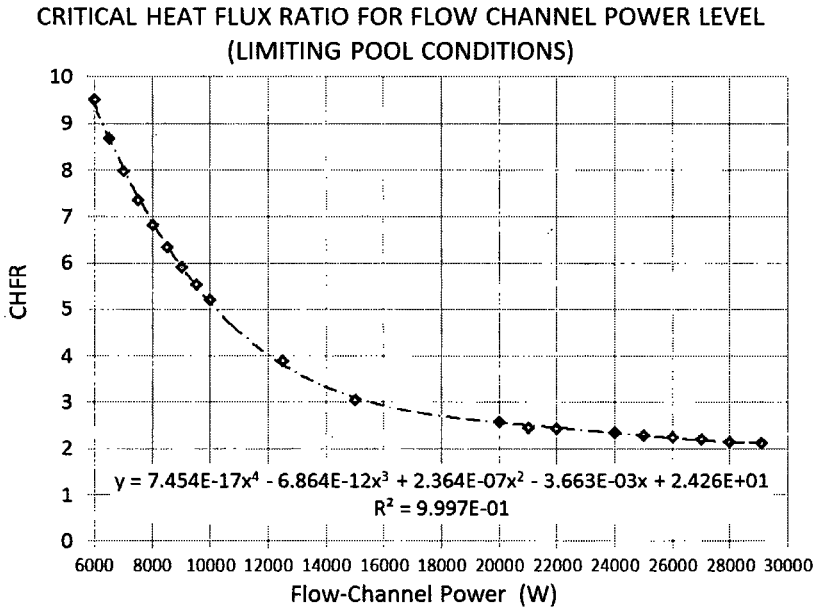

Figure 21, TRACE Critical Heat Flux, Limiting Pool Conditions

7.0 Limiting Core Configuration

Critical heat flux considerations limit the maximum power produced by a fuel element to less than approximately 30,000 W. Fuel temperature considerations limit the maximum power produced by a fuel element to less than approximately 27,000 W.

Criticality considerations (Fig. 21) show that excess reactivity reaches the maximum (k_{eff} of 1.04) with 80 elements. The maximum power produced by a fuel element by the minimum core size supporting operations at the limit of excess reactivity is on the order of 23,000-25,000 W (Fig. 22). For a more precise evaluation, the highest power level for all calculated cases was used to develop a relationship between the hot channel power and the number of fuel elements. Sensitivity of the power to changes in the number of fuel elements is taken as the derivative.

$$P_{HC} = -3.866x10^{-5} \cdot N^3 + 1.255x10^{-2} \cdot N^2 - 1.514 \cdot N + 85.24 \quad (30)$$

$$\frac{dP_{HC}}{dn} = -1.160x10^{-5} \cdot N^2 + 2.510x10^{-2} \cdot N - 1.514 \quad (31)$$

At 80 elements, the hot channel power is approximately 24,600 W with sensitivity to a change in the number of fuel elements of 2,480 W.

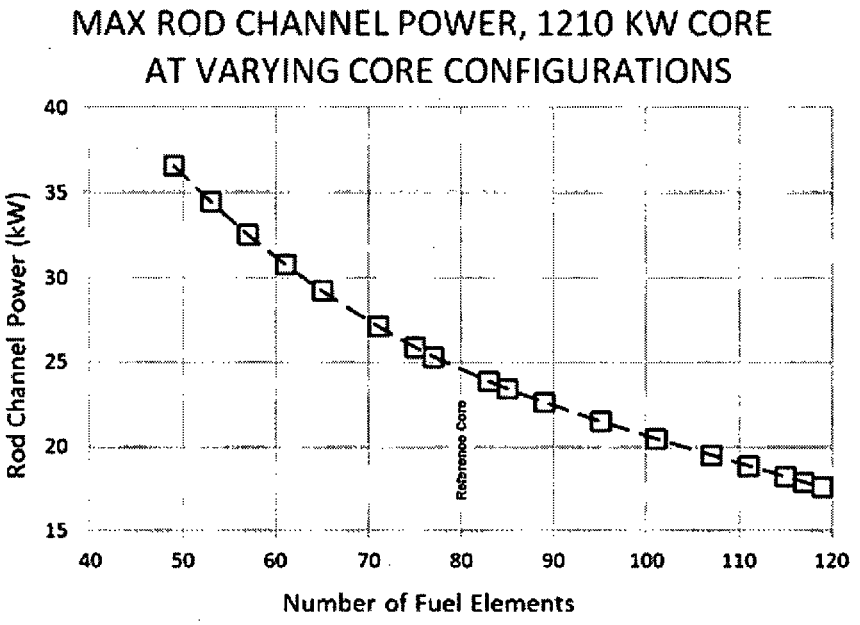

Figure 22, Highest Calculated Hot Channel Power

Calculations were performed in TRACE assuming limiting pool conditions of level and temperature at a hot channel power level of 24664 W. The minimum critical heat flux ratio remained well above 2.0 for all positions in the channel.

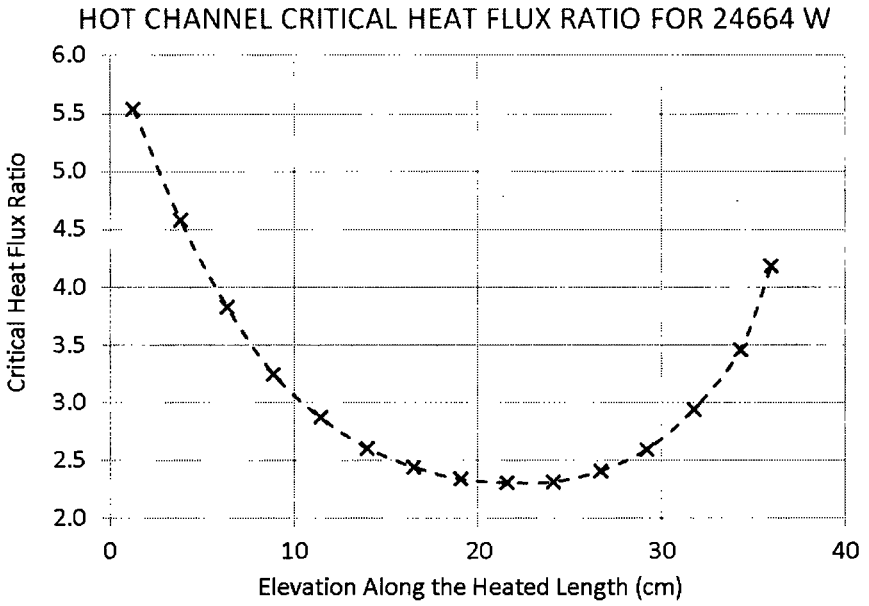

Figure 23, Limiting Core Configuration Hot Channel Critical Heat Flux Ratio

The radial temperature profile for materials in the fuel element and the (average) cooling water (Fig. 24) shows that the maximum fuel temperature remains within limits at all locations in the fuel channel. The axial profile (Fig. 25) shows the response across the radius of the fuel element is consistent with previous work that demonstrated the fuel temperature monitoring system capable of providing protection with an adequate margin to temperature limits.

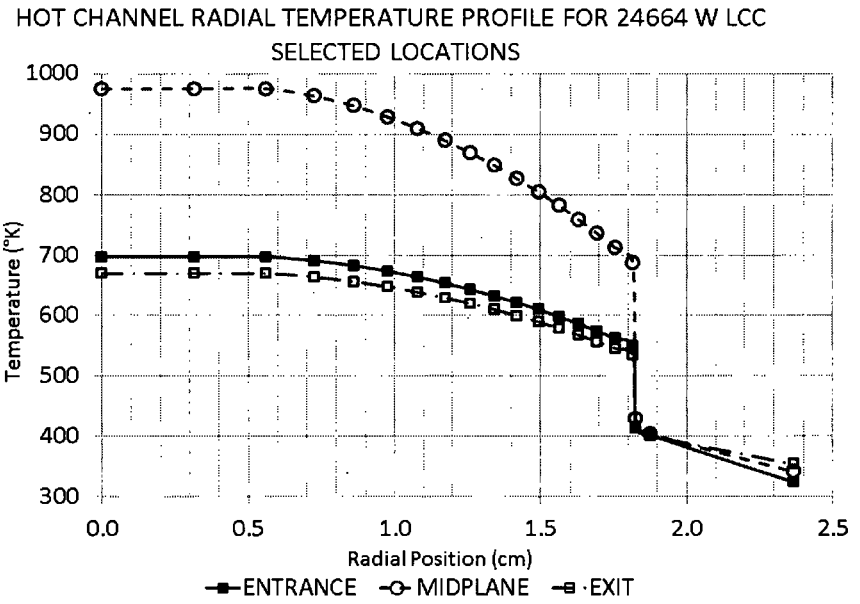

Figure 24, LCC Hot Channel Radial Temperature Profiles (Upper, Lower & Mid Heated Length)

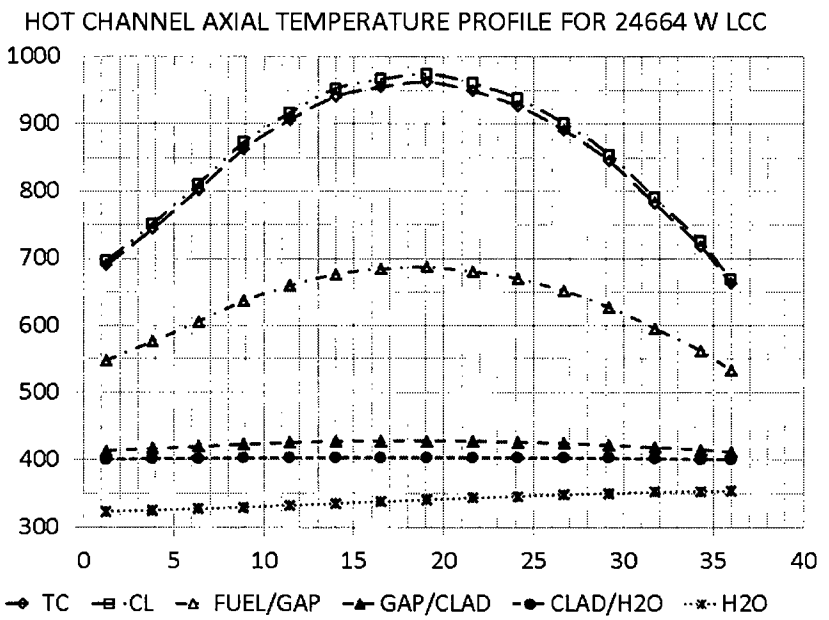

Figure 25, Limiting Core Configuration Hot Channel Axial Temperature Profiles (Heated Length)

Conservative factors in UTTRIGA analysis:

(1) Peaking factors were calculated based on a uniform average fuel temperature; the uniform average fuel temperature assumption was shown to result in higher peaking factors than a more realistic description of fuel temperature distribution.

(3) Calculated temperatures are higher than observed temperatures above approximately 750 kW, and actual thermal hydraulic conditions are therefore not as severe as calculated.

(4) Modeling a flow channel does not account for mixing with adjacent flow channels; mixing flow from adjacent channels reduces hot channel cooling temperatures.

Summary

Based on TRACE calculations at power levels up to 1210 kW (maximum measuring channel error), a minimum CHFR of 2.0 is assured in the limiting core configuration (minimum pool water level, maximum pool temperature) for all cores from 75 elements to the maximum number of fuel element locations in the core. Cores with greater than 83 elements maintain CHFR greater than 2.0 up to 1500 kW.

Therefore the minimum core configuration is selected to be 80 elements.

Hot channel power for a fuel element operating in an 80 element core at 1210 kW is approximately 24 kW. The peak centerline temperature for a 24 kW hot channel under limiting pool level and temperature is calculated by TRACE at 687 °C and by RELAP as 695 °C.

The instrumented fuel elements are capable of initiating a reactor trip prior to exceeding maximum permitted fuel temperatures in the hot channel. A trip setpoint of 500 °C accounts for differences between the sensor location and the maximum temperature of the hot channel.